REPUBLIC OF TURKEY

YILDIZ TECHNICAL UNIVERSITY

GRADUATE SCHOOL OF SCIENCE AND ENGINEERING

INFLUENCE OF CELLULOSE NANOCRYSTALS AND NANOSILICA ON MICROSTRUCTURAL AND MECHANICAL PERFORMANCE OF CEMENT-BASED MATERIALS

Ali Satar Jaber AL-ASKARY

MASTER OF SCIENCE THESIS

Department of Civil Engineering

Program of Structural Engineering

Supervisor

Asst. Prof. Dr. Didem OKTAY

July, 2022

REPUBLIC OF TURKEY

YILDIZ TECHNICAL UNIVERSITY

GRADUATE SCHOOL OF SCIENCE AND ENGINEERING

INFLUENCE OF CELLULOSE NANOCRYSTALS AND NANOSILICA ON MICROSTRUCTURAL AND MECHANICAL PERFORMANCE OF CEMENT-BASED MATERIALS

A thesis submitted by Ali Satar Jaber AL-ASKARY in partial fulfillment of the requirements for the degree of MASTER OF SCIENCE is approved by the committee on 27.07.2022 in Department of Civil Engineering, Structural Engineering Program.

Asst. Prof. Dr. Didem OKTAY
Yıldız Technical University
Supervisor

Approved By the Examining Committee

Asst. Prof. Dr. Didem OKTAY, Supervisor
Yıldız Technical University _____

Asst. Prof. Dr. Serhan ULUKAYA, Member
Yıldız Technical University _____

Asst. Prof. Dr. Buşra AKTÜRK, Member
Istanbul Bilgi University _____

I hereby declare that I have obtained the required legal permissions during data collection and exploitation procedures, that I have made the in-text citations and cited the references properly, that I haven't falsified and/or fabricated research data and results of the study and that I have abided by the principles of the scientific research and ethics during my Thesis Study under the title of Influence of Cellulose Nanocrystals and Nanosilica on Microstructural and Mechanical Performance of Cement-Based Materials supervised by my supervisor, Asst. Prof. Dr. Didem OKTAY. In the case of a discovery of false statement, I am to acknowledge any legal consequence.

Ali Satar Jaber AL-ASKARY

Signature

Dedicated to my family…

This study was financially supported by Yıldız Technical University Research Foundation (Project No: FYL-2022-4795).

ACKNOWLEDGEMENTS

I would like to express my gratitude to my supervisor for providing me with all the assistance I needed to complete my thesis. Throughout my master's degree, she provided me with invaluable assistance and encouragement, as well as extensive knowledge and precise instructions. She became pregnant when I was working on my thesis and had to care for her newborn. Despite this, she continues to help me with my thesis and keeps an eye on my progress. No matter how many times I ask her about my thesis, she always has an answer within a few minutes. I believe I am the luckiest student to be supervised by Asst. Prof. Dr. Didem OKTAY, sincere thanks.

I am grateful to Res. Asst. Tark OMÜR for his direction and assistance throughout the experimental part of my thesis. I would like to thank Eng. Nusad MIYAN for his support and assistance during my thesis study. My gratitude to Ph.D. student Mehrnosh ABOLFATHI for introducing me to my advisor, which was beginning of my success with this thesis. I am so grateful to my sister-like colleague, Ph.D. student Jinan HEYDARI, for her assistance, inspiration, advise, and support during my master's degree and life in Turkey.

Many thanks to Halil YAVAŞÇI, the technician of our Construction Materials Lab., to Ph.D. Student Ebru AYDIN from Faculty of Chemistry-Metallurgy for providing us Cellulose Nanocrystal material, AKÇANSA Cement Industry Inc. for supplying the cement, and Euclid Chemical Co. for supplying chemical admixtures.

Besides my supervisor, I would like to thank my thesis committee members for their insightful comments, suggestions, and feedback.

Last but not least, I am thankful to my mother, who is the inspiration for all of my work and dreams, and to my father, who encourages and supports me. Without their love, endurance, and support, none of this would have been possible.

Ali Satar Jaber AL-ASKARY

TABLE OF CONTENTS

LIST OF SYMBOLS

a	Hydration Degree
d	Pore Diameter
Ldx	Mass Loss in Portlandite Region
Ldh	Relative Loss of Mass Due to CSH Deyhydration
Ldc	Relative Mass Loss Due to Carbonation
Wb	Chemically Bound water
W/C	Water to Cement Ratio
2θ	Angle of Detector Position from The Incident X-Ray Beam

LIST OF ABBREVIATIONS

ASTM	American Society for Testing and Materials
AIP	Absorption after Immersion and Boiling
CNC	Cellulose Nanocrystals
CNF	Cellulose Nanofibrils
C-S-H	Calcium Hydroxide Silicate
CH	Calcium Hydroxide (Portlandite)
EDS	Energy-Dispersive Spectroscopy
ITZ	Interfacial-Transition Zone
MIP	Mercury Intrusion Porosimetry
NS	Nanosilica (Nano-SiO_2)
OPC	Ordinary Portland Cement
OPC	Ordinary Portland Cement
RH	Relative Humidity
SEM	Scanning Electronic Microscopy
SP	Superplasticizers
TGA	Thermogravimetric Analysis
TS EN	Turkish Standards Institute (English)
VPP	Volume of Permeable Pore Space (Voids)
XRD	X-Ray Diffraction
XRF	X-Ray Fluorescence

LIST OF FIGURES

LIST OF TABLES

ABSTARCT

Influence of Cellulose Nanocrystals and Nanosilica on Microstructural and Mechanical Performance of Cement-Based Materials

Ali Satar Jaber AL-ASKARY

Department of Civil Engineering

Program of Structural Engineering

Supervisor: Asst. Prof. Dr. Didem OKTAY

Nanomaterials are used in various fields to enhance material properties. In recent years, ecofriendly nanomaterials have been widely used in cement-based systems. By considering the developments in this field, the effects of cellulose nanocrystal (CNC) and nanosilica (NS) on the mechanical and microstructural performance of cement-based materials have been investigated within the scope of this experimental study.

Cement pastes and mortars were prepared with the inclusion of 0.25%, 0.50%, and 0.75% wt. for CNC groups, and similar contents for NS groups. Seven different mixtures incorporated with CNC and NS were produced to examine their fresh state performance as flow table, rheological properties and setting time. In a hardened state, compression, and water absorption tests were performed. Lastly, microstructural analyses e.g., TGA, MIP, XRD, and SEM-EDS were applied on pastes to confirm the effects of nanomaterials on cement-based composites.

The flow diameters decrease with the increase of CNCs. NS has decreased the flow diameter but did not cause a notable change compared to CNC concluding that NS has low effectivity in low quantities. CNC played as retarder admixture delaying setting time

in all of its contents, while NS reduced the setting time significantly in comparison to CNC addition. In rheological measurements, both CNC and NS samples exhibited a rise in yield stress within the increasing of nanomaterials dosages, where CNC0.75 showed the highest yield stress, meanwhile, the plastic viscosity was seen to be improved mostly in NS samples and gradually increased with the increasing of NS dosages. A compressive strength test was performed at the ages of 3, 7, 28, and 90 days. The results for CNC concluded that increasing CNC content in the mixture increased the compressive strength where it showed high compressive strength in 0.50% dosage for 28 days and 0.75% CNC content scored higher in 90 days. NS inclusion exhibited higher compressive strength in 0.25% content within 28 days while in 90 days 0.75% scored higher. Water absorption and void content has been reduced gradually in the CNC incorporated samples, while NS samples showed no remarkable effect. Microstructural analyses were mostly supportive to compressive strength results. The highest degree of hydration was obtained in CNC0.50 in 28 days, while the NS samples exhibited an incremental change in hydration degree within the early ages. C_3S and C_2S were mostly seen in CNC samples, while NS was showing both CSH and $Ca(OH)_2$ in XRD results and those were supportive and agreed in SEM-EDS results.

Keywords: Cellulose Nanocrystals (CNC), Nanosilica (NS), Eco-friendly Material, Mechanical properties, Microstructural Analysis.

ÖZET

Selüloz Nanokristalleri ve Nanosilikanın Çimento Esaslı Malzemelerin İçyapı ve Mekanik Performansına Etkisi

Ali Satar Jaber AL-ASKARY

İnşaat Mühendisliği Anabilim Dalı

Yüksek Lisans Tezi

Danışman: Dr. Öğr. Üyesi Didem OKTAY

Nano malzemeler, malzeme özelliklerini geliştirmek için çeşitli alanlarda kullanılmaktadır. Son yıllarda, çevre dostu nano malzemeler çimento esaslı sistemlerde yaygın olarak kullanılmaktadır. Bu alandaki gelişmeler göz önünde bulundurularak, selüloz nanokristal (CNC) ve nanosilika (NS) kullanımının, CNC ve NS'nin farklı örneklerde ayrı ayrı ilave edilmesiyle çimento esaslı malzemelerin mekanik performansı ve iç yapı özellikleri üzerindeki etkileri bu deneysel çalışma kapsamında araştırılmıştır.

Çimento ağırlığının %0,25, %0,50 ve %0,75'i oranında CNC ve NS ilavesi ile çimento pastası ve harç üretimleri yapılmıştır. Yayılma, reolojik özellikler ve priz süresi gibi taze hal özelliklerini incelemek için CNCc ve NS ilavesi ile yedi farklı karışım üretilmiştir. Nano malzeme ilaveli harçların sertleşmiş hallerinde basınç dayanımı testi ve su emme testi ölçümleri de yapılmıştır. Son olarak, nano malzemelerin çimento esaslı kompozitler üzerindeki etkilerini doğrulamak için pastalarda TGA, MIP, XRD ve SEM-EDS gibi içyapı özellikleri incelemeler uygulanmıştır.

CNC oranın artması ile harçların yayılma çapları azalmıştır. NS oranının artışı ile yayılma çapı azalmış ancak CNC'li serilere kıyasla önemli bir değişiklik olmamıştır. NS yüksek oranda kullanılmadığı için yayılma çapı kayda değer şekilde etkilenmemiştir. CNC'nin priz süresi üzerinde geciktirici bir etkisi olduğu görülürken, NS CNC'ye kıyasla priz

süresini kısaltmıştır. Reolojik ölçümlerde hem CNC hem de NS numuneleri, nanomalzeme dozajlarının arttırılmasında eşik kaymagerilmesinde artış görülmüştür. CNC0.75'te en yüksek kayma gerilmesi elde edilmiştir. Plastik viskozitenin çoğunlukla NS örneklerinde iyileştiği ve NS dozajlarının artmasıyla kademeli olarak arttığı görülmüştür. Serilerdeki CNC içeriğinin arttırılması ile basınç dayanımı değerleri artmıştır. 28. günde en yüksek dayanım%0,50 oranında CNC ilave edilen seride, 90. günde ise %0,75 oranında CNC içeren seride elde edilmiştir. NS'li serilerde, 28. günde %0,25 NS içeren karışım en yüksek basınç dayanımı sergilerken, 90. günde %0,75 NS kullanılan seride daha yüksek dayanım elde edilmiştir. CNC ilaveli numunelerde su emilimi ve boşluk içeriği kademeli olarak azalırken, NS'li numunelerde kayda değer bir değişiklik olmamıştır. Basınç dayanımı değerleri içyapı analizleri ile desteklenmiştir. En yüksek hidratasyon derecesi 28. günde CNC0.50 serisinde elde edilirken NS örnekleri erken yaşlarda artan bir hidratasyon derecesi değişimi göstermişlerdir. XRD sonuçlarına göre CNC örneklerinde çoğunlukla C_3S ve C_2S görülürken, NS'li serilerde hem CSH hem de $Ca(OH)_2$'yi görülmüştür ve bu sonuçlar SEM-EDS sonuçları ile desteklenmiştir.

Anahtar Kelimeler: Selüloz Nanokristalleri (CNC), Nanosilika (NS), Çevre dostu malzeme, Mekanik özellikler, İcyapı analizleri.

1
INTRODUCTION

1.1 Literature Review

Nanotechnology is one of the most rapidly emerging multidisciplinary sectors of science and technology at the current time. It incorporates physics, chemistry, biology, material engineering, and bioengineering-related topics. It refers to materials on the molecular scale up to 100 nm, at least in one dimension, that are distinguished from their macroscopic chemical equivalents by their quantum effects [1]. For modifying the building materials chemically, nanomaterial technology has been used in civil engineering, particularly in construction chemicals. It has been proposed to use nanotechnology and nanomaterials to make developments in advanced cement composites while improving their fresh and hardened performance, durability, and their sustainability [2], [3]. Today's concrete technology is under unprecedented destination to optimize environmentally friendly building materials. In the last years, nanomaterials have arisen as a breakthrough in concrete technology, discovering frontiers for building multifunctional features toward improved eco-efficiency [2].

In recent years, scientists from all over the world have prioritized the modification of materials using eco-friendly additives and admixtures, also known as biopolymers. Concerning Portland cement concrete, a convergence of phenomena has increased interest in cellulosic-based nanomaterials. First, the demand to increase the durability and resilience of infrastructure has encouraged the scientific community to further develop and enhance the qualities of concrete, the most frequent material used for infrastructure. Second, the colossal yearly output of Portland cement and the related CO_2 emissions have sparked an interest in minimizing environmental effects [4]. Nanotechnology applications in cement and concrete have demonstrated the possibility of unique combinations of early-age and long-term characteristics [5]. In each of these fields, bio-based nanocomposites have the potential to play a significant role. In recent years, there has been a significant deal of research interest in bio-based materials due to their enormous potential for generating a range of high-value goods with minimal environmental effects [6]. They have always existed in the environment and provide an environmentally friendly alternative to manufactured polymer admixtures. Cellulose is an example of a natural polymer. Cellulose is the most prevalent biopolymer on the planet; it may be

extracted from wood, cotton, or plant biomass by the synthesis of algae, bacteria, and tunicates. Nanocellulose, which is derived from cellulose, possesses low air permeability, exceptional mechanical qualities, a low thermal expansion coefficient, and high strength. It is commonly employed in industries like medical equipment, batteries, displays, and sensors. Cellulose nanoparticles may be categorized into five groups based on their source, acquiring technique, and surface chemical characteristics: cellulose nanocrystals (CNC), cellulose nanofibrils (CNF), tunicate cellulose nanocrystals (t-CNC), algal cellulose (AC), and bacterial cellulose (BC) [7]–[9]. These materials have several potential uses in cement-based composites due to their nanoscale size, fibril morphology, reactivity surfaces for the synthesis process, and substantial specific surface area [10]. In recent years, cellulose nanocrystals (CNC) have garnered increased interest as an additive and nano-reinforcing ingredient in cementitious materials. CNC has great stiffness [11], good strength [12], high thermal conductivity [13], reduced thermal expansion [14] and are nontoxic and renewable [11]. As an additive to cement materials, CNC was shown to improve the mechanical characteristics [15], [16], raise the hydration degree [15], and improve the microstructure of cementitious composites [17]. For cementitious materials, Cao et al. [15] investigated the use of CNC as an additive to improve the cement paste performance and discovered that CNC can improve flexural strength and hydration degree for cement type V at a water to cement ratio (w/c) of 0.35. Cao et al [15] also showed a decrease in the yield stress of fresh paste, with the yield stress being lowest at a dose of 0.04 percent CNC by volume of cement. In further investigation [16], it was determined that the CNC agglomerated in the cement paste above a concentration of 1.35 percent, hence raising the yield stress of the combination. Yet, Cao et al. [15], [16] conducted their research using a CNC manufactured from a single supplier with a fixed w/c. Little is known about the consequences of CNC manufactured using various raw material sources and processing procedures. In addition, little is known about how cement composition affects the fresh paste's effectiveness. Dousti et al. [18] inserted CNCs into cement paste at a rate of roughly 0.5% and studied their effect on mechanical qualities. According to reports, the integration of CNCs increases both the compressive and tensile strengths. This improvement was due to an increase in early hydration. The rise at one day of age was nearly 60% more than the group used as a comparison. At 56 days, the difference in strength was determined to be 30 percent. In contrast, Flores et al. [17] reported that the inclusion of CNCs slowed hydration at an early age but accelerated it at later ages. In addition, the inclusion of CNC led to the discovery of high-density C-S-H

in cement paste. In CNC-cement composites, Flores et al. [17] showed a slight increase in the volume percentage of high-density C–S–H and a drop in the volume fraction of low-density C–S–H. Fourier transform infrared spectroscopy (FTIR) data from the same investigation suggested the formation of potential linkages among CNCs and hydration products. Crystalline and non-crystalline zones compensate CNCs (Figure 1.1). When acid is applied, hydronium ions enter comparatively irregular, amorphous parts, resulting in glycosidic bond hydrolysis. As time passes, just the crystal area is left, and a significant stiffness develops. In addition, CNCs have great hydrophilicity due to the presence of many hydroxyl groups on their surface [16].

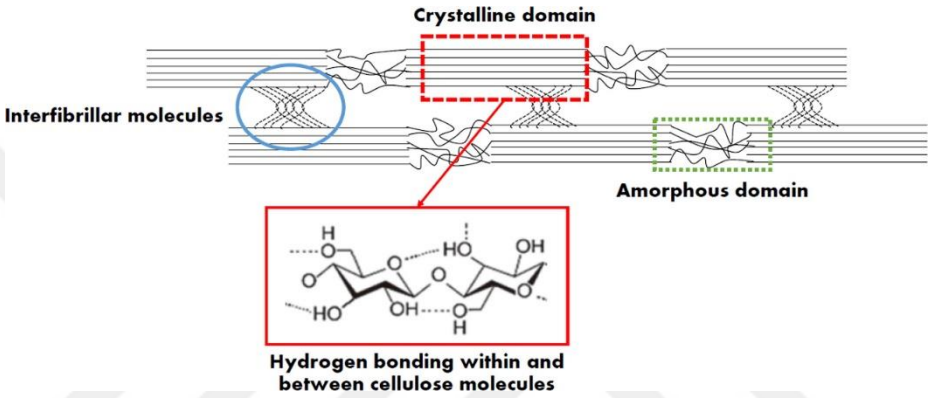

Figure 1.1 Crystals and amorphous zones of the nanocellulose fiber (Kim et al., 2016 reproduced)

As seen in Figure 1.2, the method by which CNCs increase the strength of cement is a short circuit diffusion phenomenon in which CNCs are connected to cement particles, increasing hydration of unhydrated areas by the passage of water along with the network of CNCs. Consequently, it increases the development of C-S-H (Calcium Silicate Hydration), a hydrating product that impacts the strength of cement hydration, and thereby increases the strength of the cement (up to 30 percent of bending performance) [15]. According to reports, the inclusion of CNC reduced porosity by as much as 40 percent [18]. Calamunt et al. [19] have demonstrated that cellulose nanoparticles affect the productivity of calcium aluminate cement in addition to OPC systems. Nanocellulose materials have been reported as a prospective resource for enhancing the performance of cement-based composites, taking into account all of the previously mentioned advantages.

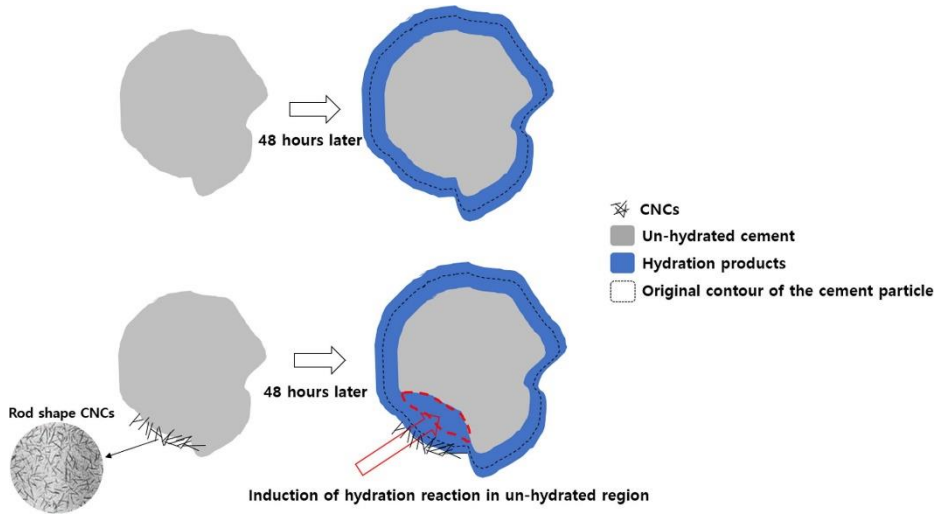

Figure 1.2 Schematic of hydration products formed surrounding cement from 0 to 48 h: on top, ordinary cement; on the bottom, hydration induction of un-hydrated regions using CNCs affixed to cement particles (short circuit diffusion) [18]

The literature review in addition to the second material of this study Nanosilica (NS), Prior research investigates the effects of nanomaterials, such as NS, on the use of nanotechnology in concrete. Nanosilica or nano-silicon dioxide (SiO_2) and its aqueous form, have garnered a great deal of interest from the scientific and technological sectors. In reality, the application of NS has been widely published in scientific literature with proven outcomes and successful implementation. The benefits of utilizing NS include, among others, strong early compressive strength, high tensile, flexural, and modulus of elasticity strength, increased durability, and low permeability. Behnood and Ziari [20] for instance, showed increases of up to 25 % in compressive strength for heated and unheated specimens with 10 wt.% percent cement substitution. Jalal et al. [21] investigated the mechanical, rheological, durability, and microstructural aspects of high-performance self-compacting concrete (HPSCC) using microsilica (MS) and NS in place of a portion of Portland cement. Different concentrations of 10 %, 2 %, and 10 % +2 % of MS, NS, and a mixture of MS and NS were evaluated. The w/b ratio was maintained at 0.38, and various binder concentrations were investigated. It was determined that the addition of 2% NS to binary mixes with a binder concentration of 400kg/m^3 enhanced the compressive strength by 45%, 55%, 70%, and 73% at 3, 7, 28, and 90 days, respectively. Since the impacts of NS on these mechanical parameters are considerable, several attempts have been undertaken to determine the optimal concentration of NS that provides concrete with the greatest compressive strength. Some researchers, like Bahadori and Hosseini [22], Berra et al. [23], and Qing et al. [24], found that the use of NS particles

significantly decreased the workability of mixtures. In contrast to this loss in workability, NS addition enhanced cohesiveness and yield stress in cement pastes. Superplasticizers have been utilized to increase the workability of the mixture, but their quantitative impacts on NS reactivity and particle dispersion are still unknown. In actuality, the rheological characteristics of new cement pastes are complicated, and further research is required. Meng et al. [25] studied the effect of NS addition with varied sizes on hydration heating of cement mortar samples. The kinetics of NS hydrations were analyzed. Results indicated that NS might increase the value and decrease the occurrence time of the exothermal peak associated with hydration. According to Figure 1.3, NS assisted in increasing the hydration degree and hydration rate in the Nucleation and crystal growth (NG) stage, reducing the length time of the Phase boundary reaction (I) stage, and decreasing the hydration rate in the diffusion reaction (D) stage. Kong et al. [26] investigated the rheological characteristics of new cement pastes with a w/c ratio of 0.4 and an NS addition of 0.5 weight percent. It was hypothesized that, if the water content were held constant, the addition of NS would enhance the packing of cement particles, reducing the gaps among them and raising the free water, so adding to the paste's fluidity. Nonetheless, the majority of writers attribute the loss in workability to the fact that not all agglomerates operate as fillers that occupy the void area among cement particles and release free water. In addition to the significant water absorption of NS nanoparticles, these agglomerates will also absorb free water that initially helps to fluidity. Some researchers [27], [28] also hypothesized that the agglomerates might dislodge the cement particles surrounding them, so increasing the void area. This conduct explains the diminished workability. Therefore, the effect of NS addition on rheological behavior depends mostly on whether or not the agglomerates can function as fillers. The conducted studies indicate that, in most instances, NS agglomeration does not operate as a filler and reduces workability. Incorporating superplasticizers into the mixtures should be the optimal approach despite the need for more research on this topic. In addition, Ashraf et al. [29] studied the impact of pure cellulose nanofibrils (CNF) and nanosilica-containing CNF on the performance of ordinary Portland cement paste (OPC). The impacts of CNFs on the rheology, hydration, creation of microscopic phases, compressive strength, and fracture characteristics of cement paste were examined. NS particles in the CNF slurry were produced using the Sol-gel technique. The impacts of CNF on cement hydration were observed to be water-to-cement ratio (w/c) dependent. The inclusion of NS particles [30] was shown to increase the aqueous solubility of CNF. The use of CNF increased the

flexural strength of cement paste by up to 75%. The inclusion of CNF had no influence on the compressive strength of the cement paste matrix. It was discovered that the use of nanosilica speeds up the cement hydration process and increases the compressive strength of concrete during the preliminary stages of development. Throughout the presence of sodium sulfate, samples containing nanosilica demonstrated a better corrosion resistance. The addition of nanosilica to cement materials functions as a nanofiller, significantly enhancing the interfacial transition zone [31].

Generally, in the literature, mechanical properties and microstructures of cement-based materials incorporated with nanomaterials have been investigated. However, there are limited studies about the effects of nanosilica and nano cellulose on the rheological properties of cementitious materials. Within the scope of this study, not only the mechanical properties and microstructure but also the rheological properties (yield stress and plastic viscosity) of nanosilica and cellulose-added pastes will be investigated and the performance of two different nanomaterials will be compared.

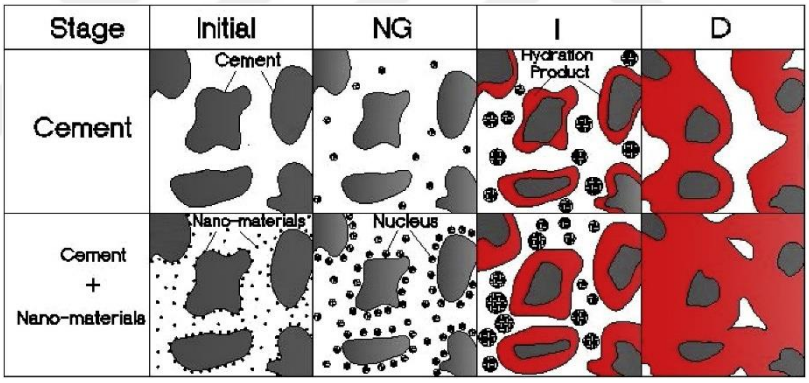

Figure 1.3 Model for the hydration of cement both with and without NS [25]

1.2 Thesis Objectives

Consequently, the cement-based material manufacturing processes of today are facing an unparalleled drive to optimize eco-efficient building materials. Cement is not beneficial to the environment since the manufacture of one ton of cement releases an average of 0.70 tons of CO_2 into the atmosphere. Therefore, it is vital to reevaluate cementitious mixture components and incorporate more eco-friendly materials. Increasing usage of supplemental cementitious materials is stimulated by the present push for more sustainable cementitious composites. With the inclusion of supplemental cementitious materials, nanomaterials present a significant growth opportunity, particularly in sustainable construction or green building applications due to their environmental

protection and efficiency. Considering the nanomodification of cement-based materials, cellulose nanocrystals (CNC) and nanosilica (NS) have more potential for increasing cement-based mixtures' (compressive and flexural) strength, reducing the overall porosity, accelerating the development of C-S-H gels, and increasing the Young's modulus.

In this thesis, paste and mortar samples were produced using Portland cement. The study work of this thesis is divided into two groups in the addition of nanomaterials. The first group was CNC addition with different dosages to Portland cement, and the second group was with the addition of NS with various contents to Portland cement. In mortar preparation superplasticizer (SP) are used to achieve workability in the samples. The water to cement ratio (w/c) was not constant in all mixtures, paste samples had different w/c from mortar samples and that was depending on the test was applied to these samples.

The aim of CNC and NS addition to Portland cement is to examine the effect of these nanomaterials on the fresh and hardened state of cement pastes and mortars, and the main objectives of the study can be listed as follows:

• In fresh state, to investigate the effects on workability, setting time, and rheology changes with the addition of CNC and NS to cement mixtures.

• In the hardened state, to investigate the effects of CNC and NS additions on cement mixtures, whether it decrease or increase the water absorption, void ratio, and compressive strength.

• Study the effects of these nanomaterials in enhancing the microstructure, mineralogy, and void structure of the paste samples, and there effects in improving the hydration degree.

The process that has been followed in this study, in which various tests were performed to examine the mechanical and microstructure performance of mortar and paste samples is presented in Figure 1.4.

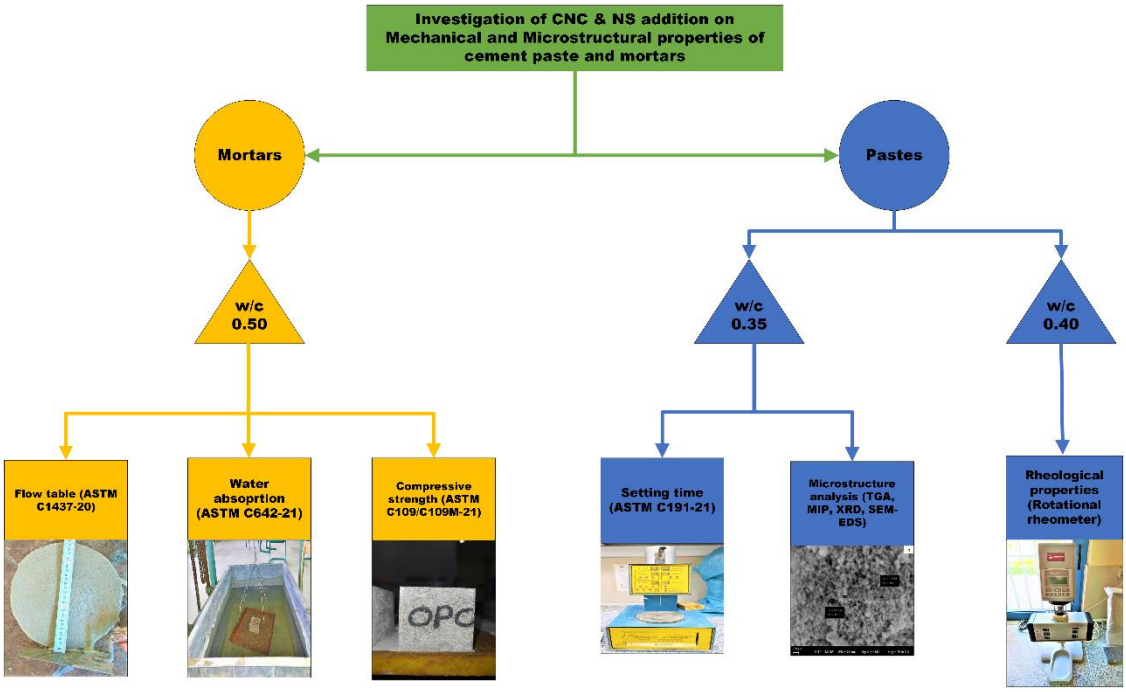

Figure 1.4 Flow chart of the experimental study

1.3 Hypothesis

The mechanical performance and microstructure of cement-based mortars can be improved with the addition of nanomaterials. By using nanosilica and cellulose nanocrystals in cementitious materials, the compressive strength of mortars can be increased while the void ratios decrease. The workability of mortar is adversely affected by the addition of nanomaterials. However, workable mortars can be obtained if nanomaterials are employed up to a certain usage rate.

2
GENERAL INFORMATION

2.1 Nanoscience (Nanotechnology)

Nano in linguistics terms according to the Oxford English Dictionary (OED) means dwarf, which comes from the classical Latin ancient Greek language, Indicating the division of one by billon [32]. Nanomaterials can be defined as any material that has an external dimension of approximately 1-100 nm, owns an internal shape, or that its forming surface is in the term of a nanoscale [33]. The nanomaterials are in their nanoscale state thanks to the recent developments in microscopies which gave scientists and researchers the ability to discover the advantages of these types of materials. Nanomaterials have been classified by scientists into many groups, where materials with nanostructures are classified as zero-dimensional, one-dimensional, two-dimensional, and three-dimensional nanostructures [34]. Nanomaterials have advantages that include being high-precision particles with a precision of less than 50 nm or with dimensions close to 50 nm [34]. It is possible to form nanostructured materials at different scales, which are 0D (atomic groups, clustered groups, and clusters), 1D and 2D (modified multiple layers and overlayer nanostructured), and 3D (nanoparticle size) [34] as shown in Figure 2.1.

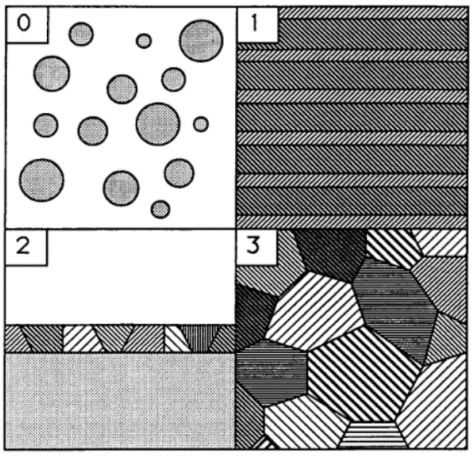

Figure 2.1 Schematic for four classes of nanomaterials based on integral modulation dimensionality: Classification of nanomaterials: 0D spheres and clusters; 1D nanofibers, wires, and rods; 2D films, plates, and networks; and 3D nanomaterials [34]

It has been considered since the statement belong the physician Richard Feynman “There’s plenty of room at the bottom” in 1959 the starting of the nanotechnology era [35]. Nanoscience or in other terms nanotechnology recently has been used in research and studies in wide fields such as biology, physics, chemistry, and construction materials science of engineering.

In addition, nanotechnology described in terms of nanoscience, it is also can be described in terms of nanoengineering (nano-modification) both explain the main directions of nanotechnology [5]. Nanotechnology has changed the world's view of materials science in terms of studies and research, attracting the researchers' inspiration in terms of the possibility of its nanoscale modification and obtaining new, more efficient materials with improved properties.

2.2 Nanotechnology in Construction

Nanotechnology has been relied upon in the field of civil engineering, especially in the field of construction materials that require chemical studies of materials. Researchers have discovered that nanotechnology has a positive influence on the physical and chemical characteristics of building materials, and this study has expanded into the area of nanotechnology research. Industry should likewise be considered in areas where nanotechnology has been developed since the utilization of nanotechnology in certain parts and cycles of development is currently expanding. Even though the development industry is as yet viewed as a moderate and customary space of modern movement, the conceivable outcomes, and viewpoints that nanotechnology gives have prompted a change in perspective. Also, both financial and natural contemplations have been driving this area to embrace new advances, producing cycles and materials. In this sense, nanotechnology came up as an extraordinary chance, because of the first physical, synthetic, and warm attributes of nanomaterials (NMs) fundamentally brought about by the nano-quantum dimensional surface impacts. As of now, there are a few unique applications in construction manufacturing. The report RILEM TC 197-NCM, "Application of Nanotechnology in construction" was the principal record, to sum up, the capability of nanotechnology in the turn of events and improvement of development and building materials [36]. From that point forward, many researchers have oppressed a similar issue. For instance, Lee et al. [37] noticed that NMs will probably greatly affect

the development business more than some other areas of the economy. Right now, biomedical and electronics applications exploit the utilization of nanomaterials, however different researchers referred to numerous possible applications in constructions manufacturing [38] for example, working on the essential properties of conventional development materials (for example concrete). By adding new functionalities to existing materials, such as self-cleaning, antimicrobial, and contamination-reduction properties to paints, coatings, or glass, various nanoparticles (NPs) are being used to achieve significant improvements in substantial strength, toughness, and maintainability, among others. In research center settings, climate-responsive anticorrosion coatings constructed using nano embodiment technologies are showing promise in this sector. For instance, silica aerogels that fill a current need for more slender, transparent, yet powerful protection; or nano encapsulated erosion inhibitors to combat steel consumption; produce self-detecting structures, which allows extensions and structures to detect their own breaks, consumption, and stresses, which may ultimately lead to underlying failures. In this sense, a few applications have been created for this area somewhat recently, working on the exhibition and toughness of materials, just as the energy effectiveness and security in structures. The assortment of utilizations goes from more solid cement to self-cleaning windows and dividers. Nevertheless, there are basic hindrances to be defeated to expand the market infiltration of these latest items and advancements. The Final Report of "Observatory Nano" [39] introduced two significant obstructions: (I) the expense of new handling innovations and new materials as the greatest hindrance and (ii) the buyer incredulity about the presentation of such superior materials. The most important goals of the development of advanced engineering are through the development of sustainable & renewable infrastructure materials and components, which is a radical alternative to conventional engineering patterns. When mentioning renewable and sustainable materials, it is worth mentioning that improved materials in nanotechnology have advanced properties such as impact resistance, bending resistance, fracture resistance, tensile resistance, and modulus of elasticity [40]. The present substantial innovation faces an uncommon push towards improving eco-proficient development materials. Throughout the most recent couple of years, nanotechnology has arisen as a leap forward in substantial innovation investigating new boondocks for designing multifunctional properties towards higher eco-proficiency [2]. Because nanotechnology empowers planning nanomodified concrete; whereby concrete microstructure can be custom fitted

to accomplish explicit beneficial properties [41]. The U.S. Geographical Survey assessed those 4.1 billion metric huge loads of cement were created in 2018 [42]. Besides, it has been for quite some time realized that cement factories represent 5–8% of all-out CO_2 discharge around the world [43]–[45]. In such a manner, it is generally accepted that nanotechnology would hoist nanomodified composites to recreate the components of regular frameworks improved until flawlessness during an extended period. This is to a great extent owing to the complex various leveled structure shown by normal frameworks [46]. The potential for nanotechnology to open new scenes in a composite plan to recreate normal framework shapes, truth be told, is a promising specialty market in substantial innovation as distinguished by the RILEM TC 197-NCM report [36]. Significant exploration regions in nanomodification of cement have so far fundamentally covered nanosilica (NS) [47]; nano-titanium dioxide ($nTiO_2$ [48], [49]; nanoclay [50]; carbon nanotubes (CNT) [51]; and carbon nanofibers (CNF) [2].

It is commonly known that nanoscale materials have superior physical and chemical properties, including enhanced mechanical, electrical, and thermal capabilities, reduced density, and superior chemical and thermal stability. It is possible to build cementitious nanocomposites with vastly varied characteristics, hence extending the lifetime of cementitious materials [52] due to the existence of a large number of distinct nanomaterial types. Nanostructures like nanofibers, nanotubes, and nanoparticles like nano-TiO_2 and nano-SiO_2 may be used to build a new development of high, multifunctional cementitious composites.

During the past decade, the number of publications on nanotechnology in the construction industry has grown substantially as seen in Figure 2.2. Reviewing the information, it was determined that the inclusion of carbon nanotubes (CNTs) has been the primary emphasis (58 % publications) (Figure 2.3), followed by nanosilica (34% of total publications) and nanotitanium (7% publications). The researches are mostly concerned with the influence of nanoparticles on the performance of cementitious matrices, without addressing their potential effects on human health and the environment. Consequently, it is essential to overcome the major disadvantages of nanomaterials. Regarding the pathogenic consequences of nanomaterials, scientific literature has contradictory findings. Consequently, their prospective connection with our biological system is yet unclear. In addition, their greater cost relative to the same materials on a larger scale is a significant

disadvantage; nevertheless, in the majority of circumstances, their optimal concentration is fairly low, making their cost equivalent or even cheaper than traditional materials. In addition, the fact that in order to make use of their exceptional qualities, they must be adequately disseminated throughout the matrix adds an extra stage to the construction of composites, which may be problematic for large-scale applications. Finally, the nanocomposites that have been produced should be assessed in terms of their sustainability and their environmental and economic impacts. A recent analysis provides more details on some of the most current concrete nanocomposites, assessing them in terms of ecological sustainability and economic benefits [52].

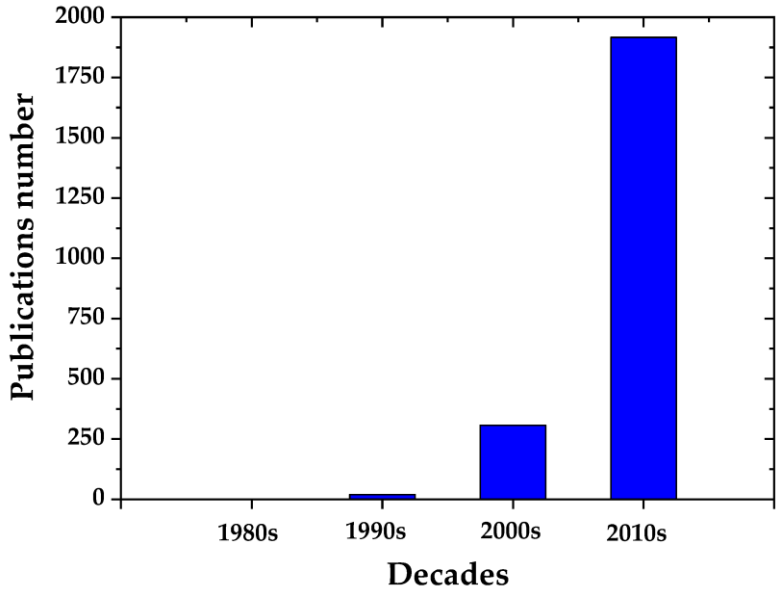

Figure 2.2 Schematic nanomaterials incorporation in cementitious composites publications per decade [53]

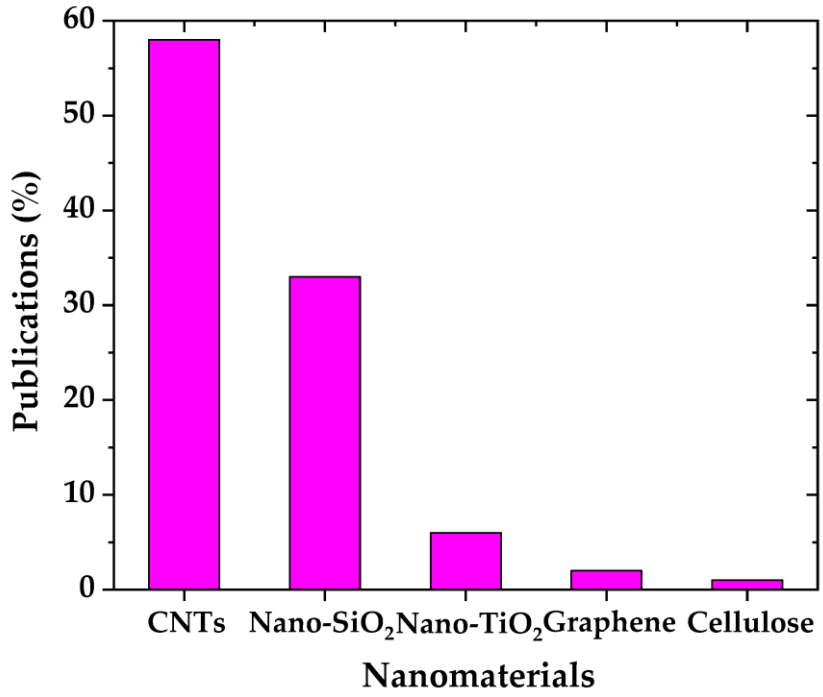

Figure 2.3 Publications (%) versus nanomaterials used in cement composites [53]

2.3 Nanocellulose

Cellulose is a plentiful natural polymer (biopolymer), and as nanotechnology has advanced, the nano version of cellulose, i.e., nanocellulose, has attracted a great deal of interest. The term microfibrillar cellulose (MFC) was created in the early 1980s by ITT Rayonier when it granted patents and published articles based on an entirely new nanocellulose composition [54]. In later decades, MFC was altered by enzymatic hydrolysis to produce CNC. Due to its exceptional mechanical qualities, transparency, capacity to create chiral nematic structures, and, most notably, its decreased health risk, environmental friendliness, and biodegradability, nanocellulose has become a viable substitute for all other nanomaterials in a variety of applications. Researchers are using nanocellulose in a variety of applications. It can serve as a reinforcing agent for a variety of matrices due to its good mechanical characteristics and the existence of free hydroxyl groups that can be adjusted to meet specific requirements. The biomedical area is also investigating nanocellulose for medication delivery, enzyme immobilization, tissue culture, etc. Due to its transparency and barrier qualities, it may be used in packaging and as flexible transparent films [55], [56]. As shown in Figure 2.4, nanocellulose may be

created primarily through two distinct methods: the top-down technique and the bottom-up approach.

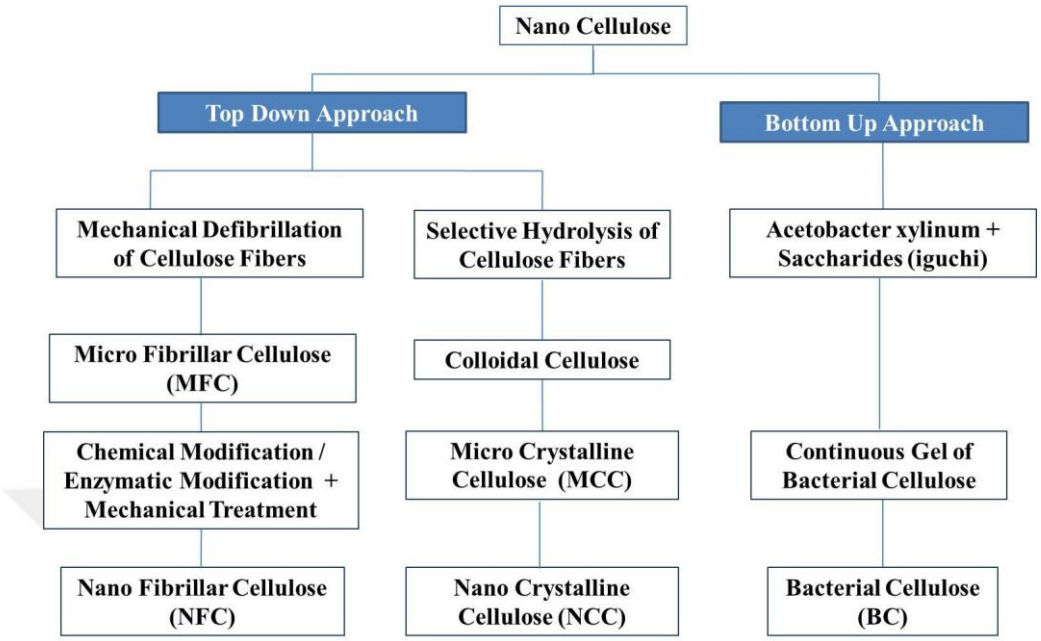

Figure 2.4 Flowchart of nanocellulose preparation [55]

The cellulose structure seen in Figure 2.5 is composed of repeated D-anhydroglucose molecules, in which the glucose components are composed of six-membered chains known as pyranoses. C1 of one pyranose ring is linked to C4 of another pyranose ring, forming a β1-4 glycosidic bond. β1-4 glycosidic bond in cellulose gives both stability and a stretched structure resembling a ribbon. The alternating pyranose chains are joined at 180° angles and create hydrogen bonds between both the monomers of the same fibrils and also with the monomers of adjacent fibrils. Van der Waal forces and intra-molecular hydrogen bonds in between hydroxyl and oxygen of monomers lead to parallelism stacking of cellulose molecules, resulting in the production of microfibrils with a diameter of 5-50 nm [57]–[59]. A highly structured distribution of cellulose chains forms the crystalline portion of cellulose fibrils, whereas disordered configurations of cellulose chains constitute the amorphous area of cellulose fibrils.

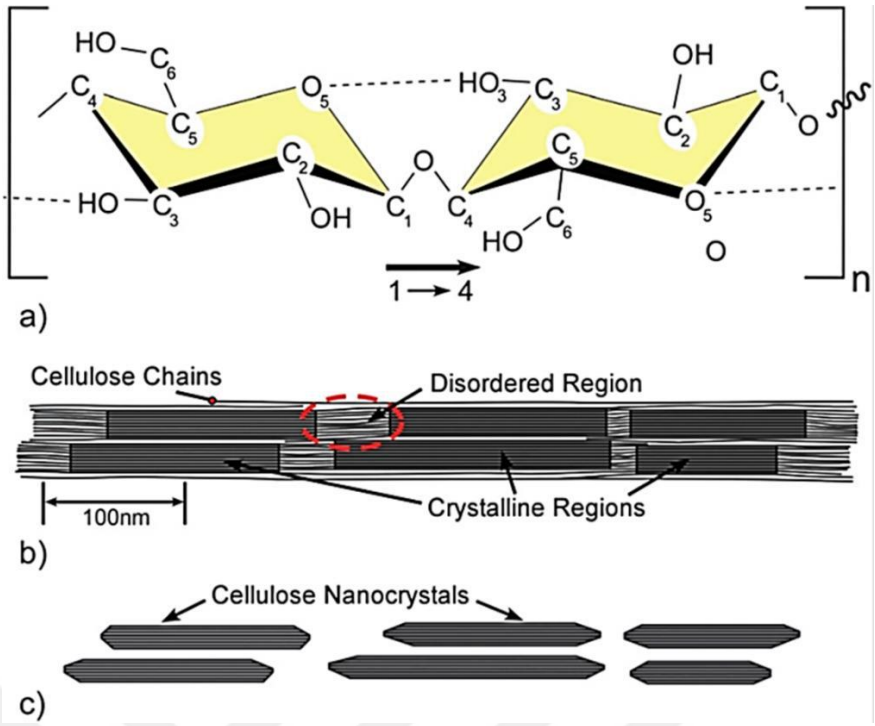

Figure 2.5 Cellulose structure: (a) chemical structure, (b) amorphous and crystals areas, and (c) cellulose nanocrystals [60]

2.3.1 Nanocellulose Categorizations

Generally, several forms of cellulose-based particles are employed, and they are commonly referred to as cellulose nanoparticles (CN) [12]. Numerous cellulose-based nanoparticles with at least one individual nanoscale dimension have been accorded this term. Microcrystalline cellulose (MCC), microfibrillated cellulose (MFC), nanofibrillated cellulose (NFC or CNF), cellulose nanocrystal (CNC) particles, and bacterial nanocellulose (BNC) are the most often utilized cellulose nanoparticles [12]. The formation of nanocellulose from plants is shown in Figure 2.6(a). Acid hydrolysis can be used to synthesize CNC. In this mechanism, as illustrated in Figure 2.6(b), the strong acid may remove the amorphous zone while preserving the nanocrystals in cellulose [19], [61], [62]. CNF is produced by mechanically treating cellulose, and its inner structure encompasses both crystalline and amorphous states [63], [64]. Due to the fact that the crystallinity of BNC is produced by bacteria between common high plant fibers and animal fibers, as seen in Figure 2.6(c), its manufacturing [61], [65] consists mostly of bacterial fermentation and purification. The variation in size, surface chemistry,

and crystallinity of these cellulose nanoparticles may be the consequence of a variety of variables, including their intrinsic features and extraction techniques.

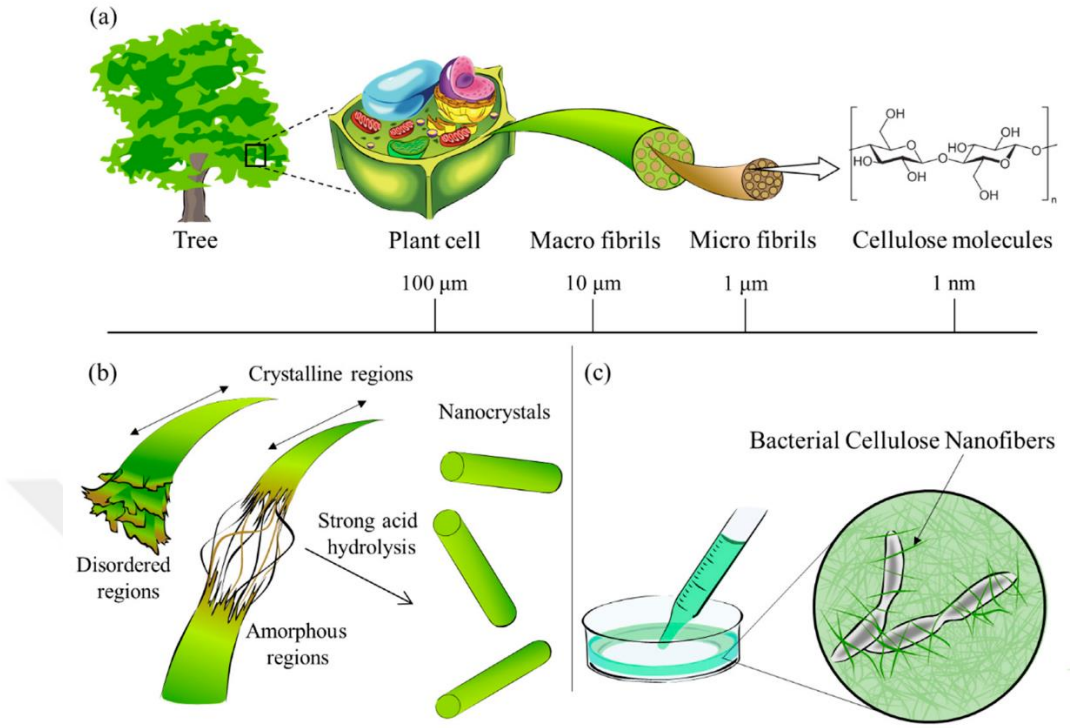

Figure 2.6 Process for manufacturing nanocellulose (a) The microscale to nanoscale structure of cellulose obtained from plants; (b) the extraction procedure of cellulose nanocrystal; and (c) the synthesis of bacterial nanocellulose [66]

2.3.2 Cellulose Nanocrystal (CNC)

Cellulose nanocrystals (CNC) nanoparticles are nanorods produced from cellulose by dividing the amorphous phases of the nanofiber presented in Figure 2.7 [67]. Bondeson et al. [68] produced CNC by acid pretreatment after dissolving wood pulp or cotton with sulfuric acid at a concentration of 65%. CNC currently on the market has a rod-like shape with a diameter of around 5 and 10 nm and a length less than 300 nm. In recent years, its mechanical, optical, and surface characteristics have been well described [69]–[71]. It provides superior strength and elastic modulus, as well as being lightweight, nontoxic, chemically modifiable, and, unlike most other nanomaterials, is biosourced sustainably and very affordable. According to Dufresne (2012) [72], the cellulose molecule contains an exceedingly complicated hydrogen-bonding network with numerous isotropic and anisotropic phases. In an isotropic phase, the substructure of cellulose, which can be called fibrils, is aligned in the same direction, however, in an anisotropy phase, numerous

layers of isotropic phases produce a fibril layer with varied orientations [69]. This is crucial because the isotropic and anisotropic aspects affect their ultimate size and aspect ratio. This combination of properties makes it desirable not just as an additive, but also for nano-engineering cement-based systems. It is proposed that CNCs can provide new opportunities for cementitious composites with improved mechanical performance. The small size of CNCs allows for reduced interfiber spacing, more interactions between cellulose and the cement system, and as a result, CNCs have a greater potential to alter micro-cracking and can increase the system's strength [15]. Recently, it was shown that CNCs enhance the flexural strength of cement composites by increasing the degree of hydration (DOH) [15], which may be facilitated by a phenomenon known as short circuit diffusion (SCD). The fundamental need for SCD is the adsorption of CNCs on the surface of cement particles, which acts as a channel for the preferential transfer of water from pores to unhydrated cement cores. In addition, when CNCs are combined with superplasticizers (SP) in cement, the SP will promote the hydration of cementitious composites by facilitating the dispersion of cement particles via space stabilization. Due to the potential difference, however, CNCs may be adsorbable on cement particles. A high concentration of CNCs hinders cement particle interaction with water, hence delaying hydration [16], [73], [74]. In addition, during later phases of hydration, the SCD impact decreases and the steric stabilizing action of SP becomes the predominant factor. Figure 2.8 depicts the combined effect diagram [75].

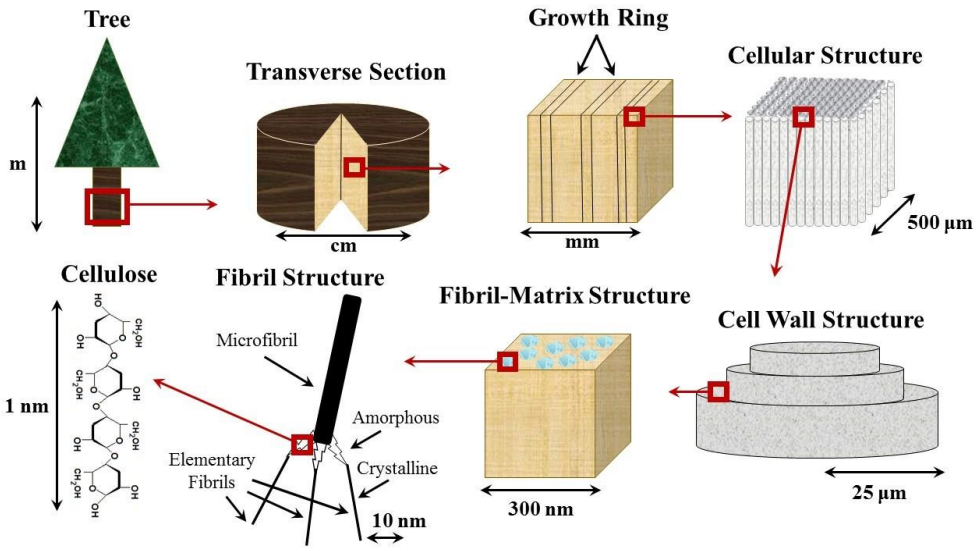

Figure 2.7 A graphical representation of CNC hierarchy [72]

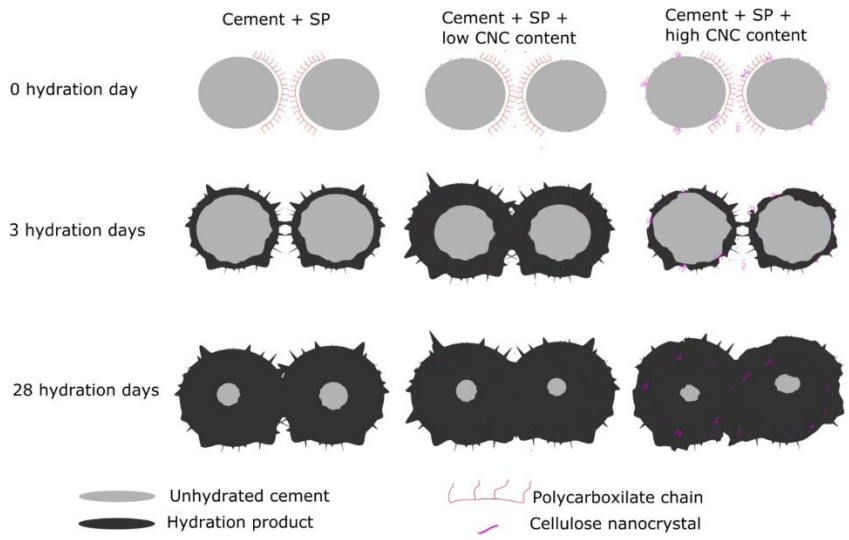

Figure 2.8 On the hydration of cement, the combined action of steric stability of superplasticizer and short circuit diffusion of cellulose nanocrystal [75]

2.4 Nanosilica (Nano-SiO_2)

NS is a white amorphous powder with a typical particle diameter between 10 and 100 nm [76], [77]. The structure of NS, as seen in Figure 2.9, indicates that each silicon atom makes single covalent connections with four oxygen atoms to create a tetrahedron [79]. It has a three-dimensional chain structure at the molecular level. It possesses saturable chemical bonds and hydroxyl groups in various bonding phases [80], and also, its molecular and structural formulae are identical: SiO_2.

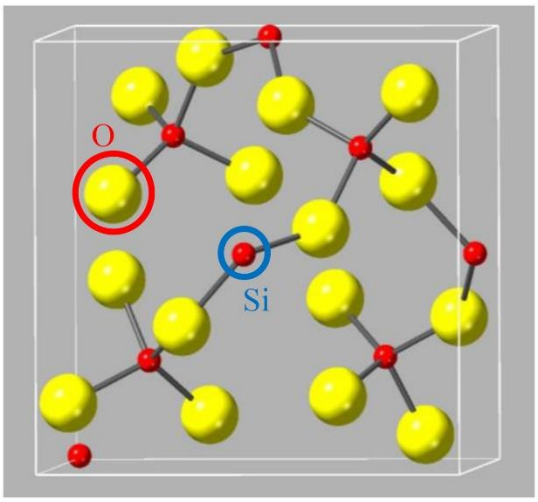

Figure 2.9 Crystal structure of NS [81]

NS and silica fume (SF), which are classified as inorganic materials, may greatly enhance the pore structure due to their filling action, a good influence on hydration, and favorable microstructure [82]. Recent research indicates that hydrothermal SiO_2 nanomaterials can accelerate the rate of clinker mineral hydration by 20–30 % [83]. Due to its pozzolanic reactivity and tiny particle size (the nanoparticles may fill the crevices between particles of C-S-H gel, functioning as a nano-filler), NS can increase the compressive strength of cement-based materials and make the microstructure denser [84]–[86]. According to a prior study [34], SF and NS are also novel types of surface protection materials. This is due to the fact that SF and NS can increase chloride penetration resistance, hence enhancing the corrosion resistance of concrete. SF may bring a higher level of reactivity; so, it has a stronger hydration acceleration impact than NS [87], [88] As illustrated in Figure 2.10, when an enough quantity of NS fills the gaps among the cement particles, the free water in the voids may be released, hence enhancing the fluidity of the cementitious materials. The smaller NS agglomerates tend to displace the surrounding cement particles and absorb a proportion of the free water, resulting in an expansion of the voids inside the cement particles. Yet, when the dose of NS is too high and cannot be adequately disseminated, since NS has a high specific surface areas and surface energy, its flocculation action will form big aggregates that cannot fill the space among cement particles, however, it will absorb a substantial quantity of free water. Rapidly increasing cement paste viscosity causes agglomeration of cement particles and a decrease in cement paste's fluidity [81].

A prior work [89] has shown that NS pozzolanic reaction products are more compact than silica fume products. In addition, it was determined that nanoSiO_2 may reduce the water absorption of hardened cement mortar by using either its strong pozzolanic reaction or its filling impact on the surface of the mortar. In a separate study [90], NS is able to fill the pores among the aggregates and hydration productions, hence enhancing the ITZ's density. NS can simultaneously promote the cement hydrations and have a reaction with $Ca(OH)_2$ (Figure 2.11) to raise the C–S–H gel concentration, optimize the pore structure, reduce the aggregation of $Ca(OH)_2$ crystals in the internal interface, and enhance the $Ca(OH)_2$ crystals to achieve a column-shaped morphology with skeleton-supporting ability. Therefore, it can enhance ITZ compaction [81]. additions of up to 5 % NS had a deleterious effect on the microstructure of cementitious composites. The integration of

NS refines the pore structure and decreases the pore volume of cement pastes containing ultra-high volume fly ash, according to a more recent study [91]. Similarly, microstructural experiments conducted by Sikora et al. [92] indicated that NS has a considerable effect on the pore properties of concretes, resulting in denser and stronger microstructures. Several research have indicated that 1 % NS is the optimal amount to improve the mechanical characteristics (compressive and flexural strength) of the cement-based materials matrix [93]–[96]. NS has also been demonstrated to increase the longevity of the matrix by decreasing its water absorption, capillary absorption, rate of water absorption, coefficient of water absorption, and water permeability relative to conventional concrete [84]. It has also been shown that the inclusion of silica nanoparticles dramatically decreased chloride ion penetration [97].

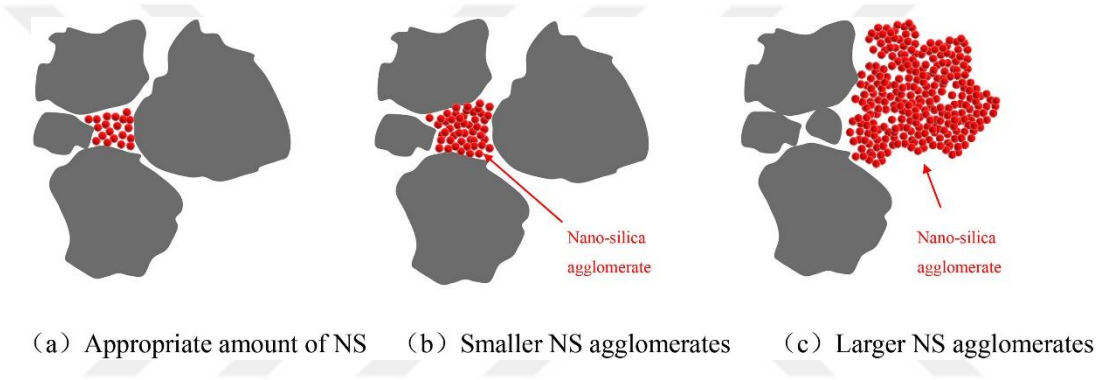

Figure 2.10 NS effect in filling between cement particles [81]

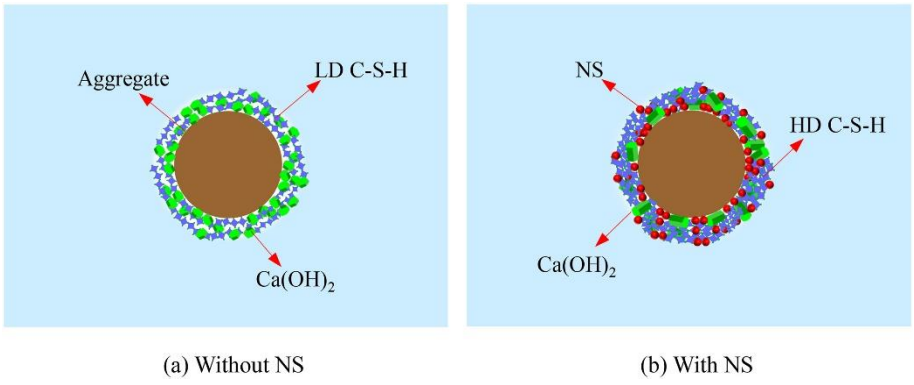

Figure 2.11 A schematic diagram presenting the impacts of NS on cement-based materials ITZ [81]

3
MATERIALS AND METHODS

3.1 Materials and Mixing Designs

This section describes the properties of the physical and chemical materials that were used in this study as well as explaining the mixes proportions of the productions. In this study, cement mortar was prepared to examine the mechanical properties for nanosilica as well as nanocrystals cellulose samples. Several tests have been studied to ensure their effects and quality before using them in mixtures.

3.1.1 Materials

Standard sand was used according to TS EN 196-1 (Figure 3.1b). In order to obtain a workable mortar with low water amount, a polycarboxylate based superplasticizer (Plastol Ultra 218) was employed in all mixtures (Figure 3.1c). OPC, CNC, and NS properties are explained in the following sections.

3.1.1.1 Ordinary Portland Cement (OPC)

In the experimental study, Portland cement (OPC) CEM I 42.5 R has been used (Figure 3.1a). Chemical and physical properties of OPC are shown in Table 3.1 The X-ray diffraction (XRD) analysis for OPC presented in Figure 3.2. It identified the main phases: C_3S, C_2S; and the minor phases C_4AF, C_3A, and CSH_2 [98].

3.1.1.2 Cellulose Nanocrystals (CNC)

Cellulose nanocrystals (CNC) were brought from CelluForce NCC® XRF results are presented in Tables 3.1 and 3.2. Zeta potential examination has been performed using Malvern Zetasizer device, the results of CNC was -41.9 millivolts (mV) with nano size distributions of 203 nm. Upper positive or a negative zeta potential higher than 30 mV results to a better stability of colloidal. With a lower zeta potentials absolute value refers to colloids tendency to agglomerate [15]. CNC patterns are presented in Figure 3.3a, are consistent with the crystal structure of cellulose-1β (PDF# 00-056-1718 from the International Centre of Diffraction Data). Segal's method [99] in Equation (3.1) was used to compute the crystallinity index of the CNC based on their XRD patterns. CNC had an

estimated crystallinity of 88.2%, indicating that more amorphous regions of CNC have been removed during their preparation as it confirmed in scanning electron microscopy (SEM) image for CNC in Figure 3.3b. Similar values were reported in Ref. [100] for CNC from CelluForce.

$$Crys.I = \frac{I_{002} - I_{am}}{I_{002}} \times 100 \quad (3.1)$$

3.1.1.3 Nanosilica (NS)

As it known in general, micro grains of hydrated calcium silicate gels, nanoscale of individual pores, capillaries pores, and large-sized crystals produced from hydration process are the compositions of normal cement pastes. Wherefore, nano-sized materials should occupy the pores in the cement paste. For this, NS has the ability with its amorphous phases to make a significant benefit for cement mixes. NS most beneficial property is the pozzolanic reaction that performed with calcium hydroxides in the production of calcium silicates hydrations.

Nanosilica (NS) was obtained from Nanografi company. XRD for NS are shown in Figure 3.4a expressing the diffraction peaks of NS amorphous and purity of to 99.5 + % in SiO_2 at 22º with low index of crystallinity, and a similar has been shown in Scanning electron microscopy (SEM) image for NS (Figure 3.4b). The zeta potential of NS was measured and results in -8.94 mV with a nano size distributions of 391 nm. which indicates the NS highly agglomerated clusters.

Figure 3.1 a) Portland cement (OPC) CEM I 42.5 R, b) Standard sand, c) Polycarboxylate Superplasticizer (SP)

Table 3.1 Chemical and physical properties of cement (OPC)

Chemical Properties			
Compositions (%)	**OPC**	**NS**	**CNC**
CaO	81.5	0.3	5.6
SiO_2	5.3	97.7	-
Al2O_3	0.3	-	-
Fe_2O_3	5.9	0.5	2.4
MgO	1.6	-	-
Na_2O	-	-	-
K_2O	1.1	-	-
SO_3	2.6	-	52.8
PdO	-	-	22.4
Loss on ignition	1.7	-	-
Physical Properties			
Specific surface area m^2/g	0.378	150-550	400
Bulk density g/cm^3	3.1	<0.1	0.7

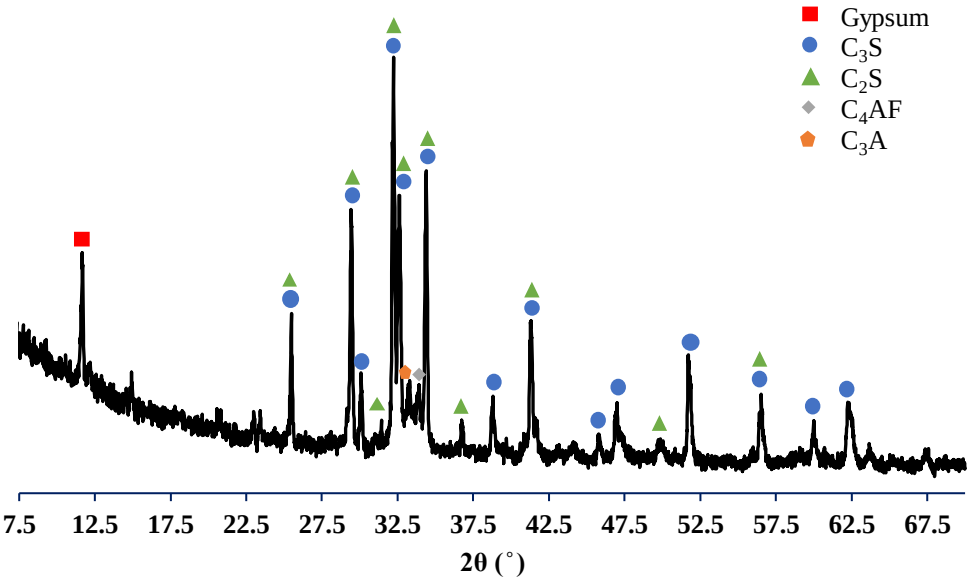

Figure 3.2 X-ray diffraction (XRD) of Portland cement (CEM I 42.5 R)

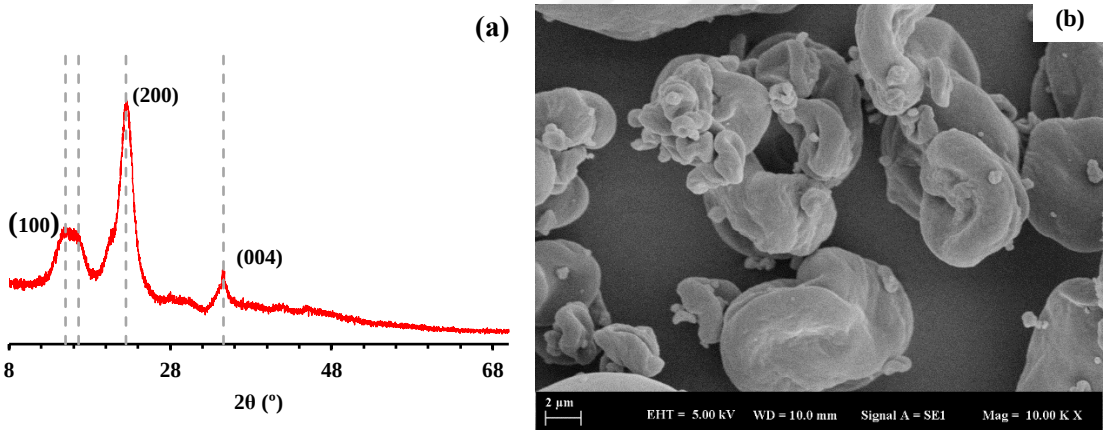

Figure 3.3 a) XRD of cellulose nanocrystals (CNC), b) SEM image for CNC

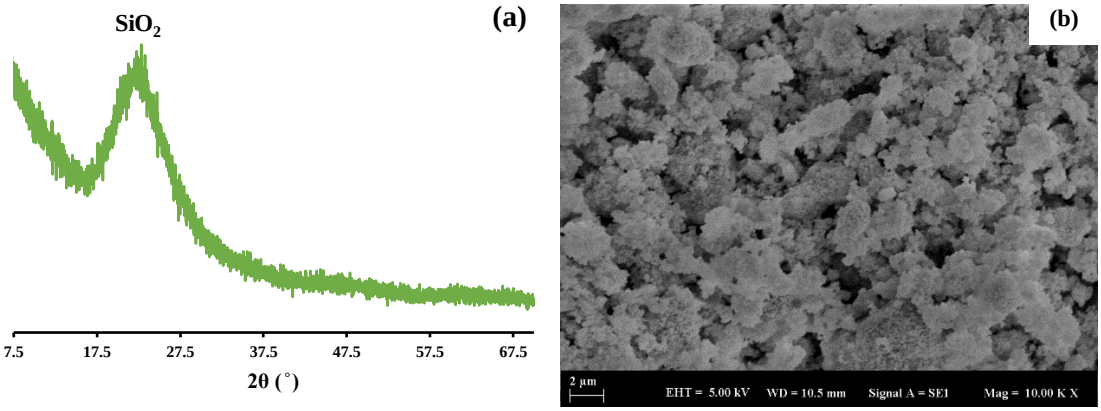

Figure 3.4 a) XRD of nanosilica (NS), b) SEM image for NS

3.1.2 Mixing Designs

Mixing has been done according to ASTM C305 [101]. NS and CNC have been added to the mixtures by mass of cement. According to the experiments applied in this study, pastes and mortars mixing was used. In Figure 3.5'a and Figure 3.5b paste mixer and mortar mixer respectively given. The w/c ratio was different for paste and mortar samples depending on the test performed for samples and it will be explained in methods and testing of this study. Mix proportions mixture and codes are given in Table 3.2.

Table 3.2 Mix Proportions and Mixture Codes

Samples names	Water (g)	OPC (g)	Sand (g)	NS (%)	CNC (%)	SP (%)
OPC	225	450	1350	-	-	1.2
CNC0.25	225	450	1350	-	0.25	1.2
CNC0.50	225	450	1350	-	0.50	1.2
CNC0.75	225	450	1350	-	0.75	1.2
NS0.25	225	450	1350	0.25	-	1.2
NS0.50	225	450	1350	0.50	-	1.2
NS0.75	225	450	1350	0.75	-	1.2

Figure 3.5 a) Kitchen mixer for paste preparation, b) Mortar mixer

3.1.3 Preparation of CNC and NS Liquid Suspensions

Both materials were prepared as liquid suspension by the biotechnology lab. in the Chemistry-Metallurgy Faculty Yildiz Technical University. CNC's and NS's suspensions have been prepared in 0.25%, 0.50%, and 0.75% dosages by the weight of the cement. CNC powder brought from Canada and produced by CelluForce company. The CNC powder was extracted from wood fiber and has been reported from the source. NS powder brought from Nanografi company with purity of 99.5+%. As mentioned before in the literature and the general information sections of this study, the use of nanomaterials in their liquid state instead of using them in the powder form is in order to avoid particles agglomeration of these materials in cement mixtures. The use of nanomaterials in their suspension state in mixtures allows the particles of these materials to diffuse well in cement mixtures, which gives the opportunity for the particles of these materials to distribute uniformly over the entire mixture.

The CNC and NS powders have been mixed individually with distilled water using high speed mixer for 10 mins. The mixes then been placed in ultrasonic bath for 30 mins. After the preparation of the CNC and NS suspension state, it was incorporated in the cement mixture for further tests in this study. The process of CNC and NS suspensions preparation was explained as schematic as presented in Figure 3.6.

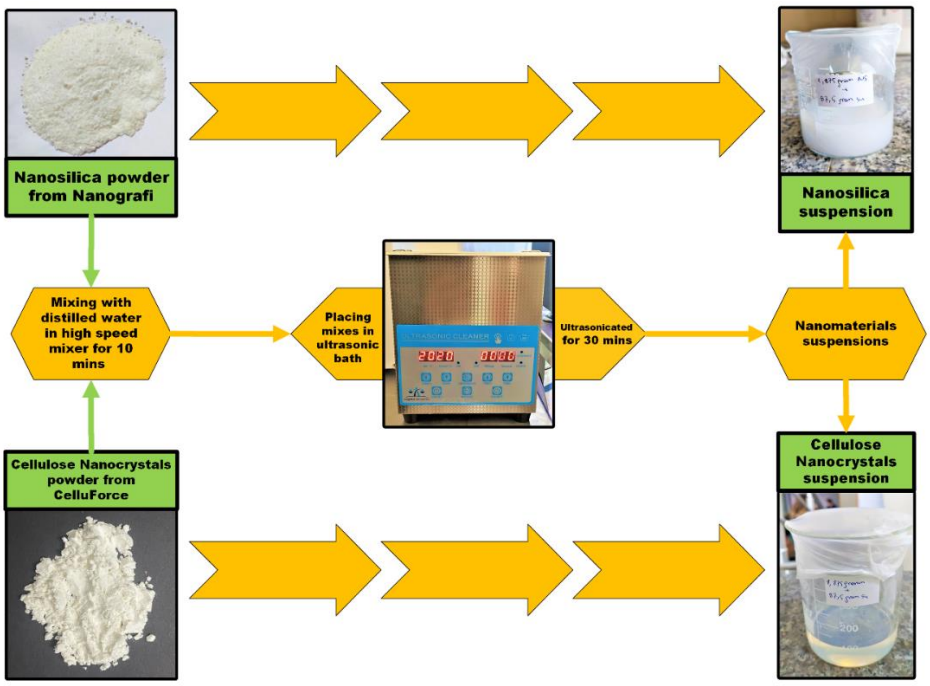

Figure 3.6 A schematic presenting the preparation process of CNC and NS suspensions

3.2 Methods and Testing Procedures

In this section, sample preparation and testing methods has been listed. Testing was applied starting from examining the fresh state of samples, then determining the mechanical strengths and behavior of samples, and lastly the microstructure tests were performed to ensure the effectivity of the additive materials in cement mixes.

3.2.1 Flow Table

In examining the mortar consistency, the flow behavior of plain mortar samples has been measured using a flow table disc with mold and tamping rod (Figure 3.7a) according to the ASTM C1437 standard [102]. This test was performed to analyze the effects of CNC and NS on the flow behavior of mortars. The mixing proportions of this test were the same as mentioned in this study, with the same addition of CNC content in its groups and similar to NS groups, and the w/c of this test was fixed at 0.50. The flow behavior was distinguished from the mortar diameters that were measured in both horizontal and vertical directions (Figure 3.7b) in each mortar using a flow table disc after the standardization of the vertical impacts. According to ASTM C1437 [102] an acceptable flow of 110 ± 5% with 25 drops in 15 s. specifies an acceptable flow of 110 ±5% with 25 drops in 15 seconds. The average of the two different diameter measurements has been considered for all mixtures.

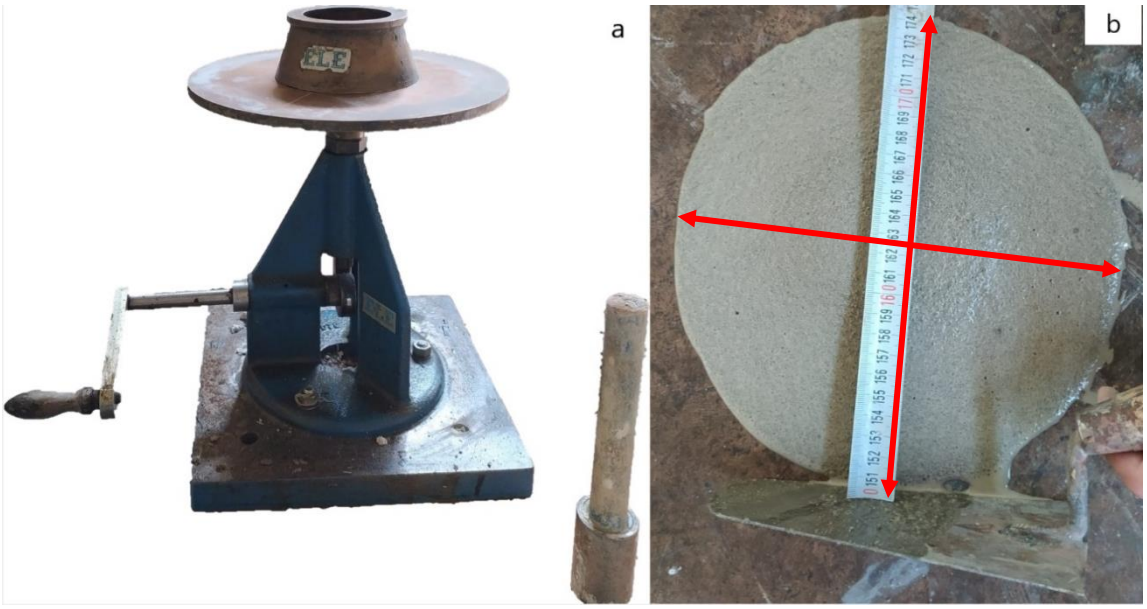

Figure 3.7 a) Flow table device with tamping rod, b) flow diameter measurements

3.2.2 Setting Time

A setting time test was applied to determine the initial and final setting time of cement-based samples. The test was performed on cement pastes with the NS and CNC groups individually. The samples were prepared using kitchen mixer as shown previously in Figure 3.5a. The mixing proportions of this test was the same as mentioned in this study with same addition of CNC content in its groups and similar to NS groups excluding the addition of sand and SP, and the w/c of this test was fixed in 0.35. The mixture then poured in a conical mold and placed into Vicat device (Figure 3.8a) and fixed as the needle penetrate the fresh mixture continuously by the time that was runs to penetrate every 10 min. After the hardening of the mixture where the finial setting time starts, the readings were collected, and the initial and final setting times were measured according to ASTM C191 [103].

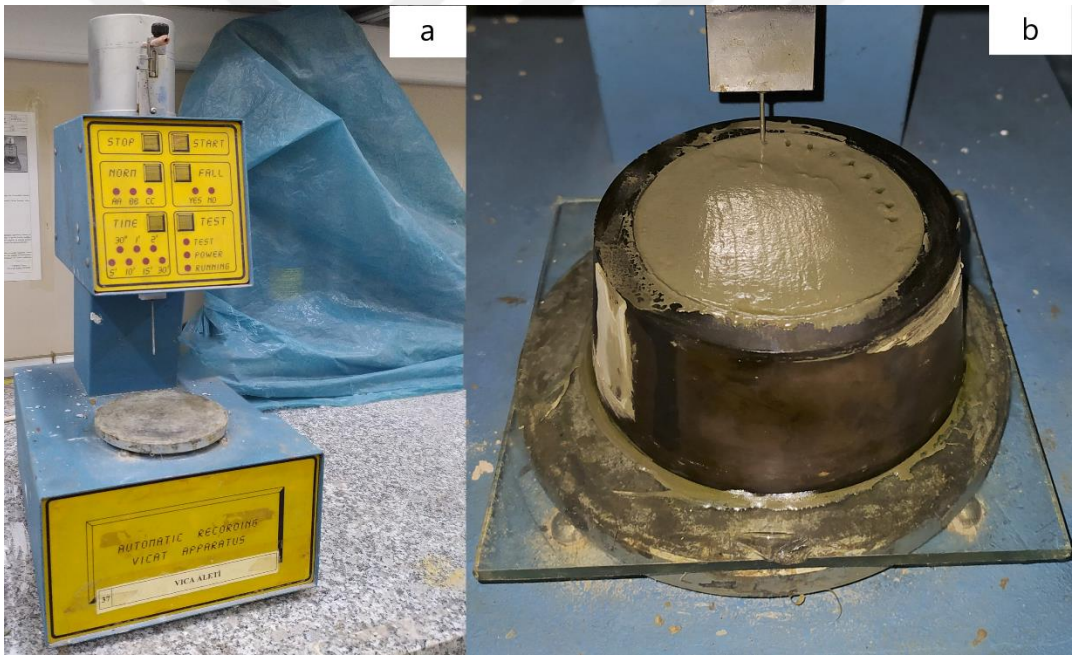

Figure 3.8 a) Vicat apparatus, b) conical mold

3.2.3 Rheological Measurements

The goal of using rheological measurements is to quantify the rheological properties of cement paste in its fresh phase with varying CNC and NS contents addition. The rheological measurements were performed using rotational rheometer device (RheolabQC) provided by AntonPaar as shown in Figure 3.9a. Cement pastes were used to be examined in this test with the addition of CNC and NS. The w/c ratio was used as

0.40, and the CNC groups were added by 0.25, 0.50 and 0.75% by the weight of cement, similar was applied to NS groups. A kitchen mixer was used to prepare the paste samples (Figure 3.5a) and the mixing of samples was according to ASTM C305 [101]. After mixing samples were poured in cylindrical cup with the ensuring of air voids removal. Vane stirrer was used in quantifying the rheological measurements as shown in Figure 3.9b. The rheological parameters of CNC or NS mixtures, such as plastic viscosity and yield stress, were determined using the rheological parameters of CNC or NS contained paste mixtures, such as plastic viscosity and yield stress, were determined using a strain-controlled mechanism. The rheological procedure performed is given in Figure 3.9 (c). Immediately after the completion of the standard paste mixing, the rheological procedure was started to be applied at a constant temperature of 20 °C. The rheological procedure was started by applying a pre-shear of 30 seconds at a shear rate of 100 s^{-1} in order to obtain a homogeneous mixture and to eliminate air bubbles, and then immediately the mixture was rested for 30 seconds. The experiment was then completed by gradually ramping up the shear rate value from 0.1 to 100 s^{-1} so that each shear rate stage would be 20 seconds, and likewise gradually ramping down from 100 to 0.1 s^{-1}. The yield stress and plastic viscosity values of CNC and NS contained paste mixtures were calculated using the Modified Bingham model as shown in Equation 3.2, which contains a second-degree term proportional to the shear rate.

$$\tau = \tau_0 + \mu \times \dot{\gamma} + c \times \dot{\gamma}^2 \tag{3.2}$$

In the modified Bingham equation, τ represents the shear stress, τ_0 denotes the yield stress (Pa), μ was the viscosity, and shear rate denotes $\dot{\gamma}$. Furthermore, the rheological index (c/μ) value is used to study the nonlinear behavior of fresh mixtures. If this value takes positive values, the shear thickening, and when it receives negative values, the shear-thinning behavior occurs in the mixtures.

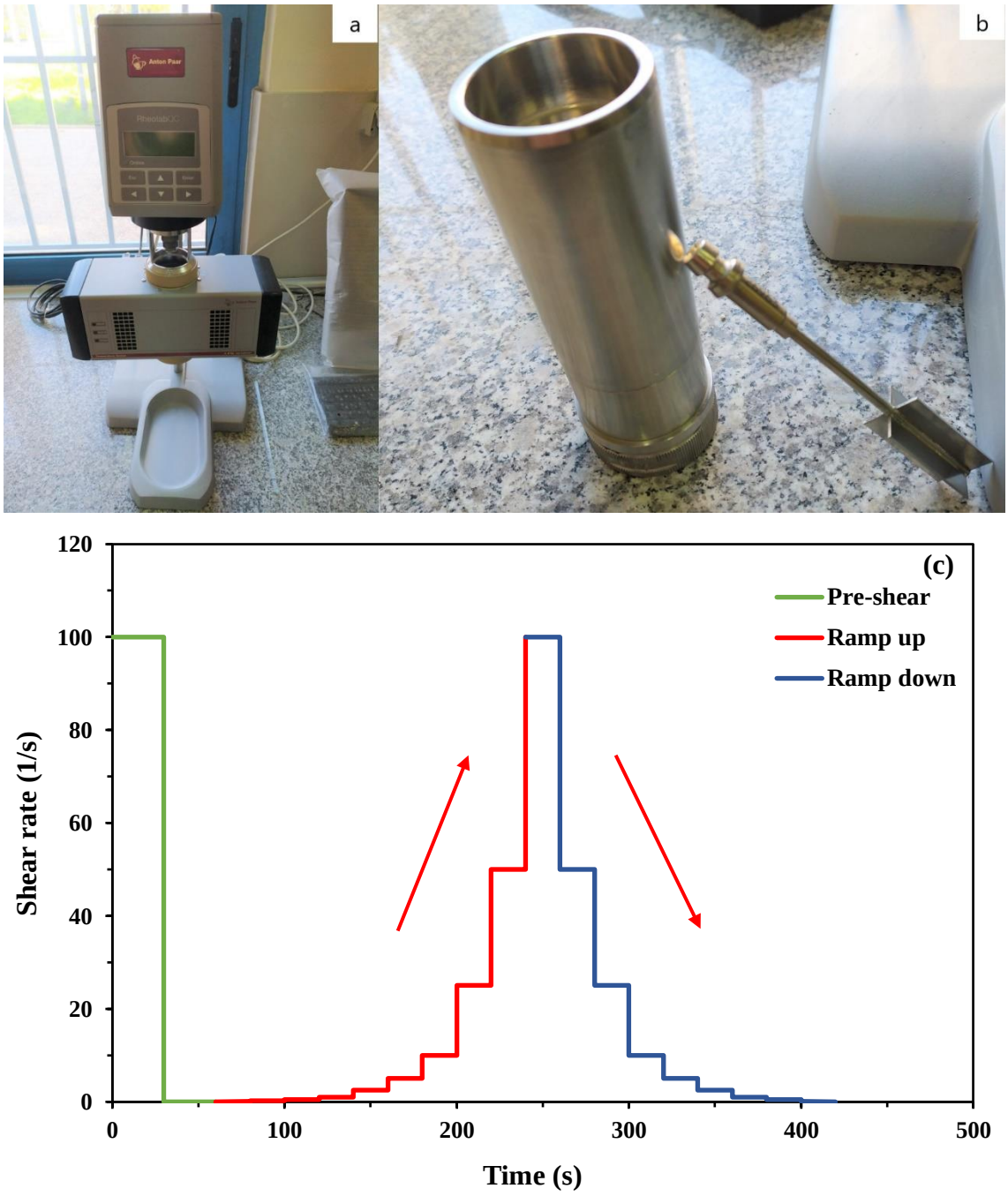

Figure 3.9 a) Rotational rheometer, b) Vane stirrer with circular cup, c) applied rheology procedure

3.2.4 Compressive Strength

Mechanical performance has been examined for the mortar samples using compressive strength test. Three cubes of 50 mm cement mortars for each series were prepared, and the mixed proportions of mortars mentioned previously was applied in this test with adjusting w/c by 0.50. The mixture was casted and vibrated in the molds (Figure 3.10a)

after that, it was covered by cling film sheet (Figure 3.10b) to avoid evaporation of water, then it was stored in a temperature room at 20 ± 2 °C and within 24 ± 0.5 h for hardening. All samples placed into the moist cabinet (Figure 3.10c) were kept at 20 °C with 55% RH until the testing days (3, 7, 28, and 90 days). Cube samples of mix groups used in this study are shown in Figure 3.11 in its 90th day before testing. Samples were tested according to ASTM C109/C109M [105] using ALŞA company hydraulic test device. Compressive strength has been calculated by taking the average of three samples for each series. The samples were subjected to a compressive load with a loading rate of 4 mm/min.

Figure 3.10 a) Plastic mold (50 X 50 X 50 mm), b) molded mortars samples cover by cling film sheet, c) moist cabinet

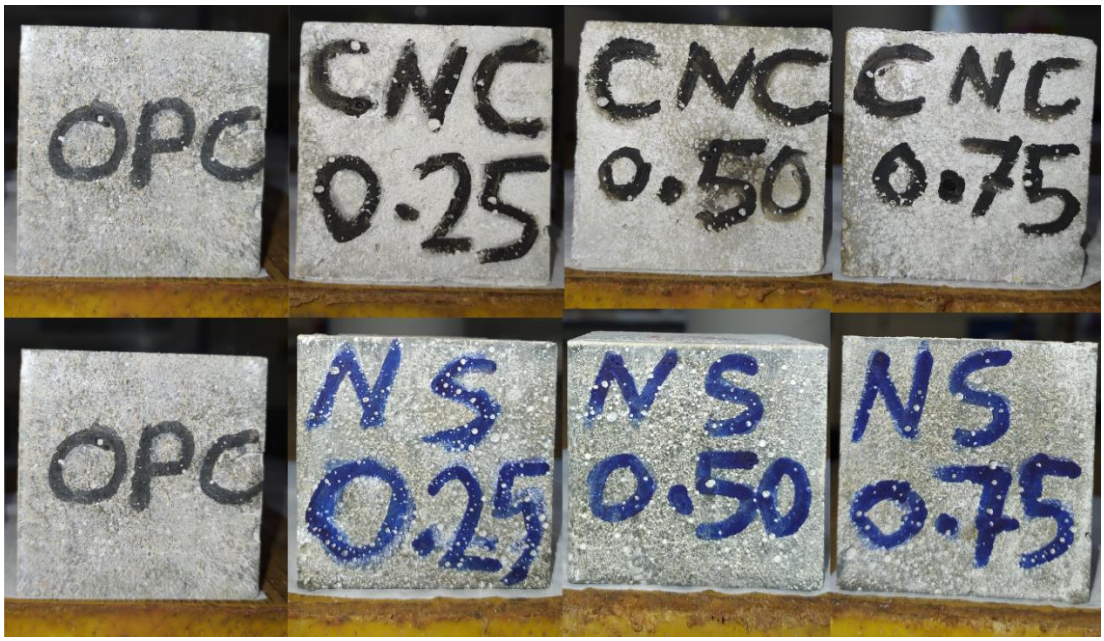

Figure 3.11 Mortar cubes of OPC, CNC0.25, CNC0.50, CNC0.75, NS0.25, NS0.50, and NS0.75

3.2.5 Water Absorption

The water absorption test was applied according to ASTM C642 [104]. For each mixture three cube specimens with dimension 50x50x50 mm were produced and the w/c was fixed to 0.50. After the standard curing of these samples for 28 days, the samples were prepared to be tested for water absorption test. Firstly, after samples were weighed individually, they were placed in oven with temperature 110 ± 5 °C for 24h (Figure 3.12a). The dry weight was taken for all samples after 24h of drying oven, and then the samples placed in water again for 48h ±5h to calculate the saturated weight after immersion. The samples, then removed from water and the surface was dried from moisture with towel and weight of samples was determined for this phase. After samples immersion in water, the samples were taken and placed to be boiled for 5h (Figure 3.12b), with the finishing of boiling time, the samples allowed to be cooled for 14±4h and the weight of samples was measured again. Finally, the samples were immersed in water while hanging in the balance to be weighed for apparent weight (Figure 3.12c). The average of the three specimens were considered for all mixtures. Absorption after immersion and boiling (AIB, %) and the volume of permeable pore space (voids) (VPP, %) of mortars could provide a general information about the pore structure. These parameters have been calculated according to the Eqs. (3.3) and (3.4), respectively.

$$AIB, \% = \left(\frac{m_{sd} - m_{od}}{m_{od}}\right) \cdot 100\% \tag{3.3}$$

$$VPP, \% = \left(\frac{g_2 - g_1}{g_2}\right) \cdot 100\% \tag{3.4}$$

Here, m_{sd} is the mass of surface-dried sample in air after immersion; m_{od} is the mass of oven-dried sample in air, g; g_2 apparent density; g_1 is bulk density, dry.

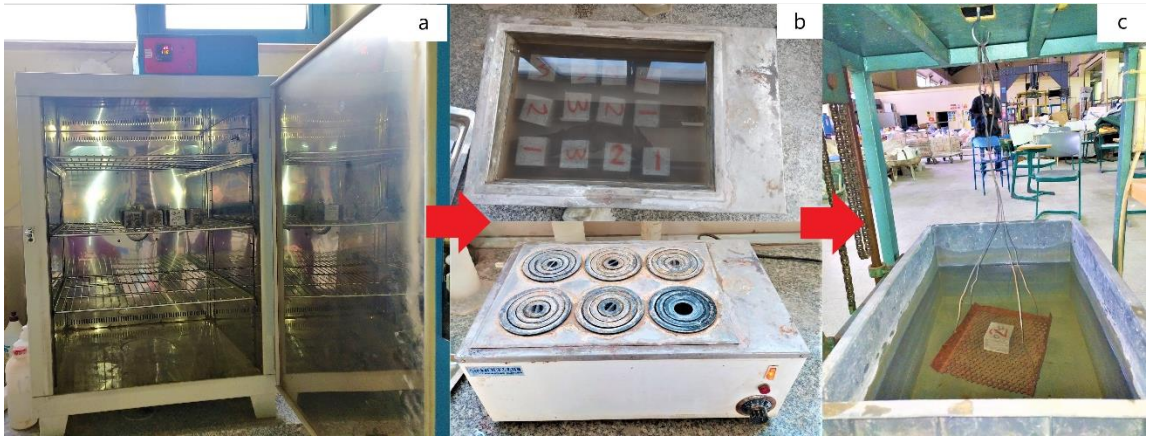

Figure 3.12 Stages of water absorption test a) standard drying oven, b) standard boiler, c) suspended weighing by immersing in water

3.2.6 Microstructure Performance

In the microstructure examination of this study, paste samples were used and the preparation was done by similar dosage used in this study for CNC and NS. The microstructure specimens were mixed with the same time of the mixing setting time examination specimens and the w/c was fixed by 0.35. The paste mixture was poured in Falcon® plastic tube (Figure 3.13a) and placed in cap to ensure it hardening and left to be stored in moist cabinet with 20 ºC and 55% ±5% relative humidity (Figure 3.11c). All the mentioned above is applicable for microstructure tests of this study (MIP, TGA, XRD, SEM-EDS).

3.2.6.1 Mercury Intrusion Porosimetry (MIP)

MIP examination was used to test the pore structure of samples and their distribution. After 28 days, the samples were removed from tube to be cut at the required aspects with the neglecting of edge and surface to avoid any cases reflecting on the results of the test. 4-8 pieces were extracted from mixtures (OPC, CNC0.25, CNC0.50, CNC0.75, NS0.25, NS0.50, and NS0.75) to be sliced with size between 3 to 5 mm avoiding large slices that may corrupt the results of the testing. The slices then placed in oven at 100 Cº temperature (Figure 3.13b). The collected pieces of each group were brought to the center lab of Yildiz Technical University to be examined in MIP test. The details reported that the device used was Quantachrome by AntonPaar company. The Pressure range set between 0.007-411 MPa that led to indicate the pore diameter approaches in 210 µm to 4 nm. The Hg surface tension was 0.48 N/m, and the contact angle of Hg was 140°.

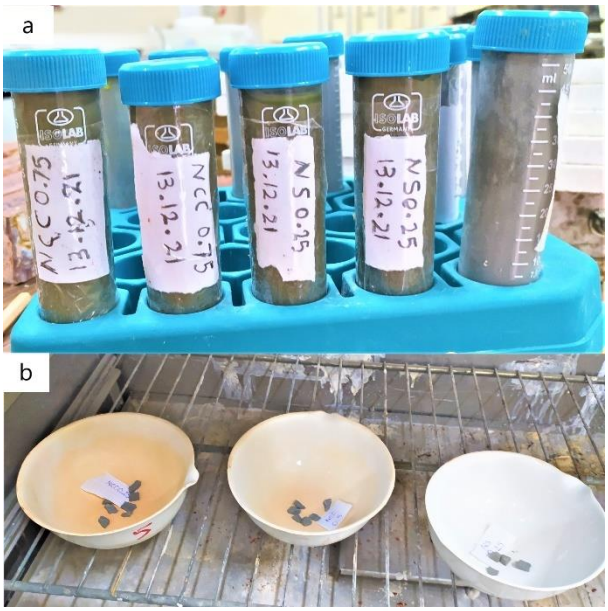

Figure 3.13 a) Falcon plastic tube with cap b) part of MIP samples prepared to be dried in the oven

3.2.6.2 Thermogravimetric Analysis (TGA)

TGA was used to evaluate weight loss and relative heat flow. Paste samples were prepared for the TGA analysis. In the 7th and 28th day of samples, the hardened pastes have taken off from the tube, then small amount was cut for each sample in its specified days with taking care not to consider the surfaces while extracting the sample for testing to neglect any moisture condensations effects, then ground into powder with using of mortar and pestle. Sieve no. 200 (75 μm) was used for the powder with a small sample of 15 to 25 mg in size. The analysis was done using Exstar TG/DTA 6300 instrument. The first derivation of the curve (DTG) for each sample was obtained to find the limits of the temperature ranges. It has been heated at constant rate of 10 ºC/min from ambient to 1000 ºC in an inert nitrogen atmosphere.

3.2.6.3 X-ray Powder Diffraction (XRD)

XRD was used in this study to examine the influence of CNC and NS addition on the hydration product chemical compositions. After 28 days of specimens mixing, the samples were taken from tube extracting XRD powder from each group. The sample that was pulverized, has been taken from the core of each specimen avoiding the surface to neglect any moisture condensations impacts. After that, it was pulverized using mortar and pestle to powder and similar to TGA the sieve no. 200 was used for the powder.

PANalytical X'Pert pro diffractometer system was used with 2θ and goniometer radius of 240 mm. The radiation sources used was Cu to determine the phase compositions. The scan parameters have an angular size between 6- 70 2θ, and step size of 0.0170 2θ with scanning step time of 30 s.

3.2.6.4 Scanning Electronic Microscopy (SEM) & Energy Dispersive Spectroscopy (EDS)

To study the microstructure development of the cement pastes with the addition of various amounts of CNC and NS, SEM-EDS tests were conducted. Firstly, the samples preparation started with removing the hardened pastes from the tube and then slicing pastes to pieces with aspects and flatness that ensuring then in impregnation process that the resin has covered the slices quite enough. To remove the free water, the slices were placed in drying oven.

Impregnation

The impregnation was done using a low viscosity epoxy resin presented in Figure 3.14a (Verpolboya mixing the A and B together). A cylindrical mold (Figure 3.14b) was used first to place the slice samples, and then poured the mixed epoxy in the mold and left to be hardened for 24h.

Polishing

After making sure the sample is hardened, the sample then removed from the mold and was marked with ink pencil from the top on each group's slice starting from OPC as 1 and ending with CNC0.75 as 7. Three SiC grinding papers were used P320, P500, and finally P1200. Firstly, it took 5-15 min for grinding the bottom part of the cylindrical sample removing the extra epoxy that covers the samples in bottom to make it flat (Figure 3.14e). At each time the sample was rinsed in ultrasonic bath (Figure 3.14d) to remove remains from the surface. After the border of slices revealed, the next is to polish the bottom of sample with diamond suspension of 1 μm and 6 μm, and lastly the sample has been polished with fumed silica 0.2 μm alkaline for final polishing (Figure 3.14c).

Testing

Once the polishing is done (Figure 3.14f), the sample has been stored in desiccator for 2 days before the testing day. In the testing day, the sample was prepared to be scanned by SEM. It was scanned by ZEISS microscopy (Figure 3.15) with 7 kV acceleration.

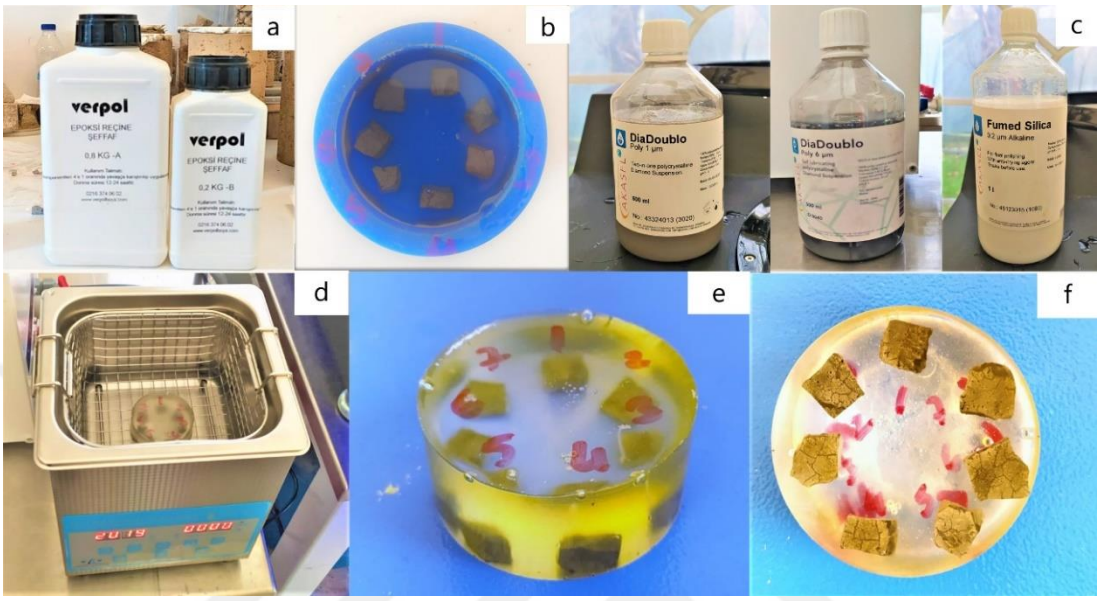

Figure 3.14 SEM-EDS sample preparation process a) Verpolboya two type epoxy resins mixture, b) Cylindrical mold, c) 1 µm and 6µm diamond suspension and fumed silica 0.2 µm Alkaline for polishing, d) Ultrasonic bath for residues removing, e) sample after removing extra resin from bottom, f) sample after polishing

Figure 3.15 ZEISS SEM-EDS device

4
RESULTS AND DESCUSSION

4.1 Fresh State Properties

In this section, the results of the flow tests conducted on the mortar samples and the rheology and setting time analyses conducted on the paste samples are examined in detail.

4.1.1 Flow Table Results

The consistency, which constitutes the flow properties and the workability for fresh mortars is presented in Figure 4.1 that shows the effect of CNC and NS on the flow table results of different batches using various amounts of CNC and NS in different mixes. To improve the deflocculation of nanoparticles, SP was used to enhance the free liquid phase performing as a lubricant and to regulate the distance among nanoparticles. On the other hand, CNC results show that the flow decreased in the increasing of CNC dosage for each group. It has decreased sufficiently from the reference sample in 0.25% and 0.50% content by 70 mm and 110 mm respectively and in 0.75% dosage remained constant. It implies the CNC has decreased the workability for all groups. Related results can be found in literature here where Lee and Kim [64] incorporated CNC in high-toughness cement composite (ECC) with the dosage of 0.4, 0.8, 1.2 vol% (cement vol%). They found from their results that the increasing of CNCs led to decrease the flow diameter [64]. With an agreement to previous studies the reduction in flowability with the addition of CNC increasingly are behind the property of hygroscopicity in absorbing and water retention which is related to the proportions between high water hydrophilicity and the increasing of CNCs in mixes, and that because of –OH combinations abundant on the surface. Similar results were conducted with Nassiri et al. [106] where they investigated the effect of inclusion CNC to cement systems, the findings of flow table results was like the CNCs reduced the flow diameter, particularly at concentrations above 0.035% wt. Another similar studies by Nasir et al. [107] where they studied three types of CNC, varied with crystallinity index, diameters, and lengths. CNC were incorporated from 0 to 1.5% by wt. of cement. The evaluation of flow table resulted in the flow of mortar gradually decreased with the addition of CNCs. They find the reason behind that with the inter-particle

resistance offered by the CNC because of their elongated morphology resulted in the reduction of the flow diameter in mixtures containing CNC. Lastly, the decrease in flow values among the investigated CNC is a result of their morphology and dimensions. The decrease in flow can be attributed to the smaller particle size, which increased the demand for water.

The findings for mixes containing NS indicate that the reduction in flow did not begin until NS0.50 compared to NS0.25. Following an increase in NS0.25, it declined by 20 mm in NS0.50 and stayed unchanged in NS0.75. If we notice that the NS decreases did not cause a notable change compared to CNC that conclude the NS has low effectivity in low quantities, that requires higher NS amounts to show an influence on flow table. Similar opinions regarding higher quantities of NS can be found in Senff et al. studies where they incorporate 3.5% and 7% of the contents of NS. They conducted the 3.5 % was 1.5 higher in flow diameter than 7% that mean in 7% content the flow diameter has been decreased and the mortar indicated a more cohesive property [108]. In other studies, it has been also found in inclusion of 1% of wt. NS has not indicated any significant effects in decreasing the flow diameter while using NS of 2% wt. and 3% of wt. as expressed a consecutive reduction of 9 mm and 12 mm compared to reference mix. In 3 to 4% dosages of NS have demonstrated higher decreasing in flow diameter (19 mm) with the increasing of NS between which have showed a significant decreases of the workability [74]. It is expected that usually a higher specific surface area in NS means an increasing in demand of water used in cement-based mixes, and that somehow makes impact on the workability.

As summarizing for the results above, it is obvious to us that the CNC dosage from lowest content (0.25% wt.) to highest content (0.75% wt.) of our studies have decreased the flow values gradually. Comparatively, NS had no significant effect on flow diameter when incorporated with low amount.

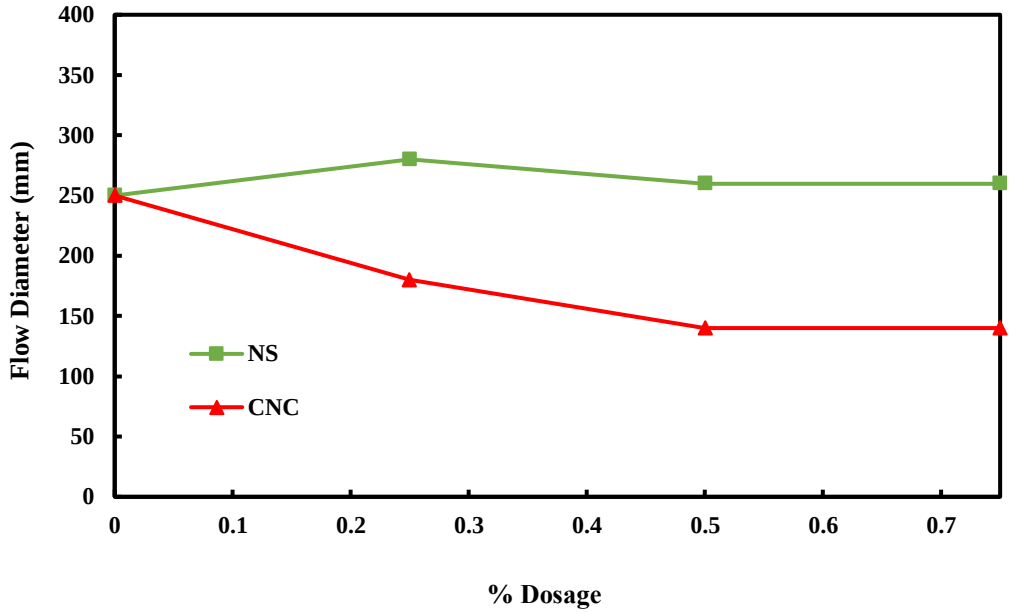

Figure 4.1 Flow diameter versus CNC and NS dosages

4.1.2 Setting Time Results

The results for initial and final setting time are presented in Figure 4.2 for selected samples containing CNC or NS compared to the OPC reference sample. As given in Figure 4.2, CNC delayed the initial setting time of the cement pastes between 30 and 60 mins. The delaying started in CNC0.50 sample, where the CNC delayed the initial setting time compared to reference by 30 mins, while the CNC0.25 showed no change in the comparison with control sample. CNC 0.75 showed the most delaying about 60 mins of reference. It is obviously showing the increasing of CNC dosage delaying the initial time. Concerning final setting time, all CNC contents showed a notable effect in delaying the final setting time than initial setting time. CNC0.25 final setting time was more than 1h from its initial time and that was no change in comparison to reference. CNC0.50 final setting time started approximately 2h after its initial time which is 1h more than final setting time of reference. The retarding effect on final setting time increased with the CNC0.75 started more than 2h of initial time and it was the most delaying content with approximately 2h from the OPC. It is concluded from the results that the more CNC inclusion the more delaying in setting time achieved.

These results in relative agreement with Nassiri et al. [106] where they tried to investigate with two nanocelluloses CNC and CNF on cement pastes. They reported the same

findings affected by CNC addition as it delayed both initial and final setting time in the increasing of CNC dosages, where the CNC playing as retarding admixture in cement mixture. Concerning CNF, they observed that it also delayed the initial and final setting time, but CNC showed a preferable setting retarder than CNF in depending on the dosage added to cement in both initial and final setting time. This effect disappears at higher concentrations, which might indeed have already aggregated, connecting cement hydrates together and causing the setting and hardening of the cement mixture [106], [109]. Jiao et al. [110] demonstrated that a higher concentration of TEMPO-oxidized CNC had a higher retarding effect, with a maximum delay of 91 minutes at 0.4 wt. percent.

In NS, the given Figure 4.2 present setting time results of cement pastes with different NS addition. It clearly shows NS shortened the setting in comparison to control mixture (OPC). This accelerating property of setting time is getting decreased by the increasing of NS incorporations to cementitious composites. Concerning the initial setting time, NS mostly achieved a reduction in the initial setting the in a NS0.25 by 60 min and then followed by a lower reduction in NS0.50 by 50 min all before the initial setting time of the reference mixture. After that we can see the disappearance of this property after the increasing of NS dosage by 0.75% (NS0.75) where it was seen increasing initial setting time by 10min beyond the reference mix. The same phenomena have been revealed in the final setting time, where NS accelerated the final setting time more than its effect on the initial setting time. The shortening of NS in cement mixtures started gradually from the lowest dosage of NS0.25 then followed by NS0.50 and NS0.75 within 70 mins, 50 mins, and 20 mins respectively in comparison to reference mixture. It clearly shows that NS property decreased with the increase of NS dosage, and it has showed higher shortening in final setting time. The explanation for these phenomena is due to the large amount of reactive unsaturated bonds in the combination of silanol groups on the top layer of cement mortar, the addition of amorphous NS as well decreases the setting time of cement mortar. These silanol groups exhibit high reaction toward CH (portlandite), resulting in the formation of a thick C S–H gel. Thus, the amorphous NS particles containing hydration products accelerate the hydration reaction [86], [111], [112].

In general, it was more obvious that CNC plays as retarding admixture, leading to delay the setting time of cement mixture in both initial and final setting time. This property was increased within the increase of CNC inclusion to cement mixtures. Comparatively, NS

played as the accelerating admixture in shortening the setting time of cement system. The NS property in accelerating the setting time was more to be seen in final setting time, while this property getting diminished within the increase of NS dosage into cement mixtures.

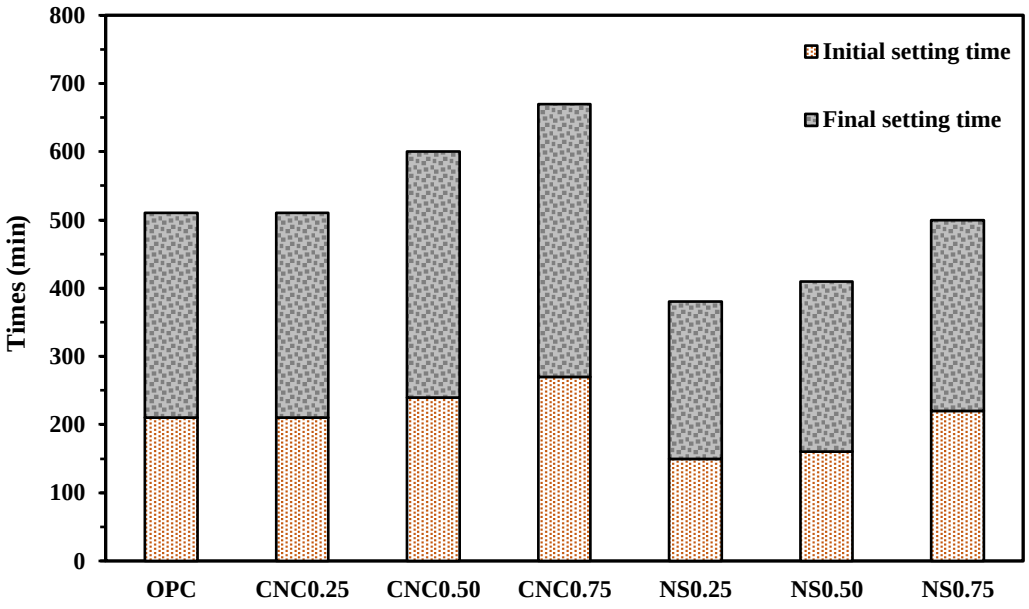

Figure 4.2 Setting time of CNC and NS samples

4.1.3 Rheological Measurements Results

The effect of CNC or NS on the rheological properties of fresh cement paste mixtures is given in Figure 4.3. The yield stress and plastic viscosity values of cement mixtures were measured as mentioned in Section 3.2.3 using the Modified Bingham model (Equation 3.2). Shear thinning behavior was observed in all cement pastes examined in this study. The regression coefficient was between 0.97 and 0.98.

From the results that are presented in Figures 4.3 and 4.4, the yield stress in CNC addition cement mixes exhibited increased with the increase of CNC content in the mixes, which showed an increase in comparison to OPC by 50%, 65%, and 70.5% within the incorporation of 0.25%, 0.50%, and 0.75% of CNC, respectively. While the addition of NS showed an increase in yield stress by 40%, 44.4%, and 54% in the addition of 0.25%, 0.50%, and 0.75% of NS, respectively. Comparatively, CNC revealed a higher effect on the increase of yield stress than the effect of NS on cement pastes. The higher increment in the yield stress was observed in the higher CNC content (0.75% wt. of cement) of this study. Similar findings have been observed in previous studies. As the CNC dose rises

(greater than 0.2%), the yield stress increases rapidly, producing a paste that is less flowable, that makes CNC in a manner comparable to that of a viscosity-modifying additive (VMA) [113] [15]. The authors are at confidence by considering the rise in yield stress to be one of the impacts of VMA. With the addition of the VMA effect, cellulose nanoparticles have been employed to increase water retention [114] and sagging resistance in cement-based systems [115]. Consequently, considering the impact of CNC on cement rheology and strength, it is claimed that CNC might serve as a dual-purpose additive at large dose by enhancing the consistency of cement-based mixes by minimizing segregation [115]. On the other hand, previous research [112], [116]–[118] shown that the yield stress increased significantly as the number of NS in the cement matrix increased. It was stated that the impact of NS on yield stress is that NS tends to absorb more free water from the mix, which may change the rheological characteristics [118]. It was also observed that the increase in friction between the particles and the dense packing of NS in the mixture is the explanation for the rise in yield stress [86], [112], [119]. Sonebi et al., [117] explain this phenomenon to the exceptionally large surface area of NS.

Meanwhile, the plastic viscosity in CNC reinforced pastes showed no changes, and it remained the same in comparison to OPC. On the other hand, NS effect on the cement pastes regarding the plastic viscosity was great, showing the increase of NS addition boosted the plastic viscosity. The plastic viscosity with the NS addition cement pastes was higher than the reference OPC by 15%, 48%, and 55.5% in the addition of 0.25%, 0.50%, and 0.75% NS, respectively. By that, NS showed higher effect concerning the plastic viscosity than CNC on the cement system, where the plastic viscosity were enhanced with the incorporation of NS and the amount of improvement has increased by gradually increasing the addition of the NS (0.25%, 0.50%, 0.75%). Regarding variations in the plastic viscosity of cement pastes containing CNC, previous authors hypothesized that despite the addition of cellulose nanomaterials, plastic viscosity remained unaffected [120], also, it was demonstrated that the cement pastes containing CNC had lower plastic viscosity than the control [106]. As NS shows a greater improvement in plastic viscosity than CNC. Earlier research [112], [116]–[118] shown that NS significantly increases the plastic viscosity of pastes. The increased plastic viscosity is attributable to the ultrafine nature of NS particles, as observed by Sonebi et al. [117]. This is the reason for altering in the kinetics of hydration, which was discovered independently [112], [117]. And

correspondingly to yield stress enhancement by NS, again as it was observed that with the increase in friction among the particles and dense packing of NS in the mix is the causative agent of an increment in viscosity [86], [112], [119].

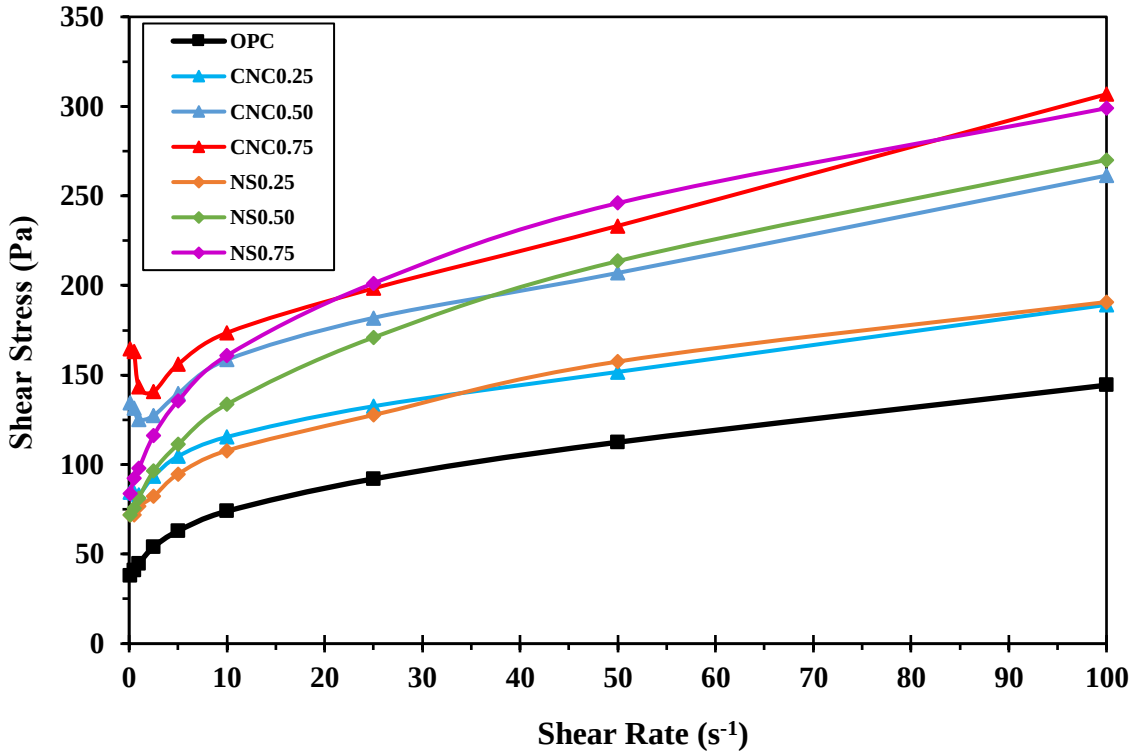

Figure 4.3 Flow curves of the mixes

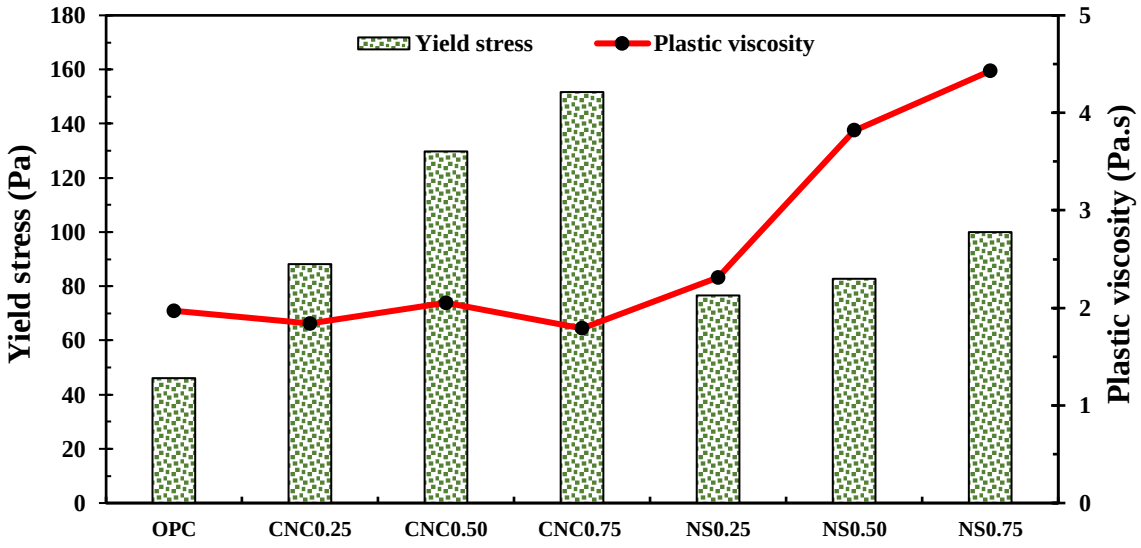

Figure 4.4 Rheological parameters using Modified-Bingham model

4.2 Hardened State Properties

4.2.1 Compressive Strength Results

Compressive strength is the most crucial parameter that must be determined in specimens of hardened cement composites. Compressive strength test results for cement mortars with the inclusion of 0.25%, 0.50%, and 0.75% wt. with 0.5 w/c ratio for CNC contained mortars, and similar contents for NS contained mortars are shown in Figure 4.5 and in Table 4.1. SP was used to enhance workability of all mortars and to regulate the distance among nanoparticle. The results were used for 3, 7, 28, 90 days of curing.

CNC results exhibited an increase in compressive strength for the 3rd day of curing by approximately 11.3% in CNC0.75 from the reference OPC. In 7^{th} day, CNC contained samples showed different trend where the increasing of compressive strength showed by CNC0.50 with 6.5% compared to the reference sample. 28 days results showed same trend followed by 7 days results in the effect of CNC on the compressive strength on the cementitious mortars where CNC0.50 expressed again the higher score in CNC contained samples, within 15.7% increase in comparison to OPC control sample. The results of CNC containing samples for 7 days and for 28 days will then need to be confirmed in the microstructure analyses within section 4.3 where 7 and 28 days were tested for TGA analysis and in 28 days were examined by MIP, XRD, and SEM. For 90 days results, CNC0.75 expressed the higher results with the increasing of 25% compressive strength compared to reference sample. The variations in compressive strength between CNC0.50 and CNC0.75 in 28 days and 90 days may account for the significant development of calcium crystals when CNC was added, since its hydrophilic nature may lead to the absorption of water into the porous structure. As noted in earlier research, the implication here is that the absorbed water may be the primary water source for the unhydrated cement particles to undergo the hydration process and generate more calcium crystals even beyond the curing interval [121]. Related results were reported by Cao et al. [15], who discovered a ring around the cement particle in the cement matrix, which was subsequently recognized as lingering CNC. Findings indicate that CNC can produce ongoing strength growth in aged cement mortar, as shown in CNC0.75 after 90 days; more investigations in the microstructure analysis section will give additional information about compressive strength.

In NS reinforced cement mortars, the 3rd day curing age compressive strength results were scored higher in NS0.75 samples by approximately 22.1% from reference. Similarly in 7th day of curing, NS0.75 was highest than other NS samples achieving about 15.9% compared to OPC. The 28th was showing different results than other days of curing age. The results in comparison to reference (OPC) achieved higher in NS0.25 by 13%. It was reported in previous studies, that the variation in the mortars strength can be related to that NS has low effect in small incorporations and the using of higher w/c decreases the effectivity of NS in case the enhancement of cement systems [112]. The growth of strength in NS contained cement mortars is related to the pozzolanic reaction. Its physicochemical impact within the mortar is responsible for the beneficial effect of NS on compressive strengths. In a subsequent hydration event, the NS combines with calcium hydroxide ($Ca(OH)_2$) freed during cement hydration to generate additional calcium silicate hydrate (C-S-H) gel. NS will indeed fill pores to boost the mortar's strength. Therefore, it is verified that the incorporation of NS into cement mortars increases their strength mostly [87]. These results will also need to be confirmed by the microstructural analysis which will be discussed in the further tests results.

In general, when the results of CNC and NS mixtures are compared, it can be said that the effect of NS on cement samples appeared to improve compressive strength in the early stages (3rd and 7th days of curing) more efficiently than CNC addition. The NS on the 3rd day was achieved within NS0.75 by 12.2% more than the CNCs' higher compressive strength results were achieved by CNC0.75. Similarly, on the 7th day, NS reinforced mortars within NS0.75 achieved higher compressive strength results than CNC's highest results (CNC0.50) by 10.1%. While CNC effect on cement systems appears more effectively in later age (28th and 90th day). At the age of 28th day, maximum compressive strength results were obtained by CNC0.50, and it was 3.1% higher than the max result in the NS (NS0.25). In the 90th curing age, CNC0.75 from CNC contained samples achieved 12% higher than the most achieved results in NS contained samples, which was in NS0.25. These comparative conclusions will need to be emphasized further in microstructural analyses.

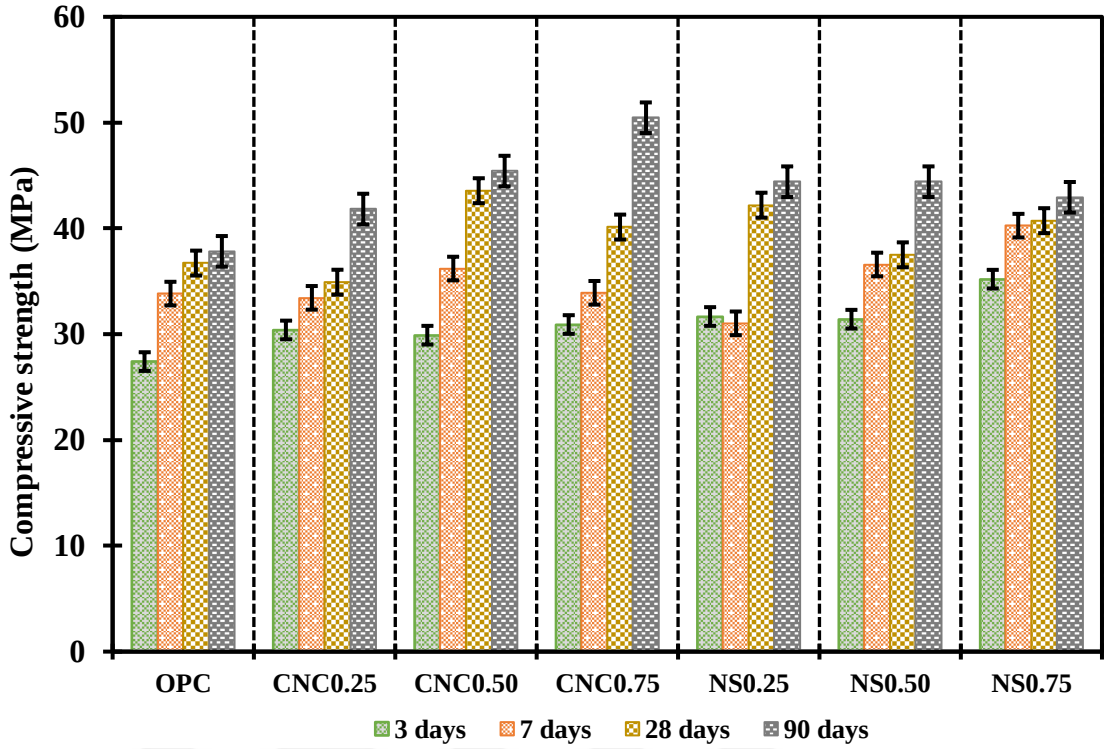

Figure 4.5 Compressive strength versus CNC and NS dosages

Table 4.1 Compressive strength results

Compressive strength (Mpa)				
Mixes	**3 days**	**7 days**	**28 days**	**90 days**
OPC	27.4 ±2.6	33.8 ±1.4	36.7 ±1.3	37.8 ±4.5
CNC0.25	30.4 ±0.6	33.4 ±0.9	34.9 ±2.3	41.8 ±3.7
CNC0.50	29.9 ±1.7	36.2 ±1.6	43.6 ±4.1	45.4 ±2.7
CNC0.75	30.9 ±1.8	33.9 ±0.9	40.1 ±4.5	50.5 ±5.5
NS0.25	31.7 ±0.3	31.0 ±0.5	42.2 ±3.9	44.4 ±1.5
NS0.50	31.4 ±2.0	36.6 ±2.8	37.5 ±2.1	44.4 ±1.7
NS0.75	35.2 ±3.9	40.3 ±1.3	40.7 ±2.3	42.9 ±4.4

4.2.2 Water Absorption Results

The water absorption test was performed on samples cured for 28 days. The results have been measured through the calculation of AIP% and VPP% using the Equations of 3.3 and 3.4. The results presented in Fig. 4.6 express the effect of CNC or NS addition on the absorptivity property of cement mortars. For CNC contained samples, CNC0.50 showed the most reduction within 3% and 3.5% from reference sample in water absorption and void content, respectively. Meanwhile, CNC0.75 and CNC0.25 exhibited higher water

absorption and void content, such as CNC0.75 results of water absorption and void content were increasing by 4.8% and 3.9% compared to reference, respectively. Similarly, CNC0.25 also showed an increase in water absorption and void content by 10.4% and 7.5% respectively in comparison to reference. The high void content and water absorption usually reduce the mechanical strength of cement systems [122]. The results of for CNC reinforced mortars trend was like the compressive strength results were CNC0.50 expressed higher compressive strength in 28 days. The decrease in water absorption and void ratio which is achieved mostly in 0.50% content, this is due to the nanopolymer's ability to seal the paste aggregate ITZ, as demonstrated by the investigation of Aguiar et al. [123]. Like our results, Wu et al. [124] reported that mortars containing 0.4 volume percent CNC had the lowest water absorption void ratio. The findings suggest that the cement matrix of CNC0.50 specimens is denser than that of other CNC-containing samples, resulting in fewer permeability spaces and less water absorption, hence enhancing the microstructure density of the specimens. The reduction in water absorption and volume of permeable voids with a CNC concentration of 0.50 wt.% may be attributable to enhanced hydration of cement [15], which will be examined further within microstructural analyses in Section 4.3.

The effect of NS addition cement mortars was like NS0.25 showed the most reduction in all nanomaterial's addition samples. NS0.25 exhibited a reduction in water absorption and void content by 12.2% and 12.6% respectively, compared to reference sample. The NS0.25 mortar sample has also been confirmed by compressive strength with higher results during 28 days upon NS contained samples. NS0.50 samples were facing increasing in water absorption and void content by 1% and 2% respectively compared to control sample. While NS0.75 also showed an increment as 3% and 2% in water absorption and void content, respectively. The instability of absorptivity and void content can be expressed to the fact that the quantity of NS used in the mixture was not appropriate for a notable change. NS has low effectivity in low quantities, that requires higher NS amounts (e.g., mostly 4%wt. and further was used in previous studies) to show an influence [108]. Also, the w/c was 0.5 with the usage of 1.2% SP. The reason has been reported that the increases in water absorption and void content may occur when mortars are formed of a large volume of water or display lower flexibility during molding conditions [112].

CNC optimum dosage was found 0.50% to be incorporated in mortar mixture according to compressive strength and confirmedly by water absorption results. CNC with dosage between 0.40%-0.50% has been reported in previous studies as the optimum dosage for CNC incorporation to enhance mechanical properties as followed by minimum void content. Comparatively, NS incorporation has shown instability in reducing water absorption and void content within NS0.50 and NS0.75 in comparison to reference sample, although the incorporation of NS with 0.25% dosage has been exhibited with great compressive strength also minimum water absorption and void content. Previous studies showed that NS present insufficient results with the increasing of w/c content while the w/c of our studies was quite higher (0.50 w/c), also NS has limited effectivity in low quantities, requiring greater levels (e.g., % wt. and beyond) to exhibit an impact.

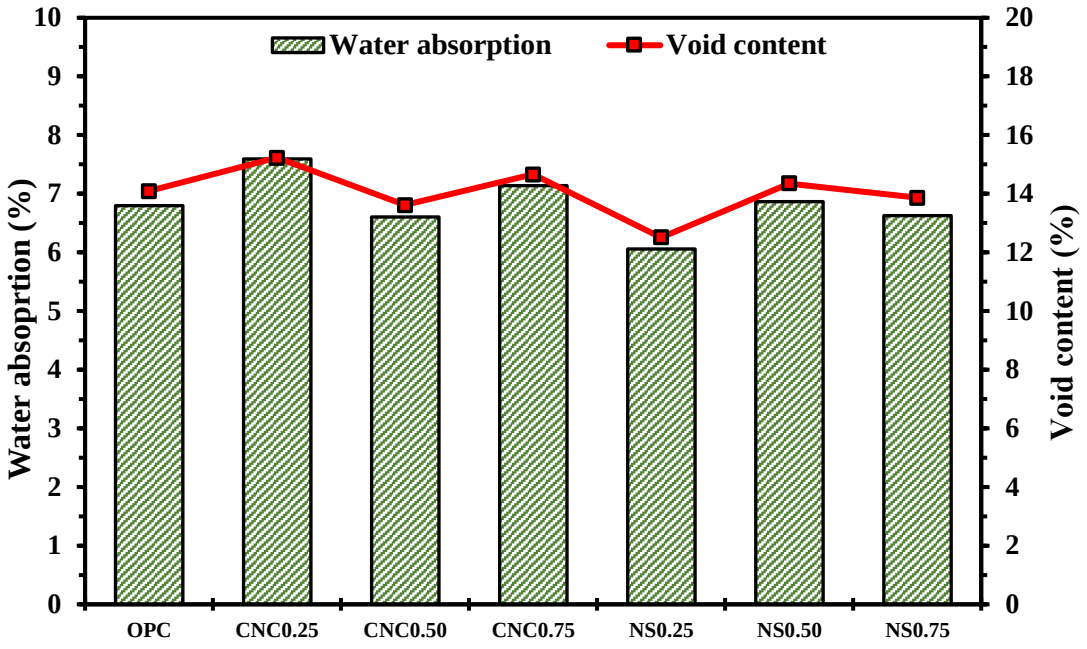

Figure 4.6 Water absorptions and void content results versus CNC and NS dosages

4.3 Microstructure Analyses

4.3.1 Mercury Intrusion Porosimetry (MIP)

Mercury Intrusion Porosimetry (MIP) was used to assess the porosity of cement paste. Figure 4.7 illustrates the outcomes. After 28 days, each mortar with OPC (reference), CNC, or NS-contained pastes was sliced into samples. Differing pore size distributions may have varying effects on the qualities of cement paste, including absorption and

overall strength. The pore structure of cement-based materials is crucial for the development of strength and transport capabilities. As hydration progresses, hydration products expand into the pores initially filled by water. In the differential pore size distribution curves, the first major peak of the differential curve, which can be seen in Figure 4.7 (b and d), shows how mercury gets into the sample through a porous network connected to the surface [125]. Pores ranges from about 0.01 μm to 0.1 μm relate to pores that are partly or completely closed by hydration products, which are intruded through or burst open as mercury intrusion force increases. Cook & Hover, [125] firstly classified the pores depends on their sizes, where they categorized into three groups based on their sizes: gel pores (<0.01 μm), mesopores (medium capillary pores) (0.01- 0.1 μm), and macropores (large capillary pores) (>0.1 μm), and this classification was employed for this study.

CNCs results (Figure 4.7a and 4.7b) revealed a CNC0.25 increase in contributive porosity (mesopores and gel pores) ranged below 0.1 μm (100 nm). As seen in Table 4.2, CNC0.25 has shown the lowest total porosity in CNC contents with 6.95% compared with reference OPC (10.57%). In the pore size distribution, the CNC0.25 critical pore diameter was not shown to have a difference from the reference within 0.048 μm for both. In comparison to the reference, the total porosity of CNC0.75 was higher than the reference by 11.61%. Furthermore, in size distribution, CNC0.75 presented a critical pore diameter lower by 0.044 μm than the reference. CNC0.50 despite having higher priority than CNC0.25 (6.95%) within the 9.06% in the CNC mixtures, it showed a refinement in pore size distribution with a critical pore size of 0.043 μm which was less than other CNC contained samples and the reference. Nanomaterials are supposed to fill in the spaces and reduce porosity, but this depends on the amount of dispersion and that nanomaterials tend to agglomerate. This is like what happened with CNC0.75 and CNC0.50, which can be explained by the fact that the CNC agglomerates absorb water, and the unreacted water might create capillary pores. In addition, CNC agglomerates may trap air, which enhances porosity [126]. Another reason is that a high quantity of CNC agglomerates attracts a huge quantity of water, resulting in capillary holes, while low quantities of CNC agglomerates attract a small amount of water, resulting in gel pores. Another reason relates to the w/c quantity that, as known, increases porosity. CNC0.25 is adjusting the larger pores and improving the pore size distribution. The results were confirmed by a

change in cumulative pore volume, which shows the rod-shaped nanoparticles added to the mix design effectively clogging the pores with a radius of less than 100 nm. The CNC particles enhance the cement hydration through the short-circuit diffusion method in which they act as seeding additives for the hydration process. When CNC is added, the shape and size of the cracks in the interfacial transition zone change. This causes the microstructure to get better and the number of holes to go down [15], [126].

NS results are presented in Figure 4.8c as cumulative intruded volume and 4.8d as differential intruded volume. From Figure 4.8c, we can see that NS0.75 scored the lowest total porosity by 6.54% and pores size below 0.10 μm exhibiting more gel pores that support CSH gel compared to the reference and overall lowest porosity in this study. NS0.25 also possessed low porosity by 7.02% compared to reference (10.57%) and possessed quite a higher number of macropores compared to other NS content and reference. NS0.50 revealed a higher number of pores below 0.1 μm compared to other NS samples but remained as an NS group behind the reference sample. The total porosity of NS0.50 was highest in the NS group in comparison to other NS mixes by 9.71% but still lower than reference OPC. NS0.50 exhibits higher porosity in the region of gel pores and mesopores where the production of CSH gel is excited. It shows the NS curves of NS0.50 and NS0.75 interface together in the macropores region, exhibiting low quantities of macropores with higher pores in mesopores and gel pores behind 0.10 μm which suggests contributive pores. It can be expressed that the higher NS content decreases the pores, especially that NS plays as filler nanomaterial, filling pores and decreasing porosity, but for sure if it was used in the ideal concentration. The optimum dosage in this test for NS was presented at 0.75% NS with lower porosity. The total pore volume of NS-containing mixtures is found to be less than that of NS-free mixtures. According to Mohammed & Azmi [127], this is related to the role of NS to densify and improve the porous structure of the mixture up to nano-size because of the increase in the pozzolanic reaction among silicon dioxide (SiO_2) and unreacted $Ca(OH)_2$ from cement hydration products to produce more C-S-H gels [127]. The high porosity of ITZ may be reduced by physiochemical effects, while boosting the C-S-H gel and filling nanopores would enhance ITZ and reduce pore size. Therefore, the hardened samples are linked, and the incorporation of NS aids in lowering the overall pore volume and subsequently the porosity [128]. The fact that the curves of the NS0.50 and NS0.75 specimens shifted to a

region of smaller pores indicates that the inclusion of NS has major impacts on pore structural modification. This work verifies the findings of previous studies that the inclusion of NS into a mixture does not necessarily affect the reduction in cement matrix porosity but has major impacts on pore structure modification [129]. Regarding pore size distribution in Figure 4.8d, NS0.50 exhibited a critical pore diameter of 0.042 μm a much lower pore diameter compared to reference and other NS mixtures. NS0.25 scored a higher critical pore diameter by 0.067 μm even more than the reference OPC (0.048 μm), while NS0.75 expressed the same as NS0.25 but a little bit lower than it with 0.058 μm. Figure 4.8d verifies the shift in the distribution of pore sizes. As mentioned above, the critical pore diameter, which is defined as the diameter that occurs most often, is much smaller for the NS0.50 mixture. This finding shows that NS influences pore refinement, and it may be due to both the filler effect and the extra C–S–H that is made by the pozzolanic reaction [130], [131]. It is well accepted that a decreased critical pore width leads to a finer pore structure [132].

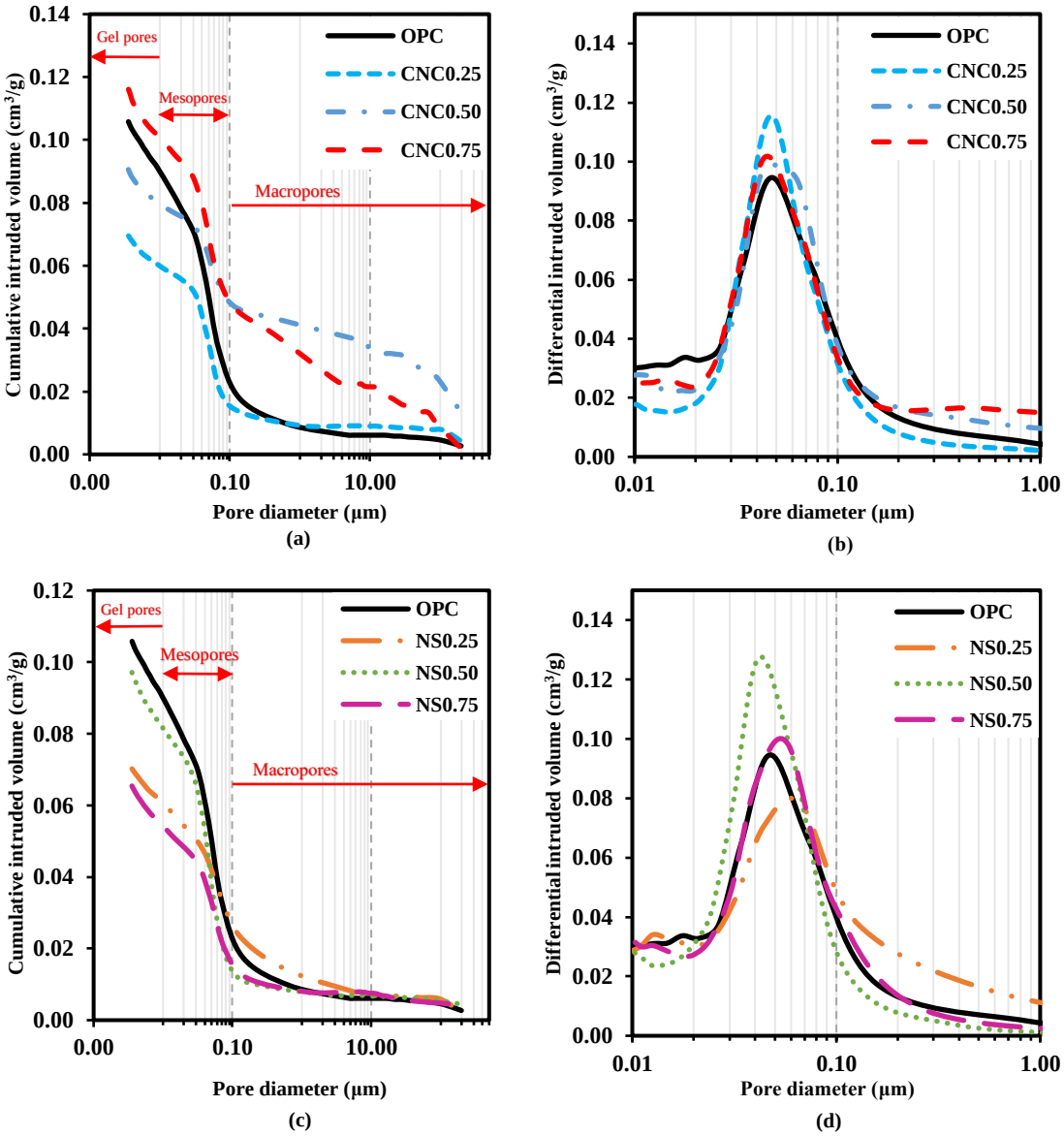

Figure 4.7 Mercury intrusion Porosimetry (MIP) results for CNCs and NS results compared to OPC a) cumulative intruded volume of CNCs compared to OPC versus pore diameter, b) differential intruded volume of CNCs compared to OPC versus pore diameter c) cumulative intruded volume of NS compared to OPC versus pore diameter, d) differential intruded volume of NS compared to OPC versus pore diameter

Table 4.2 Mixtures pore structure properties

Series	Total porosity (%)	Critical diameter (μm)
OPC	10.57	0.048
CNC0.25	6.95	0.048
CNC0.50	9.06	0.043
CNC0.75	11.61	0.044
NS0.25	7.02	0.067
NS0.50	9.71	0.042
NS0.75	6.54	0.058

4.3.2 Thermogravimetric Analysis (TGA)

Thermogravimetric curves of the CNC and NS paste samples at 7 and 28 days of curing are shown in Figure 4.8. It was observed that all the samples withstood higher temperature till 1000 °C where the reference OPC in 7 days was distinguished with a lower amount of mass loss compared to the others, while in 28 days, CNC0.25 from CNC groups was distinguished with a lower amount of mass loss compared to the others. DTG curves were plotted from the TG data and are demonstrated in the same Figure to identify the exact boundaries of various phases of the hydrated samples. The samples powder revealed three main stages of weight loss, starting from the first stage occurred from 50°C temperature to 400°C. The weight loss at this stage was caused by the dehydration of ettringite and CSH gel [133]. The second stage of weight loss occurred from 400 to 500°C and could be attributed to the dehydration of CH which is called portlandite ($Ca(OH)_2$) [134]. The final stage of weight loss was caused by the decarbonization of $CaCO_3$ from around 600 °C and above [134]. Through the carbonization of CH in the presence of air, calcium carbonate may be produced [135].

The chemically bound water (Wb) in equation 4.1 and the degree of hydration which considered as α measured in equation 4.2 were all calculated for the paste mixes by using the Bhatty's method [136].

$$Wb = Ldh + Ldx + 0.41Ldc \quad (4.1)$$

$$a = \frac{Wb}{0.24} \times 100 \quad (4.2)$$

where Ldh expressed as the relative loss of mass due to CSH deyhydration, Ldx as expresses the relative mass loss of portlandite deyhydration. Ldc give the relative mass loss due to the carbonation. The temperature ranges used to determine the Ldh, Ldx, and Ldc were 50–400 ºC, 400–500 ºC, and 600–1000 ºC for dehydration of CSH, portlandite, and carbonation, respectively. The results of bound water and hydration degree are presented in Table 4.3.

Test results showed highest hydration degree in CNC0.50 within 28 days of curing compared to reference and that was corresponding to higher mass losses of CSH and the portlandite. This demonstrates that, among the studied samples of CNC, the mixture with CNC0.50 had the greatest level of hydration in 7 and 28 days of curing. The rise in hydration degree is consistent earlier studies. Cao et al. [15] observed that the incorporation of CNC improved the degree of hydration of cement paste after 7 and 28 days of cure. They hypothesized that two factors were responsible for the rise in hydration level. The CNCs function as a water reducer, which aids in the dispersion of cement particles. Second, the CNCs function as conduits for the transmission of water to unhydrated cement particles. These two factors enhance the hydration interaction between particles of cement and water. The higher degree of hydration in CNC0.50 was also confirmed in MIP results, where CNC0.50 showed the second lowest priority in CNC samples. One potential reason for the improvement in DOH with the inclusion of CNCs at the same w/c is that the presence of CNCs helps cement particles react with water more effectively. This may be attributed to steric stabilization, the same process found in some kinds of water reduction admixtures (WRA) (e.g., polycarboxylated-based) to disperse cement particles during cement mixing, resulting in finer and more uniform cement distributions [137].

On the other hand, NS showed the highest hydration degree in the early ages of 7 days within NS0.75 and that was measured with the higher CSH and portlandite owned by

NS0.75 in 7 days results of TGA. While at the late age of 28 days NS0.25 possessed the higher hydration degree among NS samples. As it has been reported previously in this study, this was regarding the low number of NS and higher amount of w/c used in this study. In other studies, NS showed significant results with a higher number of NS (e.g., 4% wt. of cement) and a low w/c ratio (e.g., 0.35). These results that have been discussed in TGA analysis for both CNC and NS samples have showed concordance with the compressive strength results.

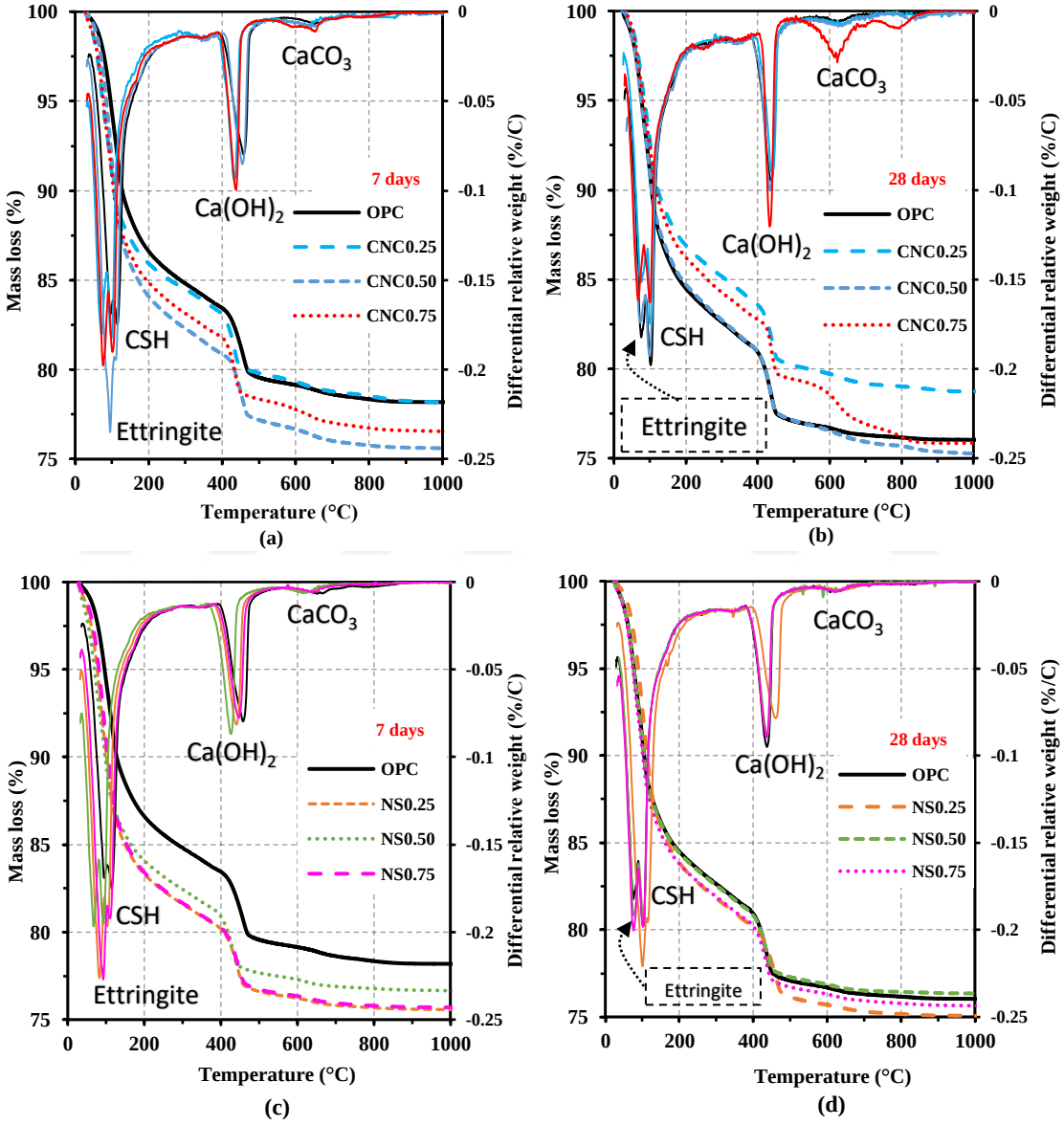

Figure 4.8 Thermogravimetric analysis (TGA) results a) CNC 7 days, b) CNC 28 days, c) NS 7 days, d) NS 28 days

Table 4.3 Chemically bound water and degree of hydration of the paste mixes

7 days					
Mix ID	**Weight Losses**			**W_b (%)**	**α (%)**
	Ldh	**Ldx**	**Ldc**		
OPC	14.415	2.961	1.978	18.19	75.78
CNC0.25	14.301	2.988	2.091	18.15	75.61
CNC0.50	15.729	3.044	1.341	19.32	80.51
CNC0.75	14.467	2.997	1.722	18.17	75.71
NS0.25	13.564	2.881	2.076	17.30	72.07
NS0.50	16.129	3.104	1.440	19.82	82.60
NS0.75	17.523	3.146	1.409	21.25	88.53
28 days					
OPC	16.129	3.105	1.440	19.82	82.60
CNC0.25	15.589	3.008	1.808	19.34	80.57
CNC0.50	18.784	3.478	1.384	22.83	95.12
CNC0.75	18.145	3.190	1.531	21.96	91.51
NS0.25	18.122	3.382	2.409	22.49	93.72
NS0.50	17.704	3.167	1.377	21.44	89.32
NS0.75	18.205	3.171	1.511	22.00	91.65

4.3.3 X-ray Diffraction (XRD)

Figure 4.9 demonstrates that XRD analysis of the seven different samples. XRD analysis was used to identify the different byproducts of the hydration process. Ca $(OH)_2$ peaks were seen in both CNC contained pastes and NS contained pastes sample powders, where the increase or decrease of these peaks indicates the degree of hydration in the composites. The presence of $Ca(OH)_2$ peaks with greater intensity in CNC and NS composites implies a greater degree of hydration, as seen in the TGA study as well. In Figure 4.9a the highest peaks at 18º, 34º, and 47º of 2θ indicated the presence of calcium hydroxide, $Ca(OH)_2$ for CNC samples, while NS samples showed at 28.6º 2θ $Ca(OH)_2$ (according to portlandite DB card PDF#04-0733). The peaks 28.6º and 32.6º 2θ in CNC contained samples and in

NS contained samples only in 32.6º 2θ peaks, is attributable to tricalcium silicate (C_3S) and dicalcium silicate (C_2S) (PDF#49-0422 for C_3S, PDF#24-0034 for C_2S), which make up most clinker components include alite and belite that indicate a partial or incomplete hydration reaction. Calcite is released because of hydration in TGA study, we might have seen calcite in the XRD analysis, but its peaks were not noticeably clear. Therefore, $CaCO_3$ was present because $Ca(OH)_2$ was partially carbonized which appeared in peak of 29.4º 2θ for CNC and NS samples [138]. It was also observed that the appearance of larnite (Ca_2SiO_4) in the peaks of 31º and 32º 2θ (PDF# 33-302).

For CNC samples powder diffractions as seen in Figure 4.10a, we can see alite and belite peaks have boosted up in CNC0.50 particularly in the peak of 32.6º 2θ compared to reference. CNC encourages the hydration of C_3S and C_2S to generate CH that was seen also in CNC0.50 that confirms the TGA analysis, hence accelerating the chemical reaction rate and enhancing the hydration heat [139]. The strength of the major peaks of calcium silicate diminishes with the addition of CNC, as a higher number of anhydrous cement phases react in the presence of CNC, where C_3S and C_2S are changed into C–S–H [140]. Therefore, the absence of these peaks in the composite sample is indicative of greater hydration and conversion of C_2S and C_3S to diverse hydration products. C-S-H gels are often significantly smaller than if the surrounding solid had inhibited their development. Since the latter includes a substantial fraction of Ca-OH bonds, it is difficult to separate [141]. Due to its amorphous nature and lack of crystallinity, the C-S-H formation is difficult to accurately characterize using XRD. Instead, the crystallinity of portlandite ($Ca(OH)_2$) was determined. This is because portlandite is a byproduct of hydration and has a crystalline structure. C-S-H has a nanometer-scale shape, and the detection of peaks verifies the existence of portlandite production as a binding agent, which in turn adds to the increased mechanical strength of cement mortar [121]. Portlandite peaks in CNC samples have been decreased while the increasing of CNC content but showed higher in CNC0.50 sample as also observed in TGA analysis. Calcite ($CaCO_3$) peak appeared decreasable in increasing of CNC content, its appearance regarding the consuming of $Ca(CH)_2$.

In addition, X-ray diffraction tests were conducted to explore the impact of NS addition on chemical composition alterations (Figure 4.9b). As previously stated, peaks of CH, calcite, C_2S, and C_3S were seen. There was a difference in the intensities of CH-related

peaks. The CH peaks were weaker in NS0.25 samples which are raised while increasing of NS content which can be seen with most of intense in NS0.75 compared to other NS and reference. As previously stated, because CSH is weakly crystalline, its peaks were not visible in the X-ray diffractograms; nevertheless, the strengthened peaks of the crystalline product portlandite revealed an increased production of hydration products in NS at all three concentrations.

The addition of CNC or NS does not create a different peak. There are peaks and minerals like OPC. Only their intensity may vary.

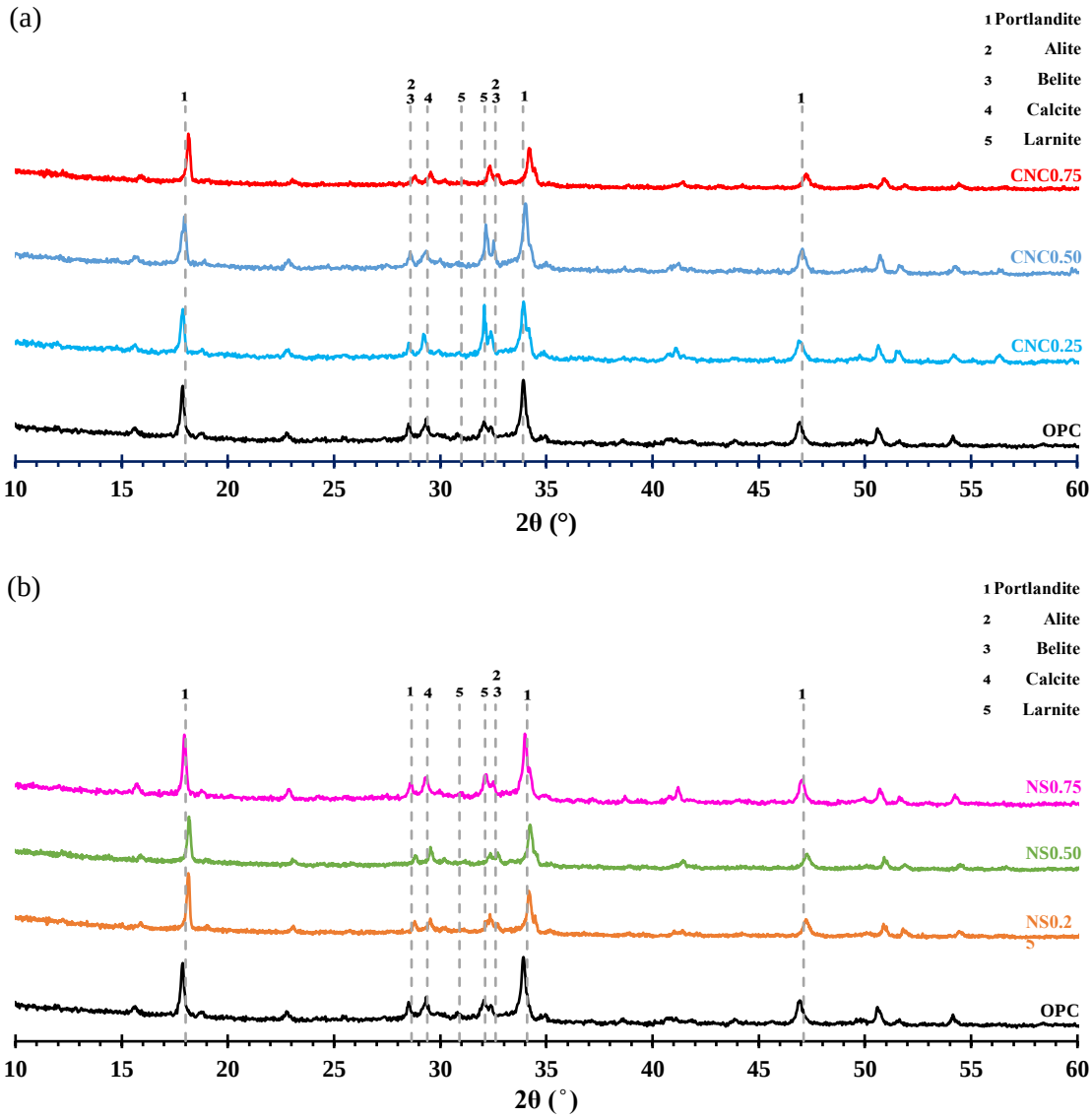

Figure 4.9 X-ray Diffraction (XRD) analysis a) CNC-contained pastes, b) NS-contained pastes

4.3.4 Scanning Electron Microscopy- Energy Dispersive Spectroscopy (SEM-EDS)

The SEM-EDS analyses were conducted at 28 days of cement samples and SEM images for each sample were given in Figure 4.10. The normal magnifications SEM images revealed hydrated parts, partial or incomplete hydrated parts, pores, and microcracks in samples. Microcracks were observed in the high pores samples in accordance with previous tests. It is possible for certain microcracks to occur, due to sample preparation (polishing) for SEM testing. The reference sample showed excessive amounts of pores compared to other samples. Unhydrated cement particles were observed in reference samples within 1.00 kX magnification. CNC reinforced samples were showing pores mostly in CNC0.25 and CNC0.75, while CNC0.50 had less pores. One noteworthy feature can be shown in the CNC contained cement pastes in formation of a ring or shell around many unhydrated cement particles found mostly within 1.00 kX and 5.00 kX magnification. This phenomenon was also seen in research conducted by Mazlan et al. [121], and its explanation was attributed to the increased development of calcium crystals when CNC were incorporated, whose hydrophilic properties led water to be absorbed into the pore structure. Correlation is made that the absorbed water was the primary water source for the unhydrated cement particles to undergo the cement hydration and form extra calcium crystals even after the curing duration. These explanations were inferred from previous studies described by Cao et al.[15], in which they explored first the exact dark ring that was noticed around the cement particle in the cement matrices, which was later described as concentrated CNC lingering around the particle. The findings additionally enhance the compressive strength results, suggesting that CNC has the capacity to offer continual strength growth in aged cement mortar. NS contained cement pastes in terms of this phenomena was showing almost different than CNC samples.

In EDS analysis, hydration products were identified using the atomic ratios of the disclosed chemical compounds to identify the C-S-H area which is present in cements with a Ca/Si ratio between 1.50 and 2.00 [134]. C_3S based on its chemical formula the Ca/Si ratio must be around 3. The carbon appeared in some picked areas in CNC reinforced samples and seemed to be higher in CNC0.25 and CNC0.75 were around 12% -17% atomic ratio, where it has disappeared totally in NS samples. The spotted picks in OPC with the number 1 and 3 were found to be CSH. The selected picks in CNC0.25,

CNC0.50, and CNC0.75 revealed to be C_3S. NS0.25, NS0.50, and NS0.75 peaks showed the appearance of CSH and the absence of C_3S also the NS particles was seen in SEM image of 20.0 kX magnifications.

As seen in EDS results that shown in Figure 4.10, carbon was observed, also the Ca and Si was found to be decreased with the increasing of CNC contents incorporation The proportionate rise in C and fall in Ca and Si indicate the existence of cellulose nanocrystals [142]. The sulfur was found to be existence in OPC and set to be decreased in the increasing of CNC content, while it was clearly visible in all NS contained mixtures.

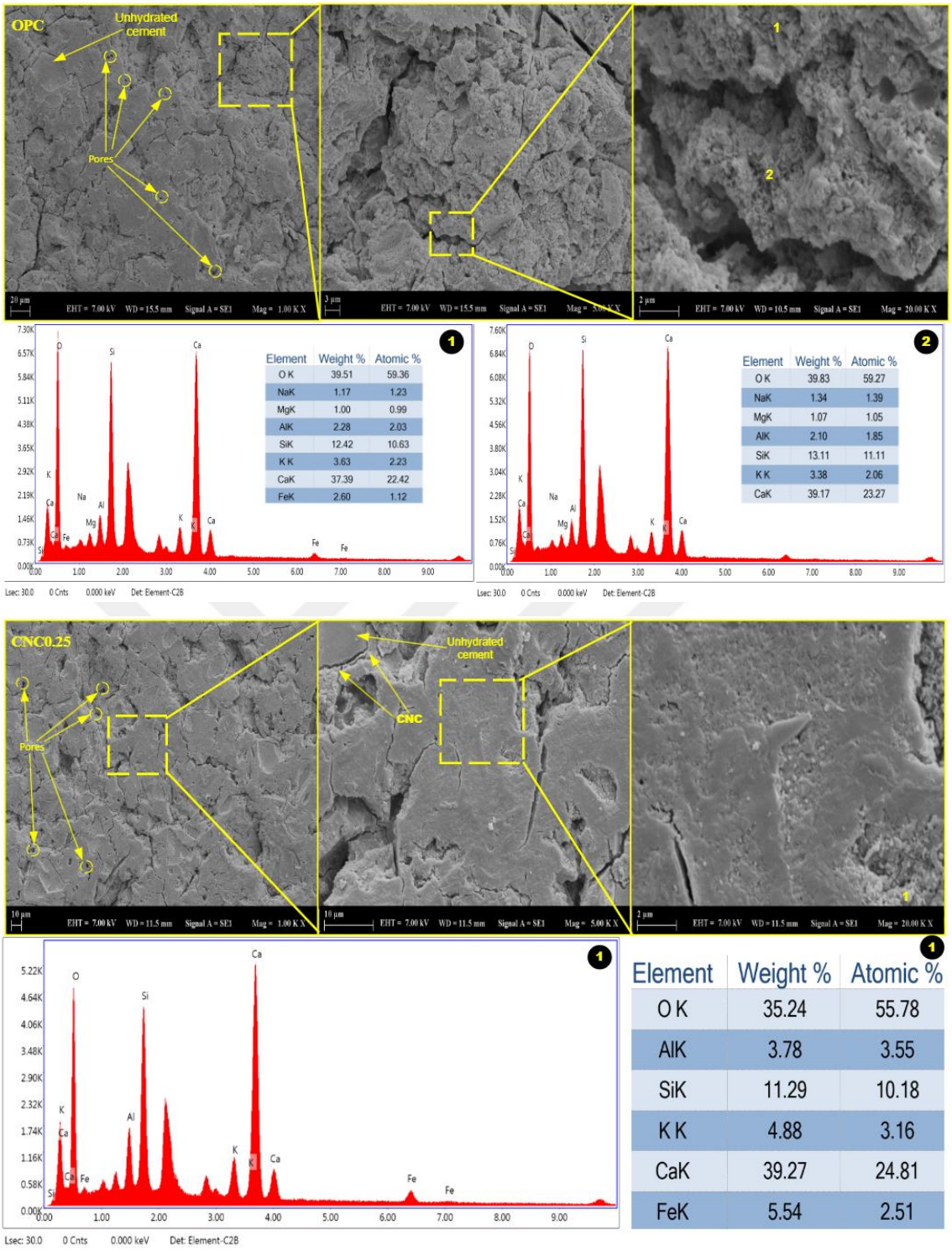

Figure 4.10 SEM-EDS image analyses for reference OPC sample, CNC reinforced cement samples, and NS reinforced cement samples

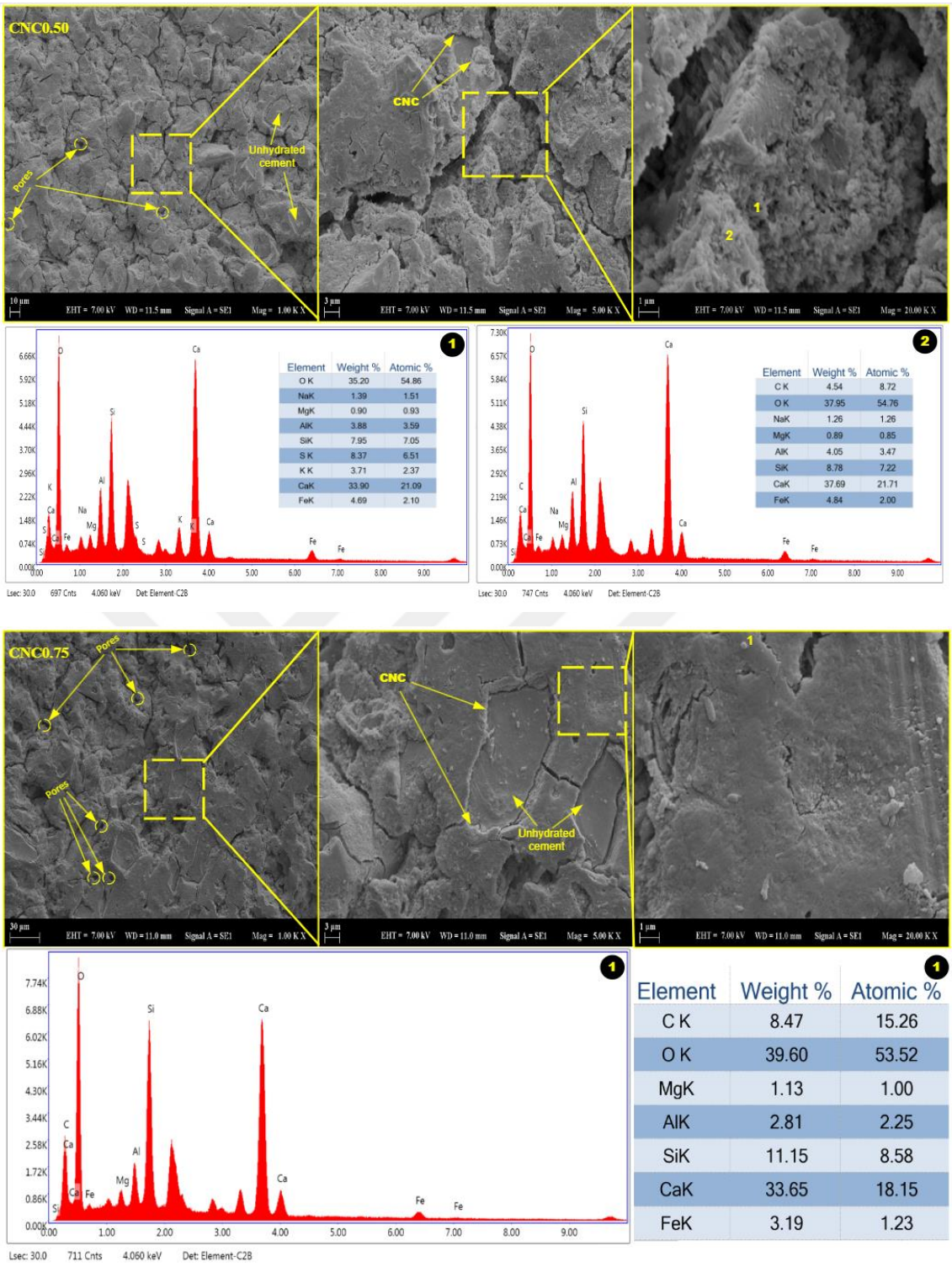

Figure 4.10 SEM-EDS image analyses for reference OPC sample, CNC reinforced cement samples, and NS reinforced cement samples (continued)

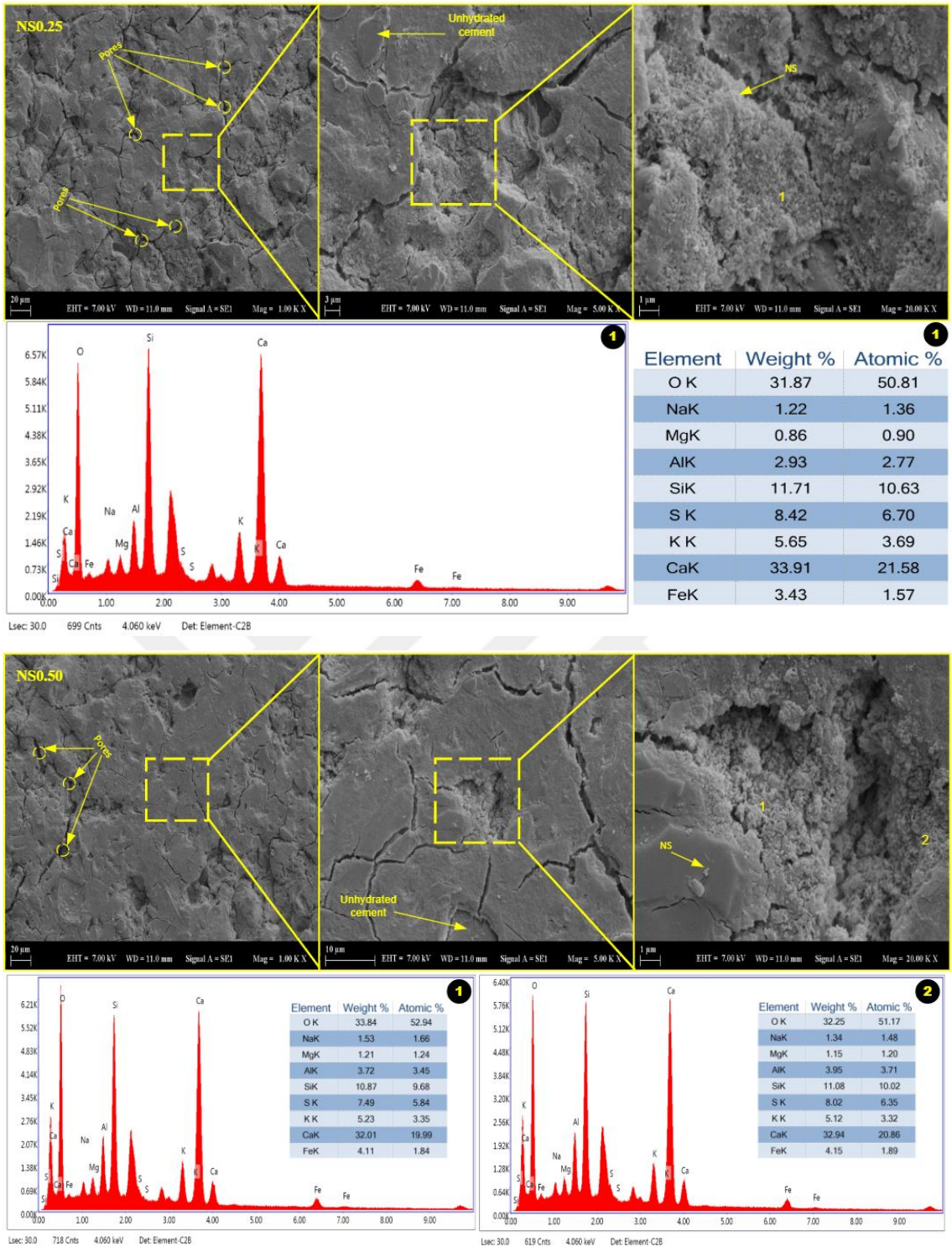

Figure 4.10 SEM-EDS image analyses for reference OPC sample, CNC reinforced cement samples, and NS reinforced cement samples (continued)

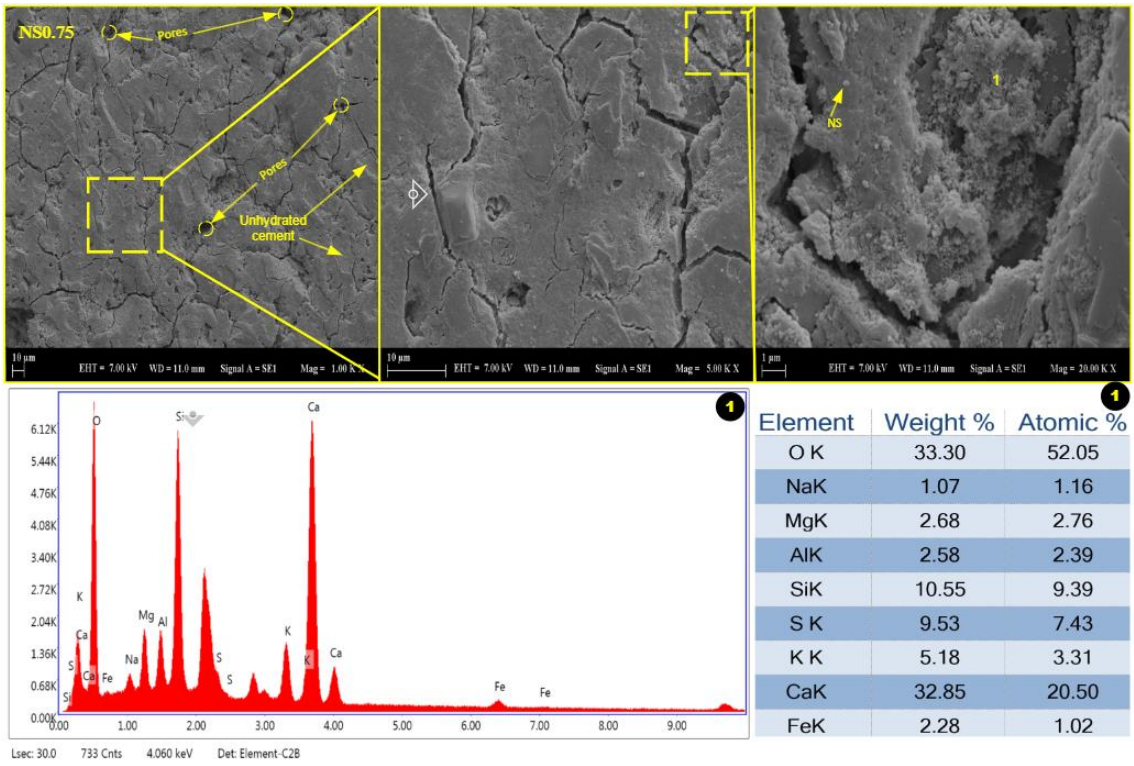

Element	Weight %	Atomic %
O K	33.30	52.05
NaK	1.07	1.16
MgK	2.68	2.76
AlK	2.58	2.39
SiK	10.55	9.39
S K	9.53	7.43
K K	5.18	3.31
CaK	32.85	20.50
FeK	2.28	1.02

Figure 4.10 SEM-EDS image analyses for reference OPC sample, CNC reinforced cement samples, and NS reinforced cement samples (continued)

5
CONCLUSIONS

The effects of using cellulose nanocrystal (CNC) and nanosilica (NS) on the mechanical and microstructural performance of cement-based materials have been investigated within the scope of this study. Cement pastes were prepared for microstructure analysis and rheological measurements with the use of 0.35 and 0.40 w/c, respectively. Fresh state properties results were obtained using flow table, setting time, and rheometer tests. While hardened state properties results were done using compressive strength and water absorption test. To confirm the validity of results, microstructure analyses (MIP, TGA, XRD, and SEM-EDS) were performed and summarized. Several important conclusions can be drawn:

- The CNC results exhibited a decrease in the **flow diameter** of the flow table with the increase of CNC contents. It has decreased sufficiently from the reference sample in 0.25% and 0.50% content by 70 mm and 110 mm, respectively. That implies the CNC has decreased the workability for all groups. While NS results expressed a low ability to decrease the flow diameter compared to CNC, they showed that the decrease in flow started only at 0.50% by 20 mm from a 0.25% content mixture. It was concluded that the NS decreases did not cause a notable change compared to CNC, showing NS has low effectivity in low quantities.
- In general, it was more obvious that CNC plays as retarding admixture, leading to delay the **setting time** of cement mixture in both initial and final setting time. This property was increased within the increase of CNC inclusion to cement mixtures. Comparatively, NS played as the accelerating admixture in shortening the setting time of cement system. The NS property in accelerating the setting time was more to be seen in final setting time, while this property getting diminished within the increase of NS dosage into cement mixtures. Despite the diminishing of shortening property in setting time, the initial and final setting time of all NS contained mixture appeared to set at lower time than CNC contained mixtures.
- CNC and NS-contained paste mixtures showed an increase in **yield stress** with the addition of the nanomaterials, wherein CNC revealed a higher effect on the

increase in yield stress than the effect of NS on cement pastes. The higher increment in the yield stress was observed in the higher CNC content (0.75% wt. of cement). Meanwhile, in the **plastic viscosity**, NS showed a higher effect concerning the plastic viscosity than CNC on the cement system, where the plastic viscosity was enhanced with the incorporation of NS and the amount of improvement has increased by gradually increasing the addition of NS.

- The addition of NS to cement samples seemed to increase early **compressive strength** (3rd and 7th day of curing) more effectively than addition of CNC. On the 3rd day, the NS was attained within NS0.75 by 12.2% greater than the higher compressive strength findings produced by CNC0.75 for the CNCs. Similarly, on the 7th day, NS reinforced mortars within NS0.75 had greater compressive strength than CNC's best results (CNC0.50) by 10.1%. While the impact of CNC on cement systems is more apparent after 28 and 90 days, CNC0.50 scored the highest at 28 days, which was 3.1 % higher than the maximum result in the NS (NS0.25). At the 90th curing age, CNC0.75 from CNC-containing samples produced outcomes that were 12% than NS0.25 from NS-containing samples.
- According to compressive strength and corroborated by **water absorption** data, the optimal proportion of CNC in mortar mixture was determined to be 0.50 percent. In comparison to the reference sample, CNC0.50 demonstrated a 3% decrease in water absorption and a 3.5% decrease in void content. Comparatively, NS incorporation indicated instability in lowering water absorption and void content within NS0.50 and NS0.75 compared to the reference sample, but NS incorporation at 0.25% dose exhibited high compressive strength as well as the lowest water absorption and void content at the age of 28^{th}. Since this w/c of our research was high (0.50 w/c), it was determined that NS produced inadequate outcomes with rising w/c content. Furthermore, NS has limited efficacy in low amounts, requiring larger amounts (e.g., 4 percent wt. and above) to have a significant impact.
- From **MIP** results we can conclude that the CNC decreased the porosity mostly in CNC0.25 with about 3.62% from OPC. Regarding the pore size distribution, CNC0.50 here showed lower pore diameter in critical size of pore than OPC within 0.043 μm. Comparatively, NS showed the effect of decreasable porosity

within NS0.75 about 4% from OPC. While NS0.50 showed refinement in pore size distribution results with pore critical diameter of 0.042 μm.

- **TGA** analysis revealed that the most common hydration products were CSH, Ca $(OH)_2$, and $CaCO_3$. The measurement of hydration degree from TGA analysis was supportive to compressive strength results, where it was found CNC0.50 owned a higher degree within 28 days, and among CNC samples, CNC0.50 owned the highest hydration degree in both 7 and 28 days. Like compressive strength, NS0.75 hydration degree was highest in the early stage of 7-day curing among all samples, and at the later age of 28 days, NS0.25 presented the highest score of NS samples.
- **XRD** peaks revealing Ca $(OH)_2$, $CaCO_3$, and clinker components including alite and belite, indicating a partial or incomplete hydration reaction. The alite and belite peaks were seen boosted up in CNC0.50, particularly, and as also observed in TGA analysis, portlandite seems to be increased in CNC0.50. Within NS samples, portlandite peaks increased with the increase of NS content and were found to be higher in NS0.75. The addition of CNC or NS does not create a different peak. There are peaks and minerals like OPC. Only their intensity may vary.
- **SEM-EDS analysis** clearly expressed that the CNC reinforced samples were showing pores mostly in CNC0.25 and CNC0.75, while CNC0.50 had a lower number of pores. In all CNC contained cement samples, C_3S was found in all picks collected from EDS results. The reason for this was that the hydrophilic property of CNC caused it to thoroughly absorb the water mixture and specifically the pore water, and the absorbed water served as the primary water supply for unhydrated cement particles to hydrate and create additional calcium crystals after curing. CNC was thought to enable continuous strength to increase in aged cement-based hardened samples. On the other hand, EDS analysis showed that the amount of C_3S in NS went down and that it looked like CSH.

From the current study and the summarized results, it is clear to us to recommend a few suggestions for future studies. It is obvious that 0.50% (wt. of cement) was the optimum content for CNC to be incorporated to the cement system to effect positively on the mechanical and microstructural properties of cement-based materials. In NS, it was clear

that the used contents of NS in this study were not showing significant effect on cement-based materials. It can be suggested to use NS in high quantities above 1% of the wt. cement to achieve better results regarding the cementitious materials. Also, it can be suggested concerning microstructural analyses, that the use of SEM-EDS and TGA in the 90 days of curing age could show more detail in the improvement of CNC in cement-based materials, because CNC was clearly decreasing the time of hydration degree due to its hydrophilic property which can be seen in compressive strength achieving perfect results in later ages of cement mixtures.

REFERENCES

[1] A. E. Oke, C. O. Aigbavboa, and K. Semenya, "Energy Savings and Sustainable Construction: Examining the Advantages of Nanotechnology," *Energy Procedia*, vol. 142, pp. 3839–3843, 2017, doi: 10.1016/j.egypro.2017.12.285.

[2] F. Sanchez and K. Sobolev, "Nanotechnology in concrete – A review," *Constr. Build. Mater.*, vol. 24, no. 11, pp. 2060–2071, Nov. 2010, doi: 10.1016/J.CONBUILDMAT.2010.03.014.

[3] P. Hou, S. Kawashima, D. Kong, D. J. Corr, J. Qian, and S. P. Shah, "Modification effects of colloidal nanoSiO2 on cement hydration and its gel property," *Compos. Part B Eng.*, vol. 45, no. 1, pp. 440–448, Feb. 2013, doi: 10.1016/J.COMPOSITESB.2012.05.056.

[4] A. Favier, C. De Wolf, K. Scrivener, and G. Habert, "A sustainable future for the European Cement and Concrete Industry," 2018, doi: 10.3929/ETHZ-B-000301843.

[5] K. Sobolev and M. F. Gutiérrez, "How Nanotechnology Can Change the Concrete World," *Prog. Nanotechnol.*, pp. 113–116, Aug. 2014, doi: 10.1002/9780470588260.CH16.

[6] R. J. Moon, G. T. Schueneman, and J. Simonsen, "Overview of Cellulose Nanomaterials, Their Capabilities and Applications," *JOM*, vol. 68, no. 9, pp. 2383–2394, Sep. 2016, doi: 10.1007/S11837-016-2018-7/FIGURES/4.

[7] E. J. Foster *et al.*, "Current characterization methods for cellulose nanomaterials," *Chem. Soc. Rev.*, vol. 47, no. 8, pp. 2609–2679, Apr. 2018, doi: 10.1039/C6CS00895J.

[8] D. Klemm, B. Heublein, H. P. Fink, and A. Bohn, "Cellulose: Fascinating Biopolymer and Sustainable Raw Material," *Angew. Chemie Int. Ed.*, vol. 44, no. 22, pp. 3358–3393, May 2005, doi: 10.1002/ANIE.200460587.

[9] M. Rajinipriya, M. Nagalakshmaiah, M. Robert, and S. Elkoun, "Importance of Agricultural and Industrial Waste in the Field of Nanocellulose and Recent Industrial Developments of Wood Based Nanocellulose: A Review," *ACS Sustain. Chem. Eng.*, vol. 6, no. 3, pp. 2807–2828, Mar. 2018, doi: 10.1021/ACSSUSCHEMENG.7B03437/ASSET/IMAGES/MEDIUM/SC-2017-03437S_0021.GIF.

[10] A. Balea, E. Fuente, A. Blanco, and C. Negro, "Nanocelluloses: Natural-Based Materials for Fiber-Reinforced Cement Composites. A Critical Review," *Polym. 2019, Vol. 11, Page 518*, vol. 11, no. 3, p. 518, Mar. 2019, doi: 10.3390/POLYM11030518.

[11] A. B. Reising, R. J. Moon, and J. P. Youngblood, "EFFECT OF PARTICLE ALIGNMENT ON MECHANICAL PROPERTIES OF NEAT CELLULOSE NANOCRYSTAL FILMS," *J-FOR J. Sci. Technol. For. Prod. Process.*, vol. 2, no. 6, 2012.

[12] R. J. Moon, A. Martini, J. Nairn, J. Simonsen, and J. Youngblood, "Cellulose nanomaterials review: structure, properties and nanocomposites," *Chem. Soc. Rev.*,

vol. 40, no. 7, pp. 3941–3994, Jun. 2011, doi: 10.1039/C0CS00108B.

[13] J. A. Diaz *et al.*, "Thermal conductivity in nanostructured films: From single cellulose nanocrystals to bulk films," *Biomacromolecules*, vol. 15, no. 11, pp. 4096–4101, Oct. 2014, doi: 10.1021/BM501131A/SUPPL_FILE/BM501131A_SI_001.PDF.

[14] J. A. Diaz, X. Wu, A. Martini, J. P. Youngblood, and R. J. Moon, "Thermal expansion of self-organized and shear-oriented cellulose nanocrystal films," *Biomacromolecules*, vol. 14, no. 8, pp. 2900–2908, Aug. 2013, doi: 10.1021/BM400794E/SUPPL_FILE/BM400794E_SI_001.PDF.

[15] Y. Cao, P. Zavaterri, J. Youngblood, R. Moon, and J. Weiss, "The influence of cellulose nanocrystal additions on the performance of cement paste," *Cem. Concr. Compos.*, vol. 56, pp. 73–83, 2015, doi: 10.1016/j.cemconcomp.2014.11.008.

[16] Y. Cao, P. Zavattieri, J. Youngblood, R. Moon, and J. Weiss, "The relationship between cellulose nanocrystal dispersion and strength," *Constr. Build. Mater.*, vol. 119, pp. 71–79, 2016, doi: 10.1016/j.conbuildmat.2016.03.077.

[17] J. Flores, M. Kamali, and A. Ghahremaninezhad, "An investigation into the properties and microstructure of cement mixtures modified with cellulose nanocrystal," *Materials (Basel).*, vol. 10, no. 5, 2017, doi: 10.3390/ma10050498.

[18] M. R. Dousti, Y. Boluk, and V. Bindiganavile, "The effect of cellulose nanocrystal (CNC) particles on the porosity and strength development in oil well cement paste," *Constr. Build. Mater.*, vol. 205, pp. 456–462, Apr. 2019, doi: 10.1016/J.CONBUILDMAT.2019.01.073.

[19] J. Claramunt, H. Ventura, R. D. Toledo Filho, and M. Ardanuy, "Effect of nanocelluloses on the microstructure and mechanical performance of CAC cementitious matrices," *Cem. Concr. Res.*, vol. 119, pp. 64–76, May 2019, doi: 10.1016/J.CEMCONRES.2019.02.006.

[20] A. Behnood and H. Ziari, "Effects of silica fume addition and water to cement ratio on the properties of high-strength concrete after exposure to high temperatures," *Cem. Concr. Compos.*, vol. 30, no. 2, pp. 106–112, Feb. 2008, doi: 10.1016/J.CEMCONCOMP.2007.06.003.

[21] M. Jalal, E. Mansouri, M. Sharifipour, and A. R. Pouladkhan, "Mechanical, rheological, durability and microstructural properties of high performance self-compacting concrete containing SiO2 micro and nanoparticles," *Mater. Des.*, vol. 34, pp. 389–400, Feb. 2012, doi: 10.1016/J.MATDES.2011.08.037.

[22] H. Bahadori and P. Hosseini, "Reduction of Cement Consumption by the Aid of Silica Nano-Particles (Investigation on Concrete Properties)," *Vilnius Gedim. Tech. Univ.*, vol. 18, no. 3, pp. 416–425, Jun. 2012, doi: 10.3846/13923730.2012.698912.

[23] M. Berra, F. Carassiti, T. Mangialardi, A. E. Paolini, and M. Sebastiani, "Effects of nanosilica addition on workability and compressive strength of Portland cement pastes," *Constr. Build. Mater.*, vol. 35, pp. 666–675, Oct. 2012, doi: 10.1016/J.CONBUILDMAT.2012.04.132.

[24] Q. Ye, Z. Zhang, L. Sheng, and R. Chen, "A comparative study on the pozzolanic

activity between nano-SiO2 and silica fume," *J. Wuhan Univ. Technol. Sci. Ed. 2006 213*, vol. 21, no. 3, pp. 153–157, Sep. 2006, doi: 10.1007/BF02840907.

[25] T. Meng, Y. Hong, H. Wei, and Q. Xu, "Effect of nano-SiO 2 with different particle size on the hydration kinetics of cement," *Thermochim. Acta*, vol. 675, no. January, pp. 127–133, 2019, doi: 10.1016/j.tca.2019.03.013.

[26] D. Kong, Y. Su, X. Du, Y. Yang, S. Wei, and S. P. Shah, "Influence of nano-silica agglomeration on fresh properties of cement pastes," *Constr. Build. Mater.*, vol. 43, pp. 557–562, Jun. 2013, doi: 10.1016/J.CONBUILDMAT.2013.02.066.

[27] R. M. Martins and A. J. F. Bombard, "Rheology of fresh cement paste with superplasticizer and nanosilica admixtures studied by response surface methodology," *Mater. Struct. Constr.*, vol. 45, no. 6, pp. 905–921, Jun. 2012, doi: 10.1617/S11527-011-9807-9/FIGURES/28.

[28] L. Senff, D. Hotza, W. L. Repette, V. M. Ferreira, and J. A. Labrincha, "Rheological characterisation of cement pastes with nanosilica, silica fume and superplasticiser additions," *http://dx.doi.org/10.1179/174367510X12663198542621*, vol. 109, no. 4, pp. 213–218, Apr. 2013, doi: 10.1179/174367510X12663198542621.

[29] K. S. Kamasamudram, W. Ashraf, and E. N. Landis, "Cellulose nanofibrils with and without nanosilica for the performance enhancement of Portland cement systems," *Constr. Build. Mater.*, vol. 285, p. 121547, 2021, doi: 10.1016/j.conbuildmat.2020.121547.

[30] Saloma, A. Nasution, I. Imran, and M. Abdullah, "Improvement of Concrete Durability by Nanomaterials," *Procedia Eng.*, vol. 125, pp. 608–612, Jan. 2015, doi: 10.1016/J.PROENG.2015.11.078.

[31] M. Jawaid, S. Boufi, and A. K. H. P. S, *Cellulose-Reinforced Nanofibre Composites*. 2017.

[32] "Home : Oxford English Dictionary." https://www.oed.com/ (accessed Jun. 18, 2022).

[33] "ISO/TS 80004-1:2015(en), Nanotechnologies — Vocabulary — Part 1: Core terms," 2015. Accessed: Jun. 18, 2022. [Online]. Available: https://www.iso.org/obp/ui/#iso:std:iso:ts:80004:-1:ed-2:v1:en.

[34] R. W. Siegel, "Nanostructured materials -mind over matter-," *Nanostructured Mater.*, vol. 4, no. 1, pp. 121–138, Jan. 1994, doi: 10.1016/0965-9773(94)90134-1.

[35] R. P. Feynman, "There's Plenty of Room at the Bottom," vol. XXIII, no. 5, 1960.

[36] W. Zhu, P. J. M. Bartos, and A. Porro, "Application of nanotechnology in construction," *Mater. Struct. 2004 379*, vol. 37, no. 9, pp. 649–658, Nov. 2004, doi: 10.1007/BF02483294.

[37] J. Lee, S. Mahendra, and P. J. J. Alvarez, "Nanomaterials in the construction industry: A review of their applications and environmental health and safety considerations," *ACS Nano*, vol. 4, no. 7, pp. 3580–3590, Jul. 2010, doi: 10.1021/NN100866W/SUPPL_FILE/NN100866W_SI_001.PDF.

[38] M. J. Hanus and A. T. Harris, “Nanotechnology innovations for the construction industry,” *Prog. Mater. Sci.*, vol. 58, no. 7, pp. 1056–1102, Aug. 2013, doi: 10.1016/J.PMATSCI.2013.04.001.

[39] “ObservatoryNano Economical Assessment / Construction sector Final report,” 2009, Accessed: Jun. 19, 2022. [Online]. Available: www.bwcv.es.

[40] P. Balaguru and S. P. Shah, *Fiber-Reinforced Cement Composites*, 1st Edition. New York: McGraw-Hill ©, 1992.

[41] D. Schodek, P. Ferreira, and M. Ashby, “Nanomaterials, Nanotechnologies and Design,” *Nanomater. Nanotechnologies Des.*, 2009, doi: 10.1016/B978-0-7506-8149-0.X0001-3.

[42] J. A. Ober, “Mineral commodity summaries 2018,” *Miner. Commod. Summ.*, 2018, doi: 10.3133/70194932.

[43] P. Juilland, E. Gallucci, R. Flatt, and K. Scrivener, “Dissolution theory applied to the induction period in alite hydration,” *Cem. Concr. Res.*, vol. 40, no. 6, pp. 831–844, Jun. 2010, doi: 10.1016/J.CEMCONRES.2010.01.012.

[44] M. Schneider, M. Romer, M. Tschudin, and H. Bolio, “Sustainable cement production—present and future,” *Cem. Concr. Res.*, vol. 41, no. 7, pp. 642–650, Jul. 2011, doi: 10.1016/J.CEMCONRES.2011.03.019.

[45] J. Cowie, E. M. (Ted) Bilek, T. H. Wegner, and J. A. Shatkin, “Market projections of cellulose nanomaterial-enabled products-- Part 2: Volume estimates,” *TAPPI JOURNAL, Vol. 13 Number 6, 2014; pp. 57-69.*, vol. 13, no. 6, pp. 57–69, 2014, [Online]. Available: https://www.fs.usda.gov/treesearch/pubs/46175.

[46] F. Pacheco-Torgal and S. Jalali, “Nanotechnology: Advantages and drawbacks in the field of construction and building materials,” *Constr. Build. Mater.*, vol. 25, no. 2, pp. 582–590, Feb. 2011, doi: 10.1016/J.CONBUILDMAT.2010.07.009.

[47] A. M. Said, M. S. Zeidan, M. T. Bassuoni, and Y. Tian, “Properties of concrete incorporating nano-silica,” *Constr. Build. Mater.*, vol. 36, pp. 838–844, Nov. 2012, doi: 10.1016/J.CONBUILDMAT.2012.06.044.

[48] J. Chen, S. C. Kou, and C. S. Poon, “Hydration and properties of nano-TiO2 blended cement composites,” *Cem. Concr. Compos.*, vol. 34, no. 5, pp. 642–649, May 2012, doi: 10.1016/J.CEMCONCOMP.2012.02.009.

[49] D. Osborn, M. Hassan, and H. Dylla, “Quantification of Reduction of Nitrogen Oxides by Nitrate Accumulation on Titanium Dioxide Photocatalytic Concrete Pavement:,” *https://doi.org/10.3141/2290-19*, no. 2290, pp. 147–153, Jan. 2012, doi: 10.3141/2290-19.

[50] N. Tregger, M. Pakula, and S. P. Shah, “Influence of Micro- and Nanoclays on Fresh State of Concrete:,” *https://doi.org/10.3141/2141-12*, no. 2141, pp. 68–74, Jan. 2010, doi: 10.3141/2141-12.

[51] M. S. Konsta-Gdoutos, Z. S. Metaxa, and S. P. Shah, “Multi-scale mechanical and fracture characteristics and early-age strain capacity of high performance carbon nanotube/cement nanocomposites,” *Cem. Concr. Compos.*, vol. 32, no. 2, pp. 110–115, Feb. 2010, doi: 10.1016/J.CEMCONCOMP.2009.10.007.

[52] N. Makul, “Advanced smart concrete - A review of current progress, benefits and challenges,” *J. Clean. Prod.*, vol. 274, p. 122899, Nov. 2020, doi: 10.1016/J.JCLEPRO.2020.122899.

[53] Z. S. Metaxa *et al.*, “Nanomaterials in Cementitious Composites: An Update,” *Mol. 2021, Vol. 26, Page 1430*, vol. 26, no. 5, p. 1430, Mar. 2021, doi: 10.3390/MOLECULES26051430.

[54] F. W. Herrick, R. L. Casebier, J. K. Hamilton, and K. R. Sandberg, “Microfibrillated cellulose: morphology and accessibility,” 1983, vol. 37, [Online]. Available: https://www.osti.gov/biblio/5039044.

[55] S. J. Eichhorn *et al.*, “Review: current international research into cellulose nanofibres and nanocomposites,” *J. Mater. Sci. 2009 451*, vol. 45, no. 1, pp. 1–33, Jan. 2010, doi: 10.1007/S10853-009-3874-0.

[56] I. Kvien, B. S. Tanem, and K. Oksman, “Characterization of Cellulose Whiskers and Their Nanocomposites by Atomic Force and Electron Microscopy,” *Biomacromolecules*, vol. 6, no. 6, pp. 3160–3165, Nov. 2005, doi: 10.1021/BM050479T.

[57] S. Rebouillat, F. Pla, S. Rebouillat, and F. Pla, “State of the Art Manufacturing and Engineering of Nanocellulose: A Review of Available Data and Industrial Applications,” *J. Biomater. Nanobiotechnol.*, vol. 4, no. 2, pp. 165–188, Apr. 2013, doi: 10.4236/JBNB.2013.42022.

[58] E. Lam, K. B. Male, J. H. Chong, A. C. W. Leung, and J. H. T. Luong, “Applications of functionalized and nanoparticle-modified nanocrystalline cellulose,” *Trends Biotechnol.*, vol. 30, no. 5, pp. 283–290, May 2012, doi: 10.1016/J.TIBTECH.2012.02.001.

[59] S. Beck, J. Bouchard, and R. Berry, “Dispersibility in water of dried nanocrystalline cellulose,” *Biomacromolecules*, vol. 13, no. 5, pp. 1486–1494, May 2012, doi: 10.1021/BM300191K/ASSET/IMAGES/MEDIUM/BM-2012-00191K_0007.GIF.

[60] N. Lin, J. Huang, and A. Dufresne, “Preparation, properties and applications of polysaccharide nanocrystals in advanced functional nanomaterials: a review,” *Nanoscale*, vol. 4, no. 11, pp. 3274–3294, May 2012, doi: 10.1039/C2NR30260H.

[61] C. Fu, C. Xie, J. Liu, X. Wei, and D. Wu, “A Comparative Study on the Effects of Three Nano-Materials on the Properties of Cement-Based Composites,” *Mater. 2020, Vol. 13, Page 857*, vol. 13, no. 4, p. 857, Feb. 2020, doi: 10.3390/MA13040857.

[62] O. A. Hisseine, W. Wilson, L. Sorelli, B. Tolnai, and A. Tagnit-Hamou, “Nanocellulose for improved concrete performance: A macro-to-micro investigation for disclosing the effects of cellulose filaments on strength of cement systems,” *Constr. Build. Mater.*, vol. 206, pp. 84–96, 2019, doi: 10.1016/j.conbuildmat.2019.02.042.

[63] X. Sun, C. Mei, A. D. French, S. Lee, Y. Wang, and Q. Wu, “Surface wetting behavior of nanocellulose-based composite films,” *Cellulose*, vol. 25, no. 9, pp. 5071–5087, Sep. 2018, doi: 10.1007/S10570-018-1927-8/FIGURES/7.

[64] H. J. Lee and W. Kim, “Long-term durability evaluation of fiber-reinforced ECC using wood-based cellulose nanocrystals,” *Constr. Build. Mater.*, vol. 238, p. 117754, 2020, doi: 10.1016/j.conbuildmat.2019.117754.

[65] M. A. Akhlaghi, R. Bagherpour, and H. Kalhori, “Application of bacterial nanocellulose fibers as reinforcement in cement composites,” *Constr. Build. Mater.*, vol. 241, p. 118061, Apr. 2020, doi: 10.1016/J.CONBUILDMAT.2020.118061.

[66] D. Miyashiro, R. Hamano, and K. Umemura, “A Review of Applications Using Mixed Materials of Cellulose, Nanocellulose and Carbon Nanotubes,” *Nanomater. 2020, Vol. 10, Page 186*, vol. 10, no. 2, p. 186, Jan. 2020, doi: 10.3390/NANO10020186.

[67] A. Dufresne, “Nanocellulose: a new ageless bionanomaterial,” *Mater. Today*, vol. 16, no. 6, pp. 220–227, Jun. 2013, doi: 10.1016/J.MATTOD.2013.06.004.

[68] D. Bondeson, A. Mathew, and K. Oksman, “Optimization of the isolation of nanocrystals from microcrystalline cellulose by acid hydrolysis,” *Cellul. 2006 132*, vol. 13, no. 2, pp. 171–180, Apr. 2006, doi: 10.1007/S10570-006-9061-4.

[69] Y. Habibi, L. A. Lucia, and O. J. Rojas, “Cellulose nanocrystals: Chemistry, self-assembly, and applications,” *Chem. Rev.*, vol. 110, no. 6, pp. 3479–3500, Jun. 2010, doi: 10.1021/CR900339W/ASSET/CR900339W.FP.PNG_V03.

[70] F. L. Dri, L. G. Hector, R. J. Moon, and P. D. Zavattieri, “Anisotropy of the elastic properties of crystalline cellulose Iβ from first principles density functional theory with Van der Waals interactions,” *Cellulose*, vol. 20, no. 6, pp. 2703–2718, Dec. 2013, doi: 10.1007/S10570-013-0071-8.

[71] M. R. Kamal and V. Khoshkava, “Effect of cellulose nanocrystals (CNC) on rheological and mechanical properties and crystallization behavior of PLA/CNC nanocomposites,” *Carbohydr. Polym.*, vol. 123, pp. 105–114, Jun. 2015, doi: 10.1016/J.CARBPOL.2015.01.012.

[72] A. Dufresne, “Nanocellulose: from nature to high performance tailored materials. De Gruyter,” *Nanocellulose*, Jan. 2012, doi: 10.1515/9783110254600.

[73] T. Fu, F. Montes, P. Suraneni, J. Youngblood, and J. Weiss, “The influence of cellulose nanocrystals on the hydration and flexural strength of Portland cement pastes,” *Polymers (Basel).*, vol. 9, no. 9, 2017, doi: 10.3390/polym9090424.

[74] S. A. Ghahari, L. N. Assi, A. Alsalman, and K. E. Alyamaç, “Fracture properties evaluation of cellulose nanocrystals cement paste,” *Materials (Basel).*, vol. 13, no. 11, 2020, doi: 10.3390/ma13112507.

[75] D. V. Filipak Vanin, V. D. Andrade, T. A. Fiorentin, D. de O. S. Recouvreux, C. A. Carminatti, and H. A. Al-Qureshi, “Cement pastes modified by cellulose nanocrystals: A dynamic moduli evolution assessment by the Impulse Excitation Technique,” *Mater. Chem. Phys.*, vol. 239, no. May 2019, p. 122038, 2020, doi: 10.1016/j.matchemphys.2019.122038.

[76] H. Yang *et al.*, “Effects of nano silica on the properties of cement-based materials: A comprehensive review,” *Constr. Build. Mater.*, vol. 282, p. 122715, May 2021, doi: 10.1016/J.CONBUILDMAT.2021.122715.

[77] S. Nandi, S. Bose, S. Mitra, and A. K. Ghosh, “Dynamic rheology and morphology of HDPE-fumed silica composites: Effect of interface modification,” *Polym. Eng. Sci.*, vol. 53, no. 3, pp. 644–650, Mar. 2013, doi: 10.1002/PEN.23299.

[78] G. Quercia, G. Hüsken, and H. J. H. Brouwers, “Water demand of amorphous nano silica and its impact on the workability of cement paste,” *Cem. Concr. Res.*, vol. 42, no. 2, pp. 344–357, Feb. 2012, doi: 10.1016/J.CEMCONRES.2011.10.008.

[79] D. M. Ritter, “Inorganic Reactions and Structure,” *Inorg. Chem.*, vol. 2, no. 3, p. 664, Jun. 1963, doi: 10.1021/IC50007A076/ASSET/IC50007A076.FP.PNG_V03.

[80] S. R. Raghavan and S. A. Khan, “Shear-Thickening Response of Fumed Silica Suspensions under Steady and Oscillatory Shear,” *J. Colloid Interface Sci.*, vol. 185, no. 1, pp. 57–67, Jan. 1997, doi: 10.1006/JCIS.1996.4581.

[81] Q. Fu, X. Zhao, Z. Zhang, W. Xu, and D. Niu, “Effects of nanosilica on microstructure and durability of cement-based materials,” *Powder Technol.*, vol. 404, p. 117447, May 2022, doi: 10.1016/J.POWTEC.2022.117447.

[82] P. Hou, X. Cheng, J. Qian, and S. P. Shah, “Effects and mechanisms of surface treatment of hardened cement-based materials with colloidal nanoSiO2 and its precursor,” *Constr. Build. Mater.*, vol. 53, pp. 66–73, Feb. 2014, doi: 10.1016/J.CONBUILDMAT.2013.11.062.

[83] Y. Sargam and K. Wang, “Influence of dispersants and dispersion on properties of nanosilica modified cement-based materials,” *Cem. Concr. Compos.*, vol. 118, no. January, p. 103969, 2021, doi: 10.1016/j.cemconcomp.2021.103969.

[84] L. P. Singh, S. R. Karade, S. K. Bhattacharyya, M. M. Yousuf, and S. Ahalawat, “Beneficial role of nanosilica in cement based materials – A review,” *Constr. Build. Mater.*, vol. 47, pp. 1069–1077, Oct. 2013, doi: 10.1016/J.CONBUILDMAT.2013.05.052.

[85] T. Ji, “Preliminary study on the water permeability and microstructure of concrete incorporating nano-SiO2,” *Cem. Concr. Res.*, vol. 35, no. 10, pp. 1943–1947, Oct. 2005, doi: 10.1016/J.CEMCONRES.2005.07.004.

[86] Y. Qing, Z. Zenan, K. Deyu, and C. Rongshen, “Influence of nano-SiO2 addition on properties of hardened cement paste as compared with silica fume,” *Constr. Build. Mater.*, vol. 21, no. 3, pp. 539–545, Mar. 2007, doi: 10.1016/J.CONBUILDMAT.2005.09.001.

[87] B. W. Jo, C. H. Kim, G. ho Tae, and J. Bin Park, “Characteristics of cement mortar with nano-SiO2 particles,” *Constr. Build. Mater.*, vol. 21, no. 6, pp. 1351–1355, Jun. 2007, doi: 10.1016/J.CONBUILDMAT.2005.12.020.

[88] J. J. Thomas, H. M. Jennings, and J. J. Chen, “Influence of Nucleation Seeding on the Hydration Mechanisms of Tricalcium Silicate and Cement,” *J. Phys. Chem. C*, vol. 113, no. 11, pp. 4327–4334, Mar. 2009, doi: 10.1021/JP809811W.

[89] P. Hou, J. Qian, X. Cheng, and S. P. Shah, “Effects of the pozzolanic reactivity of nanoSiO2 on cement-based materials,” *Cem. Concr. Compos.*, vol. 55, pp. 250–258, Jan. 2015, doi: 10.1016/J.CEMCONCOMP.2014.09.014.

[90] Z. Rong, W. Sun, H. Xiao, and G. Jiang, “Effects of nano-SiO2 particles on the mechanical and microstructural properties of ultra-high performance cementitious

composites," *Cem. Concr. Compos.*, vol. 56, pp. 25–31, Feb. 2015, doi: 10.1016/J.CEMCONCOMP.2014.11.001.

[91] Q. Huang, X. Zhu, D. Liu, L. Zhao, and M. Zhao, "Modification of water absorption and pore structure of high-volume fly ash cement pastes by incorporating nanosilica," *J. Build. Eng.*, vol. 33, p. 101638, Jan. 2021, doi: 10.1016/J.JOBE.2020.101638.

[92] P. Sikora, T. Rucinska, D. Stephan, S. Y. Chung, and M. Abd Elrahman, "Evaluating the effects of nanosilica on the material properties of lightweight and ultra-lightweight concrete using image-based approaches," *Constr. Build. Mater.*, vol. 264, p. 120241, Dec. 2020, doi: 10.1016/J.CONBUILDMAT.2020.120241.

[93] W. Li, Z. Huang, F. Cao, Z. Sun, and S. P. Shah, "Effects of nano-silica and nano-limestone on flowability and mechanical properties of ultra-high-performance concrete matrix," *Constr. Build. Mater.*, vol. 95, pp. 366–374, Oct. 2015, doi: 10.1016/J.CONBUILDMAT.2015.05.137.

[94] H. El-Diadamony, A. A. Amer, T. M. Sokkary, and S. El-Hoseny, "Hydration and characteristics of metakaolin pozzolanic cement pastes," *HBRC J.*, vol. 14, no. 2, pp. 150–158, Aug. 2018, doi: 10.1016/J.HBRCJ.2015.05.005.

[95] M. Stefanidou and I. Papayianni, "Influence of nano-SiO2 on the Portland cement pastes," *Compos. Part B Eng.*, vol. 43, no. 6, pp. 2706–2710, Sep. 2012, doi: 10.1016/J.COMPOSITESB.2011.12.015.

[96] A. A. Raheem, R. Abdulwahab, and M. A. Kareem, "Incorporation of metakaolin and nanosilica in blended cement mortar and concrete- A review," *J. Clean. Prod.*, vol. 290, p. 125852, Mar. 2021, doi: 10.1016/J.JCLEPRO.2021.125852.

[97] M. H. Zhang and H. Li, "Pore structure and chloride permeability of concrete containing nano-particles for pavement," *Constr. Build. Mater.*, vol. 25, no. 2, pp. 608–616, Feb. 2011, doi: 10.1016/J.CONBUILDMAT.2010.07.032.

[98] C. Pereira, F. Caldeira Jorge, M. Irle, and J. M. Ferreira, "Characterizing the setting of cement when mixed with cork, blue gum, or maritime pine, grown in Portugal II: X-ray diffraction and differential thermal analyzes," *J. Wood Sci.*, vol. 52, no. 4, pp. 318–324, Aug. 2006, doi: 10.1007/S10086-005-0775-Y/METRICS.

[99] L. Segal, J. J. Creely, A. E. Martin, and C. M. Conrad, "An Empirical Method for Estimating the Degree of Crystallinity of Native Cellulose Using the X-Ray Diffractometer," *Text. Res. J.*, vol. 29, no. 10, pp. 786–794, Oct. 1959, doi: 10.1177/004051755902901003.

[100] M. S. Reid, M. Villalobos, and E. D. Cranston, "Benchmarking Cellulose Nanocrystals: From the Laboratory to Industrial Production," *Langmuir*, vol. 33, no. 7, pp. 1583–1598, Feb. 2017, doi: 10.1021/acs.langmuir.6b03765.

[101] ASTM C305, "Standard Practice for Mechanical Mixing of Hydraulic Cement Pastes and Mortars of Plastic Consistency," 2020. doi: 10.1520/C0305-20.

[102] ASTM C1437, "Standard Test Method for Flow of Hydraulic Cement Mortar," 2020. doi: 10.1520/C1437.

[103] ASTM C191, "Standard Test Methods for Time of Setting of Hydraulic Cement by Vicat Needle," 2021. doi: 10.1520/C0191-21.

[104] ASTM C642, “Standard Test Method for Density, Absorption, and Voids in Hardened Concrete,” 2021. doi: 10.1520/C0642-21.

[105] ASTM C109/C109M, “Standard Test Method for Compressive Strength of Hydraulic Cement Mortars (Using 2-in. or [50 mm] Cube Specimens),” 2021. doi: 10.1520/C0109_C0109M-21.

[106] S. Nassiri *et al.*, “Comparison of unique effects of two contrasting types of cellulose nanomaterials on setting time, rheology, and compressive strength of cement paste,” *Cem. Concr. Compos.*, vol. 123, no. January, p. 104201, 2021, doi: 10.1016/j.cemconcomp.2021.104201.

[107] M. Nasir *et al.*, “Engineered cellulose nanocrystals-based cement mortar from office paper waste: Flow, strength, microstructure, and thermal properties,” *J. Build. Eng.*, vol. 51, p. 104345, Jul. 2022, doi: 10.1016/J.JOBE.2022.104345.

[108] L. Senff, D. Hotza, W. L. Repette, V. M. Ferreira, and J. A. Labrincha, “Mortars with nano-SiO2 and micro-SiO2 investigated by experimental design,” *Constr. Build. Mater.*, vol. 24, no. 8, pp. 1432–1437, 2010, doi: 10.1016/j.conbuildmat.2010.01.012.

[109] Z. Tang *et al.*, “Influence of cellulose nanoparticles on rheological behavior of oilwell cement-water slurries,” *Materials (Basel).*, vol. 12, no. 2, pp. 1–14, 2019, doi: 10.3390/ma12020291.

[110] L. Jiao, M. Su, L. Chen, Y. Wang, H. Zhu, and H. Dai, “Natural Cellulose Nanofibers As Sustainable Enhancers in Construction Cement,” *PLoS One*, vol. 11, no. 12, p. e0168422, Dec. 2016, doi: 10.1371/JOURNAL.PONE.0168422.

[111] R. Palanivelu, V. Rajendran, N. R. Dhineshbabu, T. Palanisamy, and S. Balasubramanian, “Comparative Study of Addition of Amorphous Nanosilica Particles with Different Grades of Cement Mortar,” *Int. J. Appl. Ceram. Technol.*, vol. 12, pp. E14–E22, Nov. 2015, doi: 10.1111/IJAC.12349.

[112] L. Senff, J. A. Labrincha, V. M. Ferreira, D. Hotza, and W. L. Repette, “Effect of nano-silica on rheology and fresh properties of cement pastes and mortars,” *Constr. Build. Mater.*, vol. 23, no. 7, pp. 2487–2491, Jul. 2009, doi: 10.1016/J.CONBUILDMAT.2009.02.005.

[113] F. Montes, T. Fu, J. P. Youngblood, and J. Weiss, “Rheological impact of using cellulose nanocrystals (CNC) in cement pastes,” *Constr. Build. Mater.*, vol. 235, p. 117497, 2020, doi: 10.1016/j.conbuildmat.2019.117497.

[114] J. Pourchez, P. Grosseau, and B. Ruot, “Current understanding of cellulose ethers impact on the hydration of C3A and C3A-sulphate systems,” *Cem. Concr. Res.*, vol. 39, no. 8, pp. 664–669, Aug. 2009, doi: 10.1016/J.CEMCONRES.2009.05.009.

[115] C. Brumaud, R. Baumann, M. Schmitz, M. Radler, and N. Roussel, “Cellulose ethers and yield stress of cement pastes,” *Cem. Concr. Res.*, vol. 55, pp. 14–21, Jan. 2014, doi: 10.1016/J.CEMCONRES.2013.06.013.

[116] A. Pourjavadi, S. M. Fakoorpoor, A. Khaloo, and P. Hosseini, “Improving the performance of cement-based composites containing superabsorbent polymers by utilization of nano-SiO2 particles,” *Mater. Des.*, vol. 42, pp. 94–101, Dec. 2012,

doi: 10.1016/J.MATDES.2012.05.030.

[117] M. Sonebi, M. T. Bassuoni, J. Kwasny, and A. K. Amanuddin, “Effect of Nanosilica on Rheology, Fresh Properties, and Strength of Cement-Based Grouts,” *J. Mater. Civ. Eng.*, vol. 27, no. 4, p. 04014145, 2015, doi: 10.1061/(asce)mt.1943-5533.0001080.

[118] L. B. Agostinho, de C. P. Alexandre, E. F. da Silva, and R. D. Toledo Filho, “Rheological study of Portland cement pastes modified with superabsorbent polymer and nanosilica,” *J. Build. Eng.*, vol. 34, no. November 2020, 2021, doi: 10.1016/j.jobe.2020.102024.

[119] A. Khaloo, M. H. Mobini, and P. Hosseini, “Influence of different types of nano-SiO2 particles on properties of high-performance concrete,” *Constr. Build. Mater.*, vol. 113, pp. 188–201, Jun. 2016, doi: 10.1016/J.CONBUILDMAT.2016.03.041.

[120] X. Wang, K. Wang, J. Tanesi, and A. Ardani, “Effects of nanomaterials on the hydration kinetics and rheology of Portland cement pastes,” *Adv. Civ. Eng. Mater.*, vol. 3, no. 2, pp. 142–159, 2015, doi: 10.1520/ACEM20140021.

[121] D. Mazlan *et al.*, “Effect of Cellulose Nanocrystals Extracted from Oil Palm Empty Fruit Bunch as Green Admixture for Mortar,” *Sci. Reports 2020 101*, vol. 10, no. 1, pp. 1–11, Apr. 2020, doi: 10.1038/s41598-020-63575-7.

[122] P. Kumar Mehta and Paulo J. M. Monteiro, *Concrete: Microstructure, Properties and Materials*, 3rd Edition. McGraw-Hill ©, 2006.

[123] J. Aguiar, P. Moreira, P. Lukowski, L. Czarnecki, A. Camões, and D. Van Gemert, “Ranking Procedure for Polymeric Coatings and Hydrophobic Agents for Concrete Protection / Methode zum Klassifizieren von polymeren Beschichtungen und hydrophobierenden Wirkstoffen für den Betonschutz,” *Restor. Build. Monum.*, vol. 13, no. 4, pp. 251–264, 2007, doi: doi:10.1515/rbm-2007-6143.

[124] L. ping Wu, G. ping Huang, C. shi Hu, and W. V. Liu, “Effects of cellulose nanocrystals on the acid resistance of cementitious composites,” *Int. J. Miner. Metall. Mater. 2021 2811*, vol. 28, no. 11, pp. 1745–1758, Sep. 2021, doi: 10.1007/S12613-020-2087-Z.

[125] R. A. Cook and K. C. Hover, “Mercury porosimetry of hardened cement pastes,” *Cem. Concr. Res.*, vol. 29, no. 6, pp. 933–943, Jun. 1999, doi: 10.1016/S0008-8846(99)00083-6.

[126] Y. Cao *et al.*, “The influence of cellulose nanocrystals on the microstructure of cement paste,” *Cem. Concr. Compos.*, vol. 74, pp. 164–173, 2016, doi: 10.1016/j.cemconcomp.2016.09.008.

[127] B. S. Mohammed and N. J. Azmi, “Strength reduction factors for structural rubbercrete,” *Front. Struct. Civ. Eng. 2014 83*, vol. 8, no. 3, pp. 270–281, Jul. 2014, doi: 10.1007/S11709-014-0265-7.

[128] S. Shahrul, B. S. Mohammed, M. M. A. Wahab, and M. S. Liew, “Mechanical properties of crumb rubber mortar containing nano-silica using response surface methodology,” *Materials (Basel).*, vol. 14, no. 19, 2021, doi: 10.3390/ma14195496.

[129] M. Oltulu and R. Şahin, “Pore structure analysis of hardened cement mortars

containing silica fume and different nano-powders," *Constr. Build. Mater.*, vol. 53, pp. 658–664, Feb. 2014, doi: 10.1016/J.CONBUILDMAT.2013.11.105.

[130] G. Lefever *et al.*, "The influence of superabsorbent polymers and nanosilica on the hydration process and microstructure of cementitious mixtures," *Materials (Basel).*, vol. 13, no. 22, pp. 1–16, 2020, doi: 10.3390/ma13225194.

[131] J. S. Vasconcellos, G. L. O. Martins, G. de Almeida Ribeiro Oliveira, L. M. Lião, J. H. da Silva Rêgo, and P. P. C. Sartoratto, "Effect of amine functionalized nanosilica on the cement hydration and on the physical-mechanical properties of Portland cement pastes," *J. Nanoparticle Res.*, vol. 22, no. 8, 2020, doi: 10.1007/s11051-020-04940-5.

[132] L. Cui and J. H. Cahyadi, "Permeability and pore structure of OPC paste," *Cem. Concr. Res.*, vol. 31, no. 2, pp. 277–282, Feb. 2001, doi: 10.1016/S0008-8846(00)00474-9.

[133] S. Lim and P. Mondal, "Effects of incorporating nanosilica on carbonation of cement paste," *J. Mater. Sci.*, vol. 50, no. 10, pp. 3531–3540, 2015, doi: 10.1007/s10853-015-8910-7.

[134] K. Scrivener, R. Snellings, and B. Lothenbach, *A practical guide to microstructural analysis of cementitious materials*. Boca Raton: CRC Press, 2016.

[135] N. Kabay, N. Miyan, and H. Özkan, "Utilization of pumice powder and glass microspheres in cement mortar using paste replacement methodology," *Constr. Build. Mater.*, vol. 282, p. 122691, 2021.

[136] J. I. Bhatty, "Hydration versus strength in a portland cement developed from domestic mineral wastes — a comparative study," *Thermochim. Acta*, vol. 106, no. C, pp. 93–103, Sep. 1986, doi: 10.1016/0040-6031(86)85120-6.

[137] T. Nawa, "Effect of Chemical Structure on Steric Stabilization of Polycarboxylate-based Superplasticizer," *J. Adv. Concr. Technol.*, vol. 4, no. 2, pp. 225–232, 2006, doi: 10.3151/JACT.4.225.

[138] S. Lim and P. Mondal, "Effects of nanosilica addition on increased thermal stability of cement-based composite," *ACI Mater. J.*, vol. 112, no. 2, pp. 305–316, 2015, doi: 10.14359/51687177.

[139] Q. Fan *et al.*, "Experiment and molecular dynamics simulation of functionalized cellulose nanocrystals as reinforcement in cement composites," *Constr. Build. Mater.*, vol. 341, p. 127879, Jul. 2022, doi: 10.1016/J.CONBUILDMAT.2022.127879.

[140] R. Mejdoub, H. Hammi, J. J. Suñol, M. Khitouni, A. M'nif, and S. Boufi, "Nanofibrillated cellulose as nanoreinforcement in Portland cement: Thermal, mechanical and microstructural properties," *J. Compos. Mater.*, vol. 51, no. 17, pp. 2491–2503, 2017, doi: 10.1177/0021998316672090.

[141] D. Hou, H. Ma, and Z. Li, "Morphology of calcium silicate hydrate (C-S-H) gel: a molecular dynamic study," *http://dx.doi.org/10.1680/adcr.13.00079*, vol. 27, no. 3, pp. 135–146, Sep. 2015, doi: 10.1680/ADCR.13.00079.

[142] S. Parveen, S. Rana, R. Fangueiro, and M. C. Paiva, "A novel approach of developing micro crystalline cellulose reinforced cementitious composites with

enhanced microstructure and mechanical performance," *Cem. Concr. Compos.*, vol. 78, pp. 146–161, 2017, doi: 10.1016/j.cemconcomp.2017.01.004.

PUBLICATIONS FROM THE THESIS

Conference Papers

1. A. S. J. AL-ASKARY and D. OKTAY, “Influence of Cellulose Nanocrystals and Nano Silica on Mechanical Performance of Cement-Based Materials,” in *2nd International Congress of Engineering and Natural Sciences Studies*, 2022, pp. 11–25.